Biomass Refinery and Process Dynamics Group

Novel designs for energy and nutrient recovery in municipal wastewater using a dynamic modeling approach

Thesis Biomass Refinery and Process Dynamics

Elvira Bozileva
7/26/2013

Novel designs for energy and nutrient recovery in municipal wastewater using a dynamic modeling approach

Name course	Thesis project Biomass Refinery and Process Dynamics
Number	BRD-80439
Study load	39 ECTS
Date	26/7/2013
Student	Elvira Bozileva
Registration number	s1197665
Study program	Water Technology
Supervisors	Rungnapha Khiewwijit (MSc)
	dr. ir. Karel Keesman
Examiners	dr. ir. Karel Keesman
	dr. ir. Hardy Temmink
	dr. ir. Nieck Benes
Group	Biomass Refinery and Process Dynamics

Abstract

Dynamic modelling of a novel promising scenario for municipal wastewater treatment was performed in this work. In this scenario such processes as bioflocculation, anaerobic digestion, partial nitritation and Anammox are combined in a single system. The scenario was previously identified as a more sustainable solution for the treatment of municipal wastewater compared to conventional methods, using the black-box steady-state modelling approach. In this work dynamic grey-box modelling approach was used to simulate the individual processes. Model interfacing approach was used to combine individual models into an overall model to allow a plant-wide simulation.

Several problems were identified in a course of work, such as lack of standard model for the simulation of bioflocculation process, numerical instability of a standard model used for the simulation of anaerobic digestion process and lack of a standard procedure for individual model interfacing. Ways to overcome the said problems were proposed in this work. However experimental data is now necessary to prove the proposed ideas.

Plant-wide modelling approach allowed finding the optimal operation conditions for bioflocculation and partial nitritation processes. The effect of sludge retention time, aeration intensity and influent particulates concentration was studied for bioflocculation step. Criteria used to identify the optimal operation conditions for the process of bioflocculation was the production of methane in anaerobic digestion process. The effect of sludge retention time, aeration intensity, influent particulates concentration and temperature was studied for partial nitritation step. Criteria used to identify the optimal operation conditions for partial nitritation process was obtaining the system effluent that would meet the discharge requirements denoted in EU legislation.

Contents

Acknowledgements

This master thesis was performed at Wetsus, centre of excellence for sustainable water technology (Leeuwarden). Wetsus academy provided a joined degree MSc programme in Water technology. The author would like to thank MSc Rungnapha Khiewwijit for supervising and support, dr. ir. Karel Keesman for supervising and a major help with programming in MATLAB, dr. ir. Arjen Rinzema for fruitful discussions on biofilm modelling, dr. ir. Hardy Temming for important corrections and MSc Andrii Butkovsky for useful remarks concerning practical aspects of anaerobic digestion.

1. Introduction

Wastewater treatment methods

Rapid population growth and industrialization that started in the second half of the twentieth century has resulted in high environmental stress. In attempt to decrease the stress on the environment in 1991 EU Urban Wastewater Treatment Directive [1] was adopted. According to this directive all the industrial wastewater entering collecting systems as well as the discharge of wastewater and disposal of sludge from urban wastewater treatment plants became subject to general rules and regulations.

Conventional wastewater treatment technologies are able to produce the effluents that comply with the regulations marked in the Directive. However as the stress on the ecosystems steadily increases the new legislation regulating the wastewater discharge is expected to become more stringent. For the conventional wastewater treatment technologies meeting the new legislative requirements would be associated with the increase of process costs. To avoid the negative economic returns new wastewater treatment methods should be developed that would combine high efficiency of pollution removal and low expenses.

Analysis of the novel municipal wastewater treatment plants was carried out by Khiewwijit, 2013 (unpublished). Based on the results of the analysis, several novel scenarios for municipal wastewater treatment in the Netherlands have been proposed. The most sustainable scenario identified in said work is in focus of this work. The general process scheme of a promissing scenario is shown below.

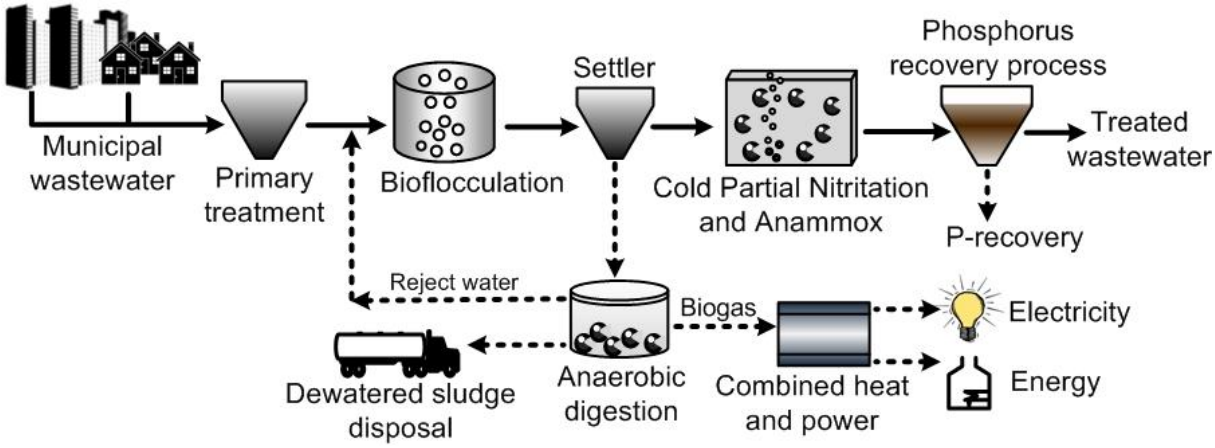

Figure 1. Wastewater treatment scenario proposed by Khiewwijit, 2013 (unpublished).

The scenario is aimed at reducing the concentration of carbon in a form of chemical oxygen demand (COD –measure of carbon content of wastewater), nitrogen and phosphorus till the discharge guidelines outlined in EU legislation [1, 2]. These compounds are typical targets of wastewater treatment techniques. Insufficient removal of these can result in uncontrolled bacteria growth and eutrophication[1] of aquatic systems.

[1] Eutrophication according to the definition given in Urban Wastewater Treatment Directive [1] is *the enrichment of water by nutrients, especially compounds of nitrogen and/or phosphorus, causing an accelerated growth of algae and higher forms of plant life to produce an undesirable disturbance to the balance of organisms present in the water and to the quality of the water concerned*.
Remark. Hereinafter *italic* font indicates a literal citation.

In this scenario, wastewater is first pre-treated in a process of bioflocculation. Here the sludge is concentrated and flocculated with the help of Extracellular Polymeric Substances excreted by the growing biomass in the reactor [3]. Only small amounts of carbon and nutrients are mineralized/consumed during bioflocculation [4]. Concentrated sludge is directed to the anaerobic digester where significant amount of organic carbon is converted to methane – an energy carrier and a source of income for the plant. Anaerobic sludge digestion is claimed to be a viable alternative to conventional aerobic activated sludge process for a variety of reasons [5-7]. However, since COD removal in anaerobic digestion is not as high as in aerobic treatment methods, aerobic post-treatment is normally recommended [8]. The effluent of bioflocculation reactor is directed to aerobic reactor where remaining COD is oxidized to CO_2 and nitrogen which is normally present in the form and ammonia is partially oxidized to nitrite. Complete oxidation to nitrate is avoided at this stage by precise regulation of process controls, such as temperature, dissolved oxygen, sludge and hydraulic retention time [9]. When nitrogen is present in the solution in the form of ammonia and nitrite at a specific ratio, it can be removed from the system via Anammox process (ANaerobic AMMonium OXidation) [10, 11]. In this process autotrophic bacteria utilizes ammonia as electron donor and nitrite – as electron acceptor, converting these compounds to nitrogen gas and small amounts of nitrate [12, 13]. Combination of partial nitritation and Anammox processes has several advantages compared to conventional nitrification-denitrification process, as outlined by several authors [14, 15].

To identify the most sustainable scenario the black-box steady-state simulation approach was used by Khiewwijit. For further analysis, mechanistically inspired approach is needed. Such approach allows evaluating the system performance at different conditions and can help to identify optimal operation conditions for different system units. Furthermore dynamic simulation results might be very valuable, since such simulation allows evaluating the system performance during plant's start-up/shut-down as well as gives an insight on the effect of the changes in system inflow on the whole process.

Some numerical problems, however, are expected for dynamic simulation of the scenario shown on Figure 1. Particularly back-loops might appear to be difficult to treat. In order to avoid computational difficulties the scenario was modified, and the actual system simulated in this work is shown on Figure 2.

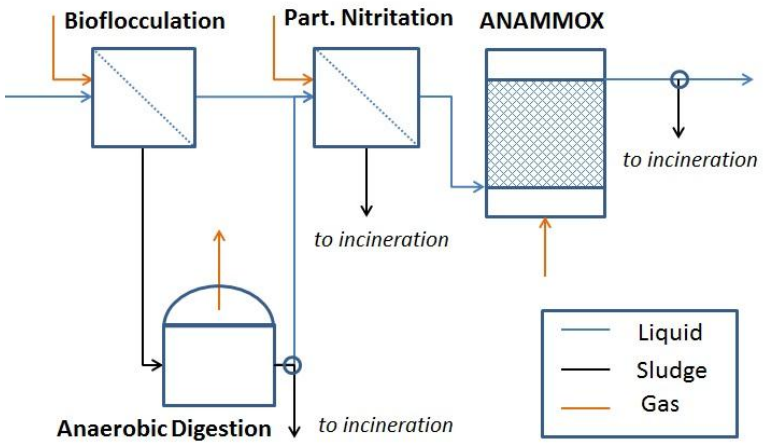

Figure 2. Wastewater treatment scenario modelled in this work.

The system shown on Figure 2 is straightforward (no back-loops are present) – the liquid fraction of anaerobic digestion that still contains high amount of nitrogen and COD [16] instead of being returned to bioflocculation unit is directed to partial nitritation reactor. Furthermore it was decided to narrow the scope of this work to removal of COD and nitrogen only. For this reason the scheme shown on Figure 2 is lacking phosphorus removal unit. Dynamic simulation of the integrated system shown on Figure 2 using the mechanistically inspired models is the objective of this work.

Modelling of the processes used for wastewater treatment

The importance of mathematical modelling of chemical, physical and biological processes cannot be overestimated. The question "Why Make Models?" was assessed among others by Bailey [17] who gave several reasons to justify the use of models in biochemical engineering. These reasons are also relevant in other fields of engineering and are the following:

- *To organize disparate information into a coherent whole,*
- *To think (and calculate) logically about what components and interactions are important in a complex system,*
- *To discover new strategies,*
- *To make important corrections in the conventional wisdom, and*
- *To understand the essential, qualitative features.*

There are in general two opposite but complementary approaches for model derivation [18]. The first approach is to build the empirical relationship from analysis and observations. Such approach is also known as black-box or input/output modelling, since in such approach model acts as a "machine" that transforms inputs into outputs using the defined relations [19]. Black-box models are relatively simple but the results obtained with these models are normally only valid for the conditions at which they were obtained, and extrapolation of the results should generally be avoided [18].

The other approach is to represent the reality based on the first principles – the fundamental laws of physics, chemistry and biology. The models derived based on this approach are called mechanistic or white-box models. The structure of such models is expected to be very complex but the behaviour of the modelled system can be predicted with high accuracy [18].

Apart from that, so called grey-box, hybrid or mechanistically inspired models can be distinguished. These models consist of some mechanistic and empirical model components, and are based on some insight about the process and the interpretation of experimental data. Grey-box models combine the advantages of both approaches: all the insight about the process builds up the white-box part, but the missing information is fitted with the black-boxes using the available experimental data [20].

In the work of Khiewwijit, 2013 (unpublished) black-box approach was used, while in this work grey-box modelling will be performed.

Improving model accuracy is usually associated with increasing its complexity. However, excessive complexity is unnecessary and should be avoided. The model should be compact and simple but adequate with respect to the purpose it is used for [21]. The main modelling purpose in this work is to predict the output of the integrated system shown on Figure 2 and to estimate the control values

that would ensure that the output of the system meets the standards of EU legislation. Thus excessive details refinement of individual system units can be omitted.

Standard models for the simulation of wastewater treatment processes

The first models that were able to simulate the behaviour of wastewater treatment systems appeared during the early seventies. The most noticeable models that appeared at that time were developed in the University of Cape Town, South Africa [22-24]. The models developed weren't widely used though due to the limitations in computer power and a complicated way in which these models were presented [25].

The situation changed after International Association on Water Pollution Research and Control (further first renamed to International Association on Water Quality and later to International Water Association – IWA) formed a Task Group. The aim of the Task Group was to create a model with the minimal complexity, which would serve as a base for future models of the activated sludge process [25]. Such model was developed in 1987, and it was called Activated Sludge Model No.1 (ASM1). The appearance of a standard model triggered the widespread use of simulation for wastewater treatment process control and optimization. One feature of ASM1, namely matrix notation (see Appendix D), appeared to be especially useful, since it significantly facilitated the interpretation of the model and the code writing.

The expansions/modifications of ASM1 soon followed which included phosphorus removal (ASM2 [26] and ASM2d [27]), and internal storage mechanism (ASM3 [28]). Nevertheless simple ASM1-based models are still widely used for the simulation of wastewater treatment processes.

High demand for a standard model that would be able to simulate anaerobic digestion process resulted in the appearance of Anaerobic Digestion Model No.1 (ADM1) [29], which was developed by IWA Anaerobic Digestion Modelling Task Group. ADM1 serves the same purposes as ASM-family models but is much more complex due to a large number of sequential and parallel steps taking place during the anaerobic digestion process.

Models used in this work are based on standard ASM1 and ADM1.

Model structure

The model is given by a number of differential equations which represent the macro balances for the species relevant to the process modelled. All the differential equations have the following structure:

$$\frac{d\xi}{dt} = D(\xi_{in} - \xi) + K \cdot r(\xi) \pm J(\xi) \qquad (1)$$

Where ξ is a vector that contains the state variables which are normally concentrations of species $\left[\frac{g}{m^3}\right]$; ξ_{in} is a vector that contains the inlet concentrations of species $\left[\frac{g}{m^3}\right]$; D is a dilution rate $\left[\frac{1}{d}\right]$ or a ratio between volumetric flow rate Q $\left[\frac{m^3}{d}\right]$ and the reactor volume V_r $[m^3]$; term $K \cdot r(\xi)$ represents the net reaction rates of the species considered in the model: K is a stoichiometric or rate equation matrix and $r(\xi)$ is a vector that contains the specific reaction rates $\left[\frac{g}{m^3 \cdot d}\right]$; term $J(\xi)$ is related to the mass transfer processes between different phases $\left[\frac{g}{m^3 \cdot d}\right]$.

ASM and ADM models provide K matrix and $r(\xi)$ vector to calculate the net reaction rate term. ADM1 additionally provides the information to calculate $J(\xi)$ term.

Apart from differential equations model can also contain algebraic equations as it is in case of ADM1. Microbalances sometimes can also be important for modelling especially in case if mass transfer between different phases needs to be considered, as it is in biofilm systems.

Integrated system modelling

While a large number of scientific papers are available on modelling of the individual processes [30-35], only a few papers concerning integrated or plant-wide modelling approach have been published [36-38]. Nevertheless importance of plant-wide modelling is acknowledged by the research community, since it allows a better understanding of the interactions between the different plant units, and consequently – finding better strategies for optimizing the plant performance [36]. When combining individual standard models into an integrated system a care must be taken to ensure that the resulting model is consistent in regard to elemental balances. This is not a simple task since the standard models, namely ASM and ADM1, use the state variables that are defined in a very different way, which makes these models incompatible. Since this work focuses on the plant-wide modelling the ways to overcome this incompatibility issue will be discussed here.

Terminology

Terminology used in this work was adapted from the paper of Carstensen et al [19]. The following terms are used particularly often:

- **State variable** – a variable that describes a mathematical "state" of a system. For example, concentrations of different species at any time during the experiment.
- **Constant** – quantity that never changes its value. For example, universal gas constant.
- **Parameter** – quantity which may have different values depending on the circumstances. For example, maximal growth rate of specific bacteria.

Apart from that, terms "control" and "disturbance" are often encountered in this work. These terms have a specific meaning:

- **Control** – system input quantity whose value can be regulated during the experiment. For example, sludge retention time.
- **Disturbance** – system input quantity whose value cannot be regulated during the experiment. For example, influent concentrations of different species.

2. Methodology

Modelling

Models with the basic structure of standard ASM [25] were used for the simulation of reactions taking place in the system. Standard ADM1 [29] was used for the simulation of anaerobic digestion.

Continuum biofilm model [39] was used to simulate mass transfer of species inside the granule in Anammox process.

ASM and ADM models use specific format and notation which allows showing large amount of information in a compact and easily understandable way. Appendix D provides an example taken form Henze et al [25] that explains format and notation used in the standard models.

Controls

In order to study the effect of changing conditions in individual reactors on the overall plant performance several controls/disturbances were chosen to be varied in a specific range. Concentration of slowly biodegradable (but unflocculated) COD in the system influent was chosen as the main disturbance. The controls selected are shown below:

Bioflocculation: Sludge retention time (SRT), overall mass transfer coefficient for oxygen ($K_{OL}a$)[2];

Anaerobic digestion: None

Partial nitritation: Sludge retention time (SRT), overall mass transfer coefficient for oxygen ($K_{OL}a$), temperature (T);

Anammox: None

It was decided to use the fixed values for controls in anaerobic digestion and Anammox to avoid obtaining hard interpretable results.

Software

Modelling of all the processes was performed in MATLAB simulation environment.

Stiff solver ODE15s was chosen to solve the sets of ordinary differential equations (ODEs) that describe each process. The choice of stiff solver can be justified because the time constants that characterize conversions of soluble and particulate species were found to differ significantly. As the result, the response times of these species to changes in the system are significantly different as well. Consequently the model describing such system becomes stiff, and the use of stiff solvers that use implicit integration methods is needed in order to decrease the computational time.

Biofilm model (Anammox process), which contains partial differential equations (PDEs) was solved using ODE solver for the integration over the time and finite difference method for the integration over space.

[2] $K_{OL}a$ cannot be controlled or measured directly. It can however be indirectly controlled by regulating the gas low rate in the reactor (see Appendix B). In this work for simplicity it is assumed that $K_{OL}a$ can be controlled.

3. Theoretical background

3.1. Bioflocculation

3.1.1. General information

Bioflocculation is the natural aggregation of colloidal particles and suspended solids mediated by microorganisms. Such aggregation is possible due to the excretion of extracellular polymeric substances (EPS) by microorganisms. EPS entraps colloidal and suspended species in aggregates (flocs) thus facilitating its settling [40].

Bioflocculation naturally happens during the activated sludge process and is regarded as important and desirable process, as it is necessary for:

- good settling and dewatering of sludge [41]; if this does not happen unsettled suspended and colloidal species including bacteria can end up in the effluent if gravity settler is used for solid-liquid separation, or clog the membrane pores if membrane process is used for this purpose;
- ensure that particulate biodegradable species are hydrolysed and converted into soluble biodegradable species, which can be removed from the systems by microorganisms: hydrolytic enyzmes accumulate in flocs and their concentration in bulk solution is negligible [42]. This implies that only flocculated biodegradable particulates can be hydrolysed. Hydrolysis, in turn, is necessary to cleave the large molecules into smaller ones. Only small molecules can pass through the cell membranes and are readily available for microorganisms to utilize.

In this paper bioflocculation is not only regarded as a **stage** of conventional activated sludge (CAS) systems, but also as a separate **process** during which wastewater pre-treatment for Anaerobic Digestion (AD) is carried out. In this process flocculation of suspended and colloidal species is promoted but the further conversions of particulate species (such as hydrolysis, substrate utilization by the microorganisms for growth and energy production) are avoided. More specifically the objectives of bioflocculation are the following:

- Capture COD for AD without allowing it to be degraded aerobically. Anaerobic digestion is characterized by less energy consumption and less sludge production than conventional aerobic treatment, also known as CAS. Therefore AD process is considered more sustainable compared to CAS [5]; see “Anaerobic Digestion” section for comparison of two wastewater treatment methods;
- Concentrate COD for AD process, because AD is more efficient for high strength wastewaters [43];
- Ensure that the concentrated COD is mainly flocculated. Colloidal and suspended species despite being partially biodegradable are poorly removed in AD process, compared to the aerobic systems, unless pre-treatment is used [44].

These objectives can be achieved if the bioflocculation process is operated at short SRT and HRT. The short SRT is necessary to prevent excessive biomass growth and associated COD mineralisation. The short HRT is needed to achieve high COD concentration in the effluent [4, 45].

Despite bioflocculation has not yet been widely recognized as a pre-treatment step for AD, the results of experiments conducted by Akanyeti et al [45] and Hernández Leal et al [4] suggest that the integration of bioflocculation and AD process seems very promising for enhancing the methane production from municipal wastewater.

3.1.2. Process Configuration

Bioflocculation is not yet an established technology for wastewater pre-treatment for AD, so only limited information is available for the reactor configurations that are suitable for this process. So far mostly lab-scale experiments with bioflocculation were conducted, and in these experiments the process took place in Membrane Bioreactor (MBR).

According to Ng and Hermanowicz [46], MBR seems a good choice as in a process operated at such extremely short HRT and SRT as necessary for bioflocculation, for example 1.2 – 6 hour for HRT and 0.2 – 5 days for SRT [4, 45, 46], inevitably not all the colloidal and suspended species would be flocculated. These unflocculated species settle poorly, meaning that they would end up in the effluent unless retained by the membrane with pore openings smaller than dimensions of suspended and colloidal particles.

For this reason MBR was chosen to model bioflocculation process in this work. Additional benefit of choosing MBR is a smaller footprint due to the possibility to operate the process at higher solids concentration and carry out several process steps in one reactor.

3.1.3. Process Microbiology and physicochemical conversions

Since bioflocculation naturally takes place in CAS systems, for modelling purposes microbial interactions similar to those in CAS would need to be considered.

Schematically the stages of bioflocculation process are shown on a figure below:

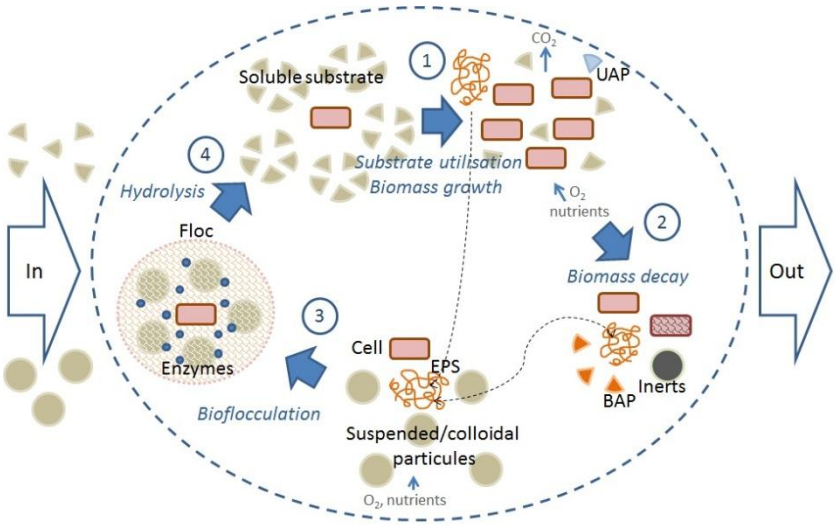

Figure 3. Schematic representation of bioflocculation.

EPS play a major role in bioflocculation. EPS are composed mainly of proteins and carbohydrate, at a smaller extent – of humic substances and nucleic acids which are produced during the biomass growth and excreted in the bulk. These compounds form a matrix that entraps different species present in the system, which results in the formation of large well settleable flocs [3]. Enzymes which are necessary for hydrolysis of particulates accumulate in flocs. Therefore, only flocculated particulates can be hydrolysed [42].

Despite the importance of EPS these compounds are normally not considered in the standard ASM models that were developed for conventional activated sludge process. However with the growing popularity of MBR new models were also developed (SMP and ASM-SMP models) that take into account formation of EPS as well as Soluble Microbial Products (SMP). In MBR these compounds can no longer be neglected as they accumulate in the reactor and may impact the microbial paths which would affect the effluent quality [47]. Apart from that, they were also reported to contribute greatly to membrane fouling [48].

In these models SMP are usually subdivided into Utilisation Associated Products (UAP) and Biomass Associated Products (BAP). UAP represent "SMP that are associated with substrate metabolism and biomass growth and are produced at a rate proportional to the rate of substrate utilisation". BAP represent "SMP that are associated with biomass decay and are produced at a rate proportional to the concentration of biomass" [49, 50].

Unmodified ASM models can also be used to simulate processes in MBR, although parameter recalibration would be required. Due to the specific conditions in MBR, e.g. smaller size of flocs and associated with that lower mass transfer resistances, many parameter values are quite different than those in CAS systems [47].

Nevertheless, neither standard ASM nor ASM-SMP models are suitable for simulation of bioflocculation process, as none of these models considers flocculation of suspended and colloidal species as a separate step. Instead suspended, colloidal and flocculated species are lumped in one state X_s and considered flocculated, meaning that flocculation is assumed instantaneous. Such assumption can be justified for CAS systems that operate at relatively long SRT and HRT, but it is not suitable for bioflocculation. Apart from that differentiation between flocculated and unflocculated species is clearly needed.

The only model where the differentiation between flocculated and unflocculated species is considered is the model of Dold et al [24]. This model is based on a dynamic model proposed in 1979 by Ekama and Marais [23] where the modified expression of Blackwell [51] is used to describe particle adsorption on the activated sludge floc. In the final form the adsorption/flocculation term in this model was expressed as:

$$\frac{dS_{bp}}{dt} = -K_a S_{bp} X_a \left(f_{ma} - \frac{X_s}{X_a}\right) \quad (2)$$

Where S_{bp} - concentration of slowly biodegradable particulate COD (unflocculated!) $\left[\frac{gCOD}{m^3}\right]$, X_s – concentration of adsorbed particulate COD (flocculated) $\left[\frac{gCOD}{m^3}\right]$, X_a – active biomass concentration

$\left[\frac{gCOD}{m^3}\right]$, K_a – slowly biodegradably COD adsorption rate $\left[\frac{m^3}{gCOD \cdot d}\right]$, f_{ma} – maximal number of adsorption sites for slowly biodegradable COD $\left[\frac{gCOD}{gCOD}\right]$.

Model of Dold et al [24] (and its further modifications), however, didn't considered the formation of EPS. Moreover, the model was calibrated for the activated sludge system, so it might not be very accurate for the simulation of bioflocculation.

In **ideal** model for bioflocculation the following species would need to be considered:

Particulate **Biomass:** heterotrophs (X_H), autotrophs (X_A);

Non-biomass: unflocculated biodegradable particulate COD (X_{un}), flocculated biodegradable particulate COD (X_s), EPS (X_{EPS}), inert particulate species (X_I), (inner cell storage (X_{STO}), only for ASM3 based models);

Soluble Dissolved oxygen (S_O), soluble biodegradable COD (S_s), ammonia species (S_{NH}), nitrate species (S_{NO}), SMP: UAP (S_{UAP}) and BAP (S_{BAP}), inert soluble species (S_I) (optionally dinitrogen (S_{N2}) and alkalinity as bicarbonate (S_{HCO})).

Although at present no model for bioflocculation has been published, a structure of ASM-SMP model can be used for such model with additional state for unflocculated slowly biodegradable COD and additional process of bioflocculation which would precede hydrolysis, as suggested by Dold et al [24].

It is clear that such model would have rather complex structure. Therefore, considering that the bioflocculation process has not yet been simulated, a more reasonable approach might be to start with simpler models that can be easily calibrated, and then proceed with the more complex and more accurate ones. A simple ASM1, which doesn't consider formation of EPS and SMP but is expanded for bioflocculation according to Dold et al [24], seems to be a good starting point.

In the model used in this work the following species are considered:

Particulate **Biomass:** heterotrophs (X_H), autotrophs (X_A);
Non-biomass: unflocculated biodegradable particulate COD (X_{un} – the same as S_{bp} in a work of Dold et al [24]), flocculated biodegradable particulate COD (X_s), particulate organic nitrogen (X_{ND}), inert particulate species (X_I);

Soluble Dissolved oxygen (S_O), soluble biodegradable COD (S_s), ammonia species (S_{NH}), nitrate species (S_{NO}), soluble organic nitrogen (S_{ND}), inert soluble species (S_I).

Influent in the system described by such model would consist of colloidal/suspended biodegradable COD X_{un} (not X_s), soluble biodegradable COD S_s, ammonia species S_{NH}, soluble inerts S_I and particulate inerts X_I. S_s can be directly utilised by heterotrophs X_H for growth, which results in increasing the amount of X_H, and energy generation, which results in production of CO_2. Particulate species X_{un} cannot be directly used as substrates for bacteria. Therefore, they first need to be adsorbed on the flocs (results in formation of X_s) and then hydrolysed (results in formation of S_s). Both flocculation and hydrolysis are mediated by microorganisms. Thus, both of these processes depend on the concentration of active bacteria in the system. For the growth of bacteria, not only the source of carbon (S_s in case of heterotrophs) but also oxygen S_O and nutrients S_{NH} should be

present in the system. Ammonia apart from being metabolised can also be used as an energy source by autotrophic bacteria X_A that oxidise it into nitrite S_{NO}. Both heterotrophs and autotrophs decay with the formation of X_s and inerts X_I, as well as release of particulate organic nitrogen X_{ND}. X_{ND} can be hydrolysed to soluble organic nitrogen S_{ND}, which is further converted into ammonia species in a process of ammonification.

Processes described above normally happen in the activated sludge systems. Obviously not all of these processes are desirable for bioflocculation. Several control handles are available to suppress the undesirable conversions. These control handles are SRT, SRT/HRT and the concentration of dissolved oxygen (DO).

SRT. SRT within the range from 0.2 – 5 days affects:

- the extent of the bioflocculation step: at lower SRT less particulates are flocculated;
- the nature of flocs formed: Ng and Hermanowicz [46] reported that at SRT = 5 days filamentous organisms were found in MBR, at SRT = 0.5 days – flocs formed were small and weak, while at SRT = 0.25 days – dispersed microorganisms were observed in the reactor;
- the extent of substrate utilisation: at lower SRT less substrate can be utilised, and below a threshold value (SRT_{min} – depends on the maximal growth rate of the microorganism) no substrate can be utilised at all and the microorganism is washed out from the reactor. In the experiment of Ng and Hermanowicz [46] nitrification completely ceased at SRT below 2.5 days;

SRT/HRT. Akanyeti et al [45] reported that in a system, where all particulates are retained by the membrane and no COD is mineralised, the concentration factor form sewage to concentrate is equal to the SRT/HRT ratio.

DO. Oxygen is an electron donor for both heterotrophs and autotrophs. At low concentration it can become a rate limiting substrate that would determine the microbial activity.

3.1.4. Model development

As it has already been mentioned, at the moment there is no model that would be able to accurately describe bioflocculation process. Desirable features of such model however can be defined:

- Flocculated and unflocculated particulate COD are modelled as two separate variables: X_s and X_{un};
- Additional process for bioflocculation during which X_{un} is converted into X_s at a rate proportional to the amount of X_{un} and the concentration of active biomass or EPS;
- Production and utilisation of EPS and SMP is considered (not considered in this work).

In this work the structure of ASM1 was chosen as a base. The set of parameter values calibrated for MBR was selected [52]. The model was expanded for an additional state - unflocculated slowly

biodegradable COD X_{un}, and additional process – bioflocculation (see Appendix E)[3]. The model is implemented for MBR. The basic scheme of the MBR system is shown on Figure 4.

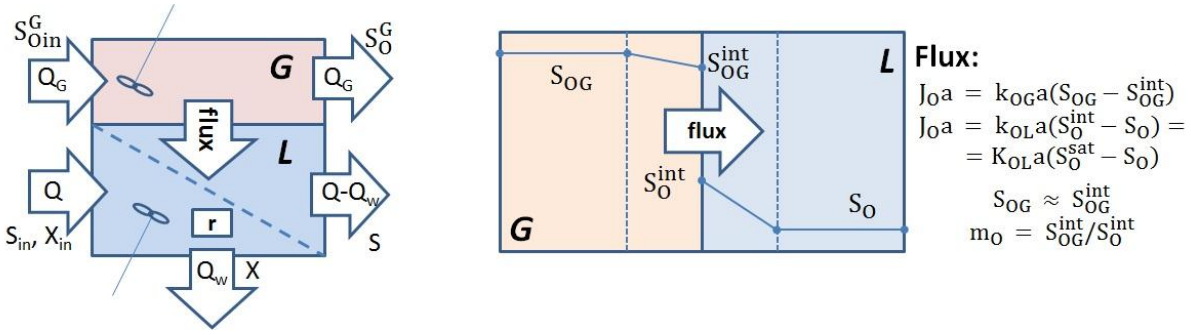

Figure 4. Bioflocculation in MBR.

In this work the model is used to attempt to simulate bioflocculaiton process. However it might also be used as a starting point for developing a model aimed at predicting the membrane fouling, because fouling was reported to depend among other on flocculation rate, shear stress, floc density and resistance to shear [53].

Assumptions

- "Liquid" volume of MBR consists of two ideally mixed compartments at equilibrium;
- Suspended growth assumed for biomass;
- All the particulates are retained by the membrane;
- Soluble species (apart from UAP and BAP) are not retained by the membrane;
- Reactions only take place in the liquid phase;
- pH is optimal;
- Nitrification is a one-step process (ammonia is oxidized directly to nitrate);
- Inhibition is negligible;
- Oxygen transfer: mass transfer resistance of the gas phase is negligible;
- Saturation concentration of oxygen (S_O^{sat}) is assumed to be only a function of temperature (see Appendix C), but the concentration of oxygen in the reactor is regulated by **overall** volumetric mass transfer coefficient of oxygen in the liquid phase (K_{OL} or $K_{OL}a$) so that $K_{OL}a(S_O^{sat} - S_O) = k_{OL}a\left(\frac{S_O^{int}}{m_O} - S_O\right)$, where S_O^{int} – is a concentration of oxygen on a gas-liquid interface.

Net reaction rates

Reaction rate for net production of specie i is calculated by multiplying the stoichiometric coefficients from column that characterizes specie i in Peterson matrix (see Appendix D) by the respective specific reaction rate expression. Reaction rates that characterize each process taking place during bioflocculation process are also given in Appendix E.

[3] Adding a state and a process would normally require recalibrating the model using the experimental data. But since experimental part is outside the scope of the present work all the parameter values from literature were adapted without changes.

Mass balances

Due to the retention mass balances for soluble species, SMP (UAP and BAP) and particulates are different.

Particulates are retained by the membrane. In general case only a fraction of particulates is retained. Therefore they would be present in both reactor compartments, so mass balance for each compartment should be written. If f is the fraction of particulates retained by the membrane then it's possible to write:

$$\textbf{Particulates}: \begin{matrix} 1st\ compartment: & \frac{dX_{i,w}}{dt} = \frac{Q}{V_r}X_{i,in} - \frac{Q_w}{V_r}X_{i,w} - f\frac{Q-Q_w}{V_r}X_{i,w} + r_{Xi,w} \\ 2nd\ compartment: & \frac{dX_{i,e}}{dt} = f\frac{Q-Q_w}{V_r}X_{i,w} - \frac{Q-Q_w}{V_r}X_{i,e} + r_{Xi,e} \end{matrix} \quad (3)$$

Where Q is the influent flow rate $\left[\frac{m^3}{d}\right]$, Q_w is the retentate flow rate $\left[\frac{m^3}{d}\right]$, V_r is the (liquid) reactor volume $[m^3]$, X_i is the concentration of particulate specie i $\left[\frac{gCOD}{m^3}\right]$, r_{X_i} is the net production rate of particulate specie i $\left[\frac{gCOD}{m^3 d}\right]$. Index w denotes retentate, and index e denotes effluent.

The complete retention of particulates by the membrane was assumed ($f = 0$), meaning that there cannot be any particulates in the second compartment ($X_{i,e} = 0$). Thus, there can also be no conversion in this compartment ($r_{Xi,e} = r_{Xi,e}(X_{i,e}) = 0$). In this case, the system is reduced to one balance:

$$\textbf{Particulates}: \quad \frac{dX_{i,w}}{dt} = \frac{Q}{V_r}X_{i,in} - \frac{Q_w}{V_r}X_{i,w} + r_{Xi,w} \quad (4)$$

Soluble species are not retained by the membrane so one mass balance for the whole reactor can be written for those:

$$\textbf{Soluble}: \quad \frac{dS_i}{dt} = \frac{Q}{V_r}S_{i,in} - \frac{Q_w}{V_r}S_i - \frac{Q-Q_w}{V_r}S_i + r_{Si} = \frac{Q}{V_r}S_{i,in} - \frac{Q}{V_r}S_i + r_{Si} \quad (5)$$

Where S_i is the concentration of soluble specie i $\left[\frac{g}{m^3}\right]$, r_{S_i} is the net production rate of soluble specie i $\left[\frac{g}{m^3 d}\right]$.

Oxygen balance differs from the balances for other soluble species since it is transferred from the gas phase:

$$\textbf{Oxygen}: \quad \frac{dS_O}{dt} = K_{OL}a(S_O^{sat} - S_O) - \frac{Q}{V_r}S_O + r_O \quad (6)$$

Where S_O is the concentration of dissolved oxygen $\left[\frac{gO_2}{m^3}\right]$, $K_{OL}a(S_O^{sat} - S_O) = k_{OL}a\left(\frac{S_O^{int}}{m_O} - S_O\right)$ is the term that describes oxygen flux from gas to liquid phase $\left[\frac{g}{m^3 d}\right]$.

Net reaction rates of different species r_{Si}, r_{Xi}, r_O can be found from Peterson Matrix $\left[\frac{g}{m^3 d}\right]$ (see Appendix E).

3.2. Anaerobic digestion

3.2.1. General information

Anaerobic digestion (AD) is a biological process, in which complex organic matter is converted to methane, some simple compounds and microbial biomass in the absence of oxygen or other external electron acceptor [54, 55]. The conversion is a multistep process. It starts with disintegration of cell with the release of complex organic molecules, followed by hydrolysis of these molecules into monomers. The monomers are then fermented into variety of acids, CO_2 and H_2. Next step is acetogenesis – production of acetate. The final step is methanogenesis. During this step methane is produced from acetate, as well as from CO_2 and H_2. Two main desirable outcomes of AD are production of methane as a renewable energy source, and reduction of the amount of solids and formation of digestate, which can be used as a fertilizer and soil conditioner.

AD is applied mainly to treat the following types of wastes: 1) municipal wastewater, 2) industrial wastewater, 3) organic slurries (e.g., animal manure and sewage sludge) and 4) municipal solid wastes [56]. Different types of wastes are treated differently; however co-digestion of several types of wastes has also obtained much attention in recent years. The reason for this increasing popularity is higher overall process efficiency that was reported for co-digesting different types of wastes. Such synergistic effect can be explained, for example, by obtaining an optimal C/N ratio for AD process [57].

This method is rather old [6, 58] but not outdated. In fact, anaerobic digestion is a viable alternative to conventional aerobic activated sludge process due to several advantages summarized, e.g., by Aiyuk et al [5]. These advantages can be classified into:

- Energy related (unlike aerobic treatment, AD is a net energy producing process);
- Environmental (due to lower growth rates of anaerobic microorganisms sludge production during AD is significantly lower; excess sludge is well stabilized; the incidence of pathogens can be decreased during AD, etc.);
- Economic and others (obtainable at very low costs; can be applied at any place at any scale; much smaller footprint; possibility to organize the process produce to alternative added value products, etc.).

However, AD process has several disadvantages which should also be mentioned [55]:

- Long process start-up (a trade-off for low sludge production – also a consequence of slow anaerobic microorganisms' growth rates);
- High sensitivity of AD microorganisms to several factors, such as overloads, inhibition (e.g. pH, free ammonia and long chain fatty acids inhibition) and other disturbances;
- Lack of complete understanding of all the complex processes involved in anaerobic digestion.

Nevertheless, the interest towards AD is high, especially for its implementation in the integrated systems where AD is combined with other treatment methods.

3.2.2. Process Configuration

Reactor configuration depends majorly on a type of influent to be treated.

There are three main reactor configurations that are currently used for anaerobic digestion of **solid wastes** [7]:

- Sequenching batch reactors (SBR) – reactors are periodically filled and emptied;
- One-stage continuously fed systems – all conversions take place in one reactor;
- Two-stage (or multistage) continuously fed systems – hydrolysis/acidogenesis and acetogenesis/methanogenesis take place in different reactors. The optimal conditions can be provided for each stage. Besides, a more sensitive methanogens can be buffered by the first stage, which results in a whole process becoming more stable.

Reactor configurations that are used for anaerobic digestion of **wastewater** were summarized by Aiyuk et al [5]:

- Continuous stirred tank reactor (CSTR) and anaerobic contact process – hydraulic retentions time (HRT) of about 20 days, suitable for high-strength wastes (COD is higher than 2gCOD/L), not suitable for high flow rates;
- Fixed film or anaerobic filter (AF) reactor – biomass growth on support ensures good retention. HRT can be varied from few hours to days, and organic loading rate (OLR) 0.4-27 kg/m^3/d;
- Upflow anaerobic sludge blanket (UASB) – operated at low upflow velocities – 1-2 m/h, solid-liquid-gas separator, rising gas bubbles provide mixing, sludge usually forms granules, suitable for concentrated and dilute wastes;
- Expanded granular sludge bed (EGSB) – modification of UASB, operated higher upflow velocities (6-15 m/h), more suitable for low temperature and diluted wastewaters;
- Internal circulation (IC) reactor – high upflow velocities (20-30 m/h), two compartments, rising bubbles passing through separators generate gas lift and ensure circulation.
- Anaerobic baffled reactor (ABR) – compartmentalized - acidogens and methanogens separated in space, good biomass retention and granulation is possible, OLR up till 36 kg/m^3/d.

In this work reactor is assumed to be a CSTR. This configuration was chosen mainly because of the modelling simplicity.

3.2.3. Process Microbiology and physicochemical conversions

Anaerobic digestion is a complex process which consists of a number of sequential and parallel steps. During these steps microbiological and physicochemical conversions take place. Physicochemical conversions that occur during AD process are acid/base equilibria, mass transfer from liquid to gas and solids precipitation.

Microbiological conversions alone are quite complex and are performed by the large community of different microorganisms that interact with each other in a complex manner. Influent of the AD

reactor often contains large fraction of large polymeric compounds. Such compounds cannot penetrate the cell wall of microorganisms and should be first hydrolysed into smaller soluble species. **Hydrolysis** step is performed extracellulary and is catalysed by the enzymes released by the living cells. During hydrolysis proteins, lipids and carbohydrates are converted into amino acids, long chain fatty acids and sugars, respectively. These soluble compounds are converted by two groups of **acidogens** into a variety of volatile fatty acids (VFAs), CO_2 and H_2. Alcohols and amines are also produced during this step. VFAs are the substrates for **acetogens** that produce acetate, CO_2 and H_2. And the latter ones are the substrates for **methanogens** that produce methane. There are two types of methanogenic microorganisms that can be encountered in AD reactor: acetoclastic and hydrogenophilic methanogens. The acetoclastic methanogens utilize acetate to produce CH_4 and CO_2, which is known as heterotrophic methanogenesis. The hydrogenophilic methanogens utilize CO_2 and H_2 to produce CH_4, which is known as autotrophic methanogenesis [59].

The chemical compounds present in the system do not only act as substrates or products for microorganisms, but can also be inhibitors for specific processes. Inhibiting effects of LCFAs, hydrogen, sulphide and free ammonia on anaerobic community are well known (see below) [60]. Sensitivity of the anaerobic microorganisms to the presence of toxic compounds as well as to conditions (pH, temperature) along with the lack of complete understanding of the processes inside AD reactor can cause poor performance of the reactor. Modelling can be a very useful tool to prevent the unfavourable conditions.

The first AD models appeared in 1960's (see the review of Lauwers et al [61]). These early models were rather rough and only took into account few processes. As the understanding of the process improved the complexity and accuracy of the models increased as well. A wide variety of AD models that appeared during 60's – 90's wasn't however used widely by practitioners, possibly because of their large number and a very specific nature. Thus, in 2002 the 'IWA Task Group on Mathematical Modelling of Anaerobic Digestion Process' has published the Anaerobic Digestion Model No.1 (ADM1) as a unified base for modelling of anaerobic digestion [29]. The model compiles the knowledge on AD. The conversions that are accounted for in this model are shown on Figure 5.

In ADM1 the following species are accounted for:

Particulate	**Biomass:** sugar degraders (X_{su}), amino acid degraders (X_{aa}), LCFA degraders (X_{fa}), valerate and butyrate degraders (X_{c4}), propionate degraders (X_{pro}), acetate degraders (X_{ac}), hydrogen degraders (X_{h2}). **Non-biomass:** composites (X_c), carbohydrates (X_{ch}), proteins (X_{pr}), lipids (X_{li}), particulate inerts (X_I).
Soluble	Sugars (S_{su}), amino acids (S_{aa}), LCFA (S_{fa}), total valerate (S_{va}), total butyrate (S_{bu}), total propionate (S_{pro}), total acetate (S_{ac}), hydrogen (S_{h2}), methane (S_{ch4}), inorganic carbon (S_{IC}), inorganic nitrogen (S_{IN}), soluble inerts (S_I).

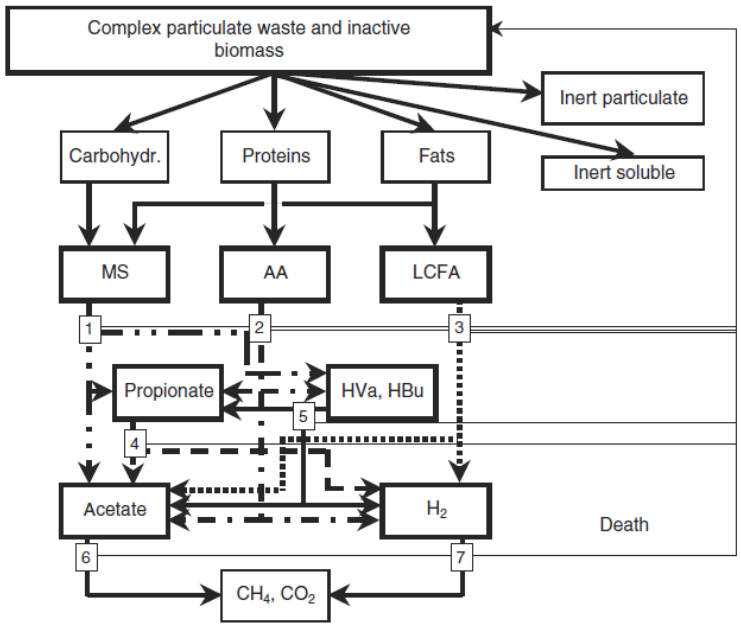

Figure 5. Conversions during AD process according to ADM1 (taken from Batstone et al [29]).

It can be seen from Figure 5 that in ADM1 **disintegration** process is added mainly to facilitate modelling of activated sludge digestion. Disintegration step simulates combined effect of such processes as lysis, non-enzymatic decay, phase separation and physical breakdown [29]. During disintegration complex particulate waste breaks down to carbohydrates, proteins, LCFA, as well as particulate and soluble inerts. Disintegration follows by hydrolysis, acidogenesis, acetogenesis and methanogenesis. These processes are modelled according to the description above with some simplifications. For example, the only outcome of acidogenesis step is conversion of carbohydrate, proteins and LCFA into propionate, butyrate, valerate, H_2 and CO_2. Production of alcohols and other acids is neglected. Only some inhibition mechanisms are considered (see below).

As any biological process AD is affected by the environmental conditions. The effects of these conditions on the process are described as followed:

Temperature. AD process is normally operated either in mesophilic (30-37^{o}C) or thermophilic (50-58^{o}C) mode. Under these two modes different microbial communities will develop. When operated in thermophilic mode, the processes energy consumption is increased due to the necessity to provide higher temperature. This, however, is compensated by the increased gas production yield and rate [62]. The effect of temperature on biological process is traditionally simulated with the exponential term [29], despite it cannot describe the system at temperature above an optimal range for each mode.

Temperature influences also physicochemical processes relevant to AD, such as gas solubility. The dependence of Henry's constant (characterizes gas solubility) as given by Rosen and Jeppsson [63] has the following form:

$$H_i(T) = H_i(T_{ref}) \exp\left(C_i\left(\frac{1}{T_{ref}} - \frac{1}{T}\right)\right) \quad (7)$$

Where $H_i(T)$ is Henry's constant of specie i at temperature T $\left[\frac{M}{bar}\right]$; $H_i(T_{ref})$ is Henry's constant of specie i at the reference temperature T_{ref} $\left[\frac{M}{bar}\right]$; C_i is a constant that characterizes specie i.

Temperature dependency of acid dissociation constants $K_{a,i}$ has similar form:

$$K_{a,i}(T) = K_{a,i}(T_{ref}) \exp\left(C_i\left(\frac{1}{T_{ref}} - \frac{1}{T}\right)\right) \quad (8)$$

Where $K_{a,i}(T)$ is acid dissociation constant of specie i at temperature T $\left[\frac{M}{bar}\right]$; $K_{a,i}(T_{ref})$ is acid dissociation constant of specie i at the reference temperature T_{ref} $\left[\frac{M}{bar}\right]$; C_i is a constant that characterizes specie i.

pH. The effect of pH on AD process is associated with activation/deactivation of microorganisms as well as with influencing acid/base equilibria of chemical species. Some forms of these species have inhibiting effect on AD microorganisms, while other don't. For example, free ammonia inhibits the process while ammonium ion does not. Maximal growth rates of different microorganisms in the AD reactor can be observed at different pH. For example, it was reported that for two-stage configuration pH in the first stage (hydrolysis and acidogenesis) stabilizes around 5.7-6.0 without any regulation, while in the second stage (acetogenesis and methanogenesis) – around 7.2-7.7 at mesophilic conditions [64]. There are different ways of simulating the effect of pH on the system. In the standard ADM1 [29] the following empirical function is given:

$$I_{pH,i} = \frac{1+2\cdot 10^{0.5\left(pH_{LL,i}-pH_{UL,i}\right)}}{1+10^{pH-pH_{UL,i}}+10^{pH_{LL,i}-pH}} \quad (9)$$

Where $pH_{UL,i}$ and $pH_{LL,i}$ are the upper and lower pH limits where 50% inhibition of the group of organisms i is observed. Other functions that describe pH inhibition are also available, but the expression above was chosen for AD modelling in this work.

Inhibition. Anaerobic microorganisms are very sensitive to the presence of specific chemical species. A detailed review on inhibition of AD was made by Chen et al [60]. In the review the inhibitory effects of the following species are discussed:

- **Ammonia.** Ammonia is an important nutrient for all living cells but its non-ionized form, free ammonia (FA), is a common inhibitor for many microorganisms. The inhibitory effect of ammonia is especially strong on methanogens [65]. Concentration of free ammonia depends on the concentration of total ammonia nitrogen, pH, temperature, presence of other ions and acclimation of microorganisms. Inhibition of ammonia is simulated by including a non-competitive inhibition term $I_{nh3} = \frac{K_{I,nh3}}{S_{nh3}+K_{I,nh3}}$ [29]. The nutrient limitation of total inorganic nitrogen is simulated with the substrate limitation term $I_{IN,lim} = \frac{S_{IN}}{S_{IN}+K_{S,IN}}$ [29].
- **Sulphate-sulphide**. Sulphate serves as an electron acceptor of sulphate reducing bacteria (SRB), which use the same C-source for growth as heterotrophic methanogens (and some other anaerobic microorganisms). If concentration of sulphate is sufficiently high,

suppression of methanogenesis is likely to occur, because SRB can outcompete methanogens as well as because they produce sulphide – compound that is toxic to many microorganisms.

- **Light metals.** At low concentrations light metal ions serve as micronutrients for microorganisms and are stimulate their growth. At high concentrations the effect is opposite: high osmotic pressure caused by high salinity results in cells' dehydration [66]. The effect of sodium inhibition is studied the best. This effect can be simulated by including a non-competitive inhibition term $I_{Na^+} = \frac{K_{I,Na^+}}{S_{Na^+}+K_{I,Na^+}}$ [67].
- **Heavy metals.** Toxicity of heavy metals for living cells is well known. Heavy metals bind to the functional groups of enzymes, which results in disrupting function and structure of these enzymes [68].
- **LCFA.** LCFA are the intermediate specie during the AD process. Accumulating of LCFA was reported to have inhibitory effect on AD [69]. Simulating the inhibiting effect of LCFA was done, e.g., by Zonta et al [70].
- **H_2.** Hydrogen inhibits the degradation of fatty acids and alcohols during anaerobic digestion [71]. Non-competitive inhibition term $I_{h2,i} = \frac{K_{I,h2,i}}{S_{h2}+K_{I,h2,i}}$ is included in the model to account for the inhibiting effect of hydrogen on specie i.

SRT. The effect of SRT on AD was studied among others by Miron et al [72]. The study showed that for anaerobic digestion of primary sludge at 25°C in a CSTR-type digester at SRT below 8 days acidogenic conditions would form which would result in very low gas production, while at SRT above 8 days methanogenic conditions would occur. The extent of hydrolysis was also found to be a function of SRT.

C/N. As it was mentioned, despite nitrogen is an important nutrient for all living cells, high concentrations of free ammonia species inhibit many biological processes. For this reason optimal C/N ratio should be maintained in the system to avoid its failure. The optimal C/N ratio for AD is in the range from 15/1 to 30/1 [73].

In order to avoid making the standard model overly complex and thus impractical, some processes/effects that occur during AD were neglected in ADM1. These were summarized by Blumenstaat and Keller [33] and are shown below:

- Production of lactate from glucose fermentation;
- Sulphate reduction and sulphide inhibition;
- Nitrate reduction;
- LCFA inhibition;
- Competitive uptake of H_2 and CO_2 between hydrogenotrophic methanogenic archaea and homoacetogenic bacteria;
- Solids precipitation due to high alkalinity or other chemical precipitation reactions.

3.2.4. Model development

Standard Anaerobic Digestion Model No.1 [29] developed by the 'IWA Task Group on Mathematical Modelling of Anaerobic Digestion Process' has been chosen in this work. Parameter values were

corrected according to Rosen and Jeppsson [63]. The model is implemented for CSTR. The basic scheme of the system is shown on Figure 6.

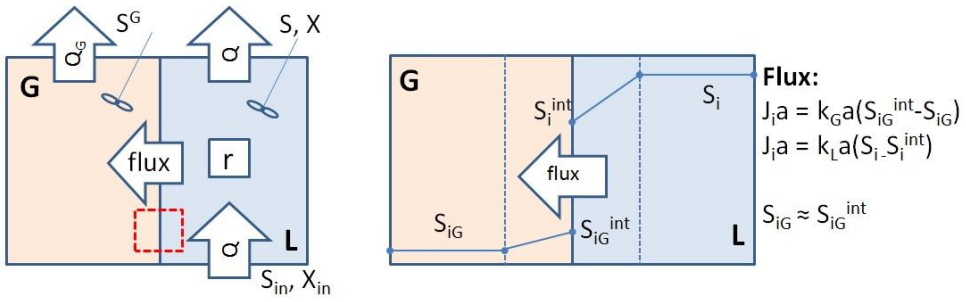

Figure 6. Anaerobic Digestion process scheme.

Assumptions

- All the particulate species are suspended (no aggregate formation); as a consequence mass transfer limitations due to biomass aggregate formation (a common phenomenon in digesters) are neglected – the effects of mass transfer are "accounted for" in the kinetic parameters used in the model which are in fact lumped. This is done to avoid model over-parameterisation which would make it impractical;
- Gas and liquid phases are completely mixed;
- Reactions take part only in the liquid phase;
- Association/dissociation processes are much quicker than the microbial conversions (see Asid/Base equilibria);
- CH_4, CO_2 and H_2 transfer form liquid to gas phase is much quicker than the microbial conversions;
- Inhibition only by free ammonia and hydrogen as well as due to pH and nutrient (nitrogen) limitation;

Acid/Base equilibira

ADM1 provides the expressions that allow calculating the concentrations of ionized/ unionized form of states either from algebraic or from differential equations. The algebraic equations are used if association/dissociation processes are assumed instantaneous. In case if differential equations are chosen to describe association/dissociation reactions, extra states need to be added to the system to account for both acid and base form of species. Apart from that, the system becomes very stiff as the reaction rates of acid/base conversions are much faster than those related to microbial conversions. In this work concentrations of acid and base forms of some compounds are calculated from algebraic equations meaning that these forms are assumed to be at equilibrium.

For an equilibrium reaction:

$$HA \rightleftarrows H^+ + A^-$$

The following expression can be used to find S_{A^-}:

$$S_{A^-} = \frac{S_A^{TOT}}{1+\frac{S_{H^+}}{K_{a,A}}} \quad (10)$$

Where HA is the acid form of a specie (CO_2, HAc, HPro, HBu, HVa and NH_4^+), A^- - base form of a specie (HCO_3^-, Ac^-, Pro^-, Bu^-, Va^- and NH_3), S_A^{TOT} – total concentration of both acid and base forms ($S_A^{TOT} = S_{HA} + S_{A^-}$), $K_{a,A}$ – acid dissociation constant of A, $S_{H^+} = 10^{-pH}$.

Inhibition

All the processes associated with microorganisms' growth are affected by inhibition as followed:

- Uptake of sugars – by inhibition due to pH and total N limitation ($I_5 = I_{pH,aa} \cdot I_{IN,lim}$);
- Uptake of amino acids – by inhibition due to pH and N limitation ($I_6 = I_{pH,aa} \cdot I_{IN,lim}$);
- Uptake of LCFA – by inhibition due to pH, N limitation and hydrogen ($I_7 = I_{pH,aa} \cdot I_{IN,lim} \cdot I_{h2,fa}$);
- Uptake of valerate – by inhibition due to pH, N limitation and hydrogen ($I_8 = I_{pH,aa} \cdot I_{IN,lim} \cdot I_{h2,c4}$);
- Uptake of butyrate – by inhibition due to pH, N limitation and hydrogen ($I_9 = I_{pH,aa} \cdot I_{IN,lim} \cdot I_{h2,c4}$);
- Uptake of propionate – by inhibition due to pH, N limitation and hydrogen ($I_{10} = I_{pH,aa} \cdot I_{IN,lim} \cdot I_{h2,pro}$);
- Uptake of acetate – by inhibition due to pH, N limitation and free ammonia ($I_{11} = I_{pH,ac} \cdot I_{IN,lim} \cdot I_{nh3}$);
- Uptake of hydrogen – by inhibition due to pH and N limitation ($I_{12} = I_{pH,h2} \cdot I_{IN,lim}$).

These inhibition terms are included in the expressions for specific (and net reaction rates) given in Appendix F.

Net reaction rates

Reaction rate for net production of specie i is calculated by multiplying the stoichiometric coefficients from column that characterizes specie i in Peterson matrix by the respective specific reaction rate expression. Reaction rates that characterize each process taking place in AD system are also given in Appendix F.

Mass balances

Particulate, soluble and gaseous species behave differently in the system. Differential equations that describe these species are given below.

Particulate. Mass balance for each particulate specie i is given by equation:

$$\frac{dX_i}{dt} = \frac{Q}{V_L}\left(X_{i,in} - X_i\right) + r_{Xi} \tag{11}$$

Where Q is a flow rate of the liquid phase $[m^3/d]$; V_L is volume of the liquid phase $[m^3]$; $X_{i,in}$ is input concentration of specie i $[kgCOD/m^3]$; X_i is concentration of specie i in the reactor $[kgCOD/m^3]$; r_{Xi} is reaction rate of net production of specie i $\left[\frac{kgCOD}{m^3 d}\right]$.

Soluble. Mass balance for each soluble specie i except for CH_4, CO_2 and H_2 is given by equation:

$$\frac{dS_i}{dt} = \frac{Q}{V_L}\left(S_{i,in} - S_i\right) + r_{Si} \tag{12}$$

Where $S_{i,in}$ is input concentration of specie i $[kgCOD/m^3]$ (for CO_2 - $[kmolC/m^3]$, for total inorganic nitrogen (IN) - $[kmolN/m^3]$) ; S_i is concentration of specie i in the reactor $[kgCOD/m^3]$ (for CO_2 - $[kmolC/m^3]$, for total inorganic nitrogen (IN) - $[kmolN/m^3]$); r_{Si} is reaction rate of net production of specie i $\left[\frac{kgCOD}{m^3 \cdot d}\right]$ (for CO_2 - $\left[\frac{kmolC}{m^3 d}\right]$, for total inorganic nitrogen (IN) - $\left[\frac{kmolN}{m^3 d}\right]$)– can be found from Peterson matrix given in Appendix F.

CH_4, CO_2 and H_2 apart from being produced/utilized in the liquid phase are also transferred to the gas phase, so a flux term should also appear in the respective mass balances:

$$\frac{dS_i}{dt} = \frac{Q}{V_L}\left(S_{i,in} - S_i\right) + r_{Si} - \rho_{T,i} \qquad (for\ i = CH_4, CO_2, H_2) \tag{13}$$

Where $\rho_{T,i}$ is a flux term for specie i and can be found form:

$$\begin{aligned}
\rho_{T,h2} &= k_L a_{h2}\left(S_{h2} - H_{h2} RT \cdot S_{h2}^G\right) \\
\rho_{T,ch4} &= k_L a_{ch4}\left(S_{ch4} - H_{ch4} RT \cdot S_{ch4}^G\right) \\
\rho_{T,co2} &= k_L a_{co2}\left(S_{co2} - H_{co2} RT \cdot S_{co2}^G\right)
\end{aligned} \tag{14}$$

Where $k_L a_i$ is local mass transfer coefficient for specie i $[1/d]$; H_i is Henry's constant for specie i $[M/bar]$; R is gas constant $\left[\frac{bar}{M \cdot K}\right]$; T is temperature $[K]$; S_i^G is concentration of specie i in gas phase $[kgCOD/m^3]$ (for CO_2 - $[kmolC/m^3]$); and $S_{co2} = S_{IC} - S_{HCO3^-}$.

Gaseous. Mass balance for each gaseous specie i is given by the equation:

$$\frac{dS_i^G}{dt} = 0 - \frac{Q_G}{V_G} S_i^G + \frac{V_L}{V_G} \rho_{T,i} \tag{15}$$

Where Q_G is gas flow rate $[m^3/d]$; V_G is volume of the gas phase $[m^3]$.

There is no input of gas in the system, so all the gaseous species that leave the system are transferred from the liquid phase where they were produced. This also means that there is no direct way to control gas flow rate Q_G, because it depends on the production and mass transfer rates of CH_4, CO_2 and H_2:

$$Q_G = \frac{RT}{P_{atm} - p_{G,H_2O}} V_L \left(\frac{\rho_{T,CH_4}}{COD(CH_4)} + \frac{\rho_{T,H_2}}{COD(H_2)} + \rho_{T,CO_2}\right) \tag{16}$$

Where $COD(CH_4) = 64\ \left[\frac{kgCOD}{kmolCH_4}\right]$; $COD(H_2) = 16\ \left[\frac{kgCOD}{kmolH_2}\right]$; P_{atm} is atmospheric pressure $[bar]$; p_{G,H_2O} is partial pressure of water vapour.

Several numerical problems, however, can occur when using this way of calculating gas flow rate, such as multiple steady states and numerical instability [63]. Alternative way of calculating Q_G suggested in ADM1 (assuming the overpressure in the head space):

$$Q_G = k_p\left(P_{gas} - P_{atm}\right) \cdot \frac{P_{gas}}{P_{atm}} \tag{17}$$

Where k_p is a coefficient related to the friction in the gas outlet $\left[\frac{m^3}{d \cdot bar}\right]$; P_{gas} is total pressure $[bar]$, can be calculated from:

$$P_{gas} = p_{G,H_2} + p_{G,CH_4} + p_{G,CO_2} + p_{G,H_2O} \quad (18)$$

Where

$$\begin{aligned} p_{G,H_2} &= S^G_{H_2} \cdot \frac{RT}{COD(H_2)} \\ p_{G,CH_4} &= S^G_{CH_4} \cdot \frac{RT}{COD(CH_4)} \\ p_{G,CO_2} &= S^G_{CO_2} \cdot RT \end{aligned} \quad (19)$$

According to Rosen and Jeppsson [63] this method of calculating flow rate results in slightly smaller values for Q_G but the numerical problems mentioned above can be avoided. For this reason the latter method for finding Q_G was chosen in this work.

pH. Many intermediates in AD process affect pH of the system, for example, acids: acetate, propionate, butyrate, valerate and carbonic acid as well as ammonia. Thus, pH (or $S_{H^+} = 10^{-pH}$) cannot be directly controlled but can be calculated from the charge balance:

$$\Theta = S_{H^+} - S_{OH^-} = S_{HCO3^-} + \frac{S_{Ac-}}{64} + \frac{S_{Pro-}}{112} + \frac{S_{Bu-}}{160} + \frac{S_{Va-}}{208} + S_{An^-} - S_{Cat^+} - S_{NH_4^+} \quad (20)$$

Since $S_{OH^-} = \frac{K_W}{S_{H^+}}$ ($K_W = 10^{-14}$ – water dissociation constant), the charge balance can be written as:

$$S_{H+} = \frac{\Theta + \sqrt{\Theta^2 + 4K_W}}{2} \quad (21)$$

This is an implicit algebraic equation ($\Theta = \Theta(S_{H^+})$) so the system can only be solved with DAE solver (differential-algebraic equation solver).

MATLAB solvers ODE15s and ODE23t can solve DAE problems (www.mathworks.com). ODE15s was chosen in this work because of the shorter computation times required by this solver.

3.3. Partial nitritation and Anammox

3.3.1. General information

Nitrogen is an important nutrient for microbial growth. Excess of nitrogen in water causes the increase of microorganisms' population, known as eutrophication. This growth of microorganisms is accompanied by the depletion of oxygen in water which negatively affects higher life forms [1]. Therefore, nitrogen removal becomes an important part of wastewater treatment.

Conventional method for N removal is a two-stage nitrification-denitrification process (Figure 7). In this process during the aerobic stage autotrophic nitrifying bacteria first convert ammonium present in wastewater to nitrite and then – to nitrate. High amount of oxygen is required for this process. During the anoxic stage heterotrophic denitrifiers convert nitrate from the aerobic stage to nitrogen gas. Organic carbon source is required at this stage to ensure bacterial growth [8].

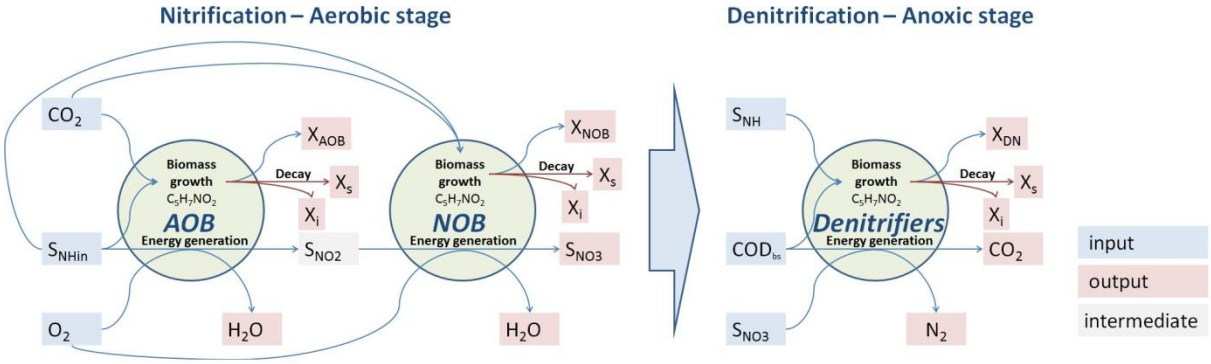

Figure 7. Conventional nitrification - denitrification process scheme (not all the interactions are shown).

The main advantage of the nitrification-denitrification process is the satisfying effluent quality toward the low amount of nitrogen (N). However, several disadvantages can be stressed, among which high oxygen consumption resulting in high energy consumption, necessity to provide additional carbon (C) source for denitrifiers, and high sludge production [8].

To overcome these disadvantages alternative methods for N removal have been proposed. Description of these methods can be found, for example, in a review of Paredes et al [15]. One of such methods is a combination of partial nitritation and Anammox processes (Figure 8). The general idea of this method is the following: during the first aerobic stage (partial nitritation) ammonium in wastewater is oxidised to NO_2^-, for which specific conditions need to be provided to inhibit the complete oxidation to NO_3^-. Apart from that it needs to be ensured that only approximately half of the ammonia is converted into nitrite, so that in the effluent of the first stage NO_2^-:NH_4^+ ratio is roughly 1.32:1. This is the stoichiometric ratio which will be required for the next stage. The optimal ratio can be obtained by varying temperature, SRT, pH and bicarbonate–to–ammonia ratio. During the second anoxic stage Anammox bacteria under anoxic conditions convert ammonium and nitrite into nitrogen gas. Ammonia is used as electron donor, while nitrite is used as electron acceptor [13]. In this way N removal can be achieved with lower oxygen requirement compared to the conventional nitrification-denitrification process. This method is especially effective for influents with high N and low soluble biodegradable COD content [74].

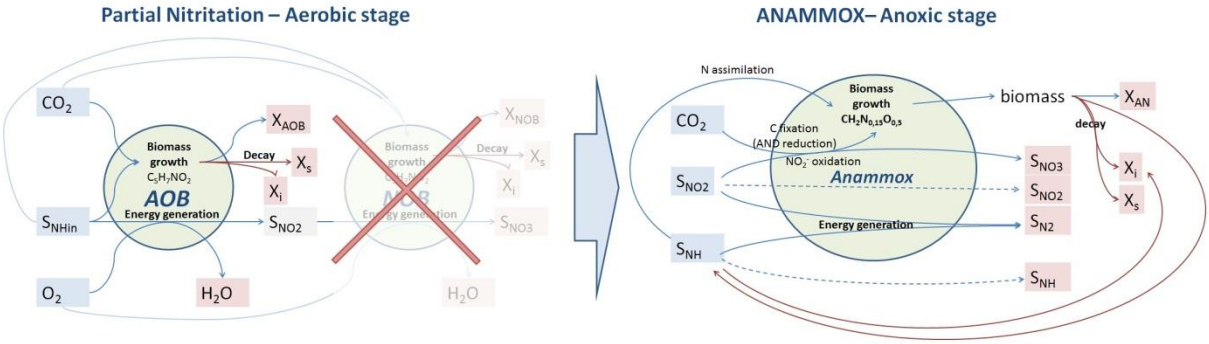

Figure 8. Partial nitritation - ANAMMOX process scheme.

3.3.2. Process configuration

There are two general approaches for nitrogen removal using Anammox process: The first approach is to use two separate reactors for partial nitritation and Anammox, such as SHARON-Anammox process (SHARON – Stable High rate Ammonia Removal Over Nitrite). Another approach is to carry out partial nitritation and Anammox in one reactor, such as Aerobic/Anoxic Deammonification, Completely Autotrophic Nitrogen Removal Over Nitrite (CANON) [75, 76] and Oxygen Limited Autotrophic Nitrification Denitrification (OLAND which is a variation of CANON process) [77]. Comparison of both approaches is shown in Table 1, based on reviews of Zhang et al [13], Paredes et al [15] and Ahn [78].

Table 1. Comparison of different approaches for N removal using ANAMMOX process.

	Types of reactors and sludge form		NH_4^+/NO_2^- control handles	Advantages	Disadvantages
Two-reactors configuration	**Partial nitritation:**		Temperature; Dissolved oxygen (DO); SRT; pH; HCO_3^-/NH_3(tot);	Easy control; Optimal conditions for each step can be provided; More stable operation; Higher nitrogen concentrations can be treated;	Higher investment; Larger footprint;
	SBR	suspended [79];			
	CSTR	suspended [14] (SHARON);			
	MBR	suspended [80] or biofilm [81];			
	ANAMMOX:				
	SBR	suspended [82]), or granular [14];			
	Gas-lift	granular [83];			
	FBR	granular [84];			
	RBC	biofilm [85];			
One-reactor configuration	**Partial Nitritation + ANAMMOX**		DO/ NH_3(tot);	More compact (thus, lower investment); Better N removal for low loaded streams;	Advanced control needed;
	SBR	suspended [86] or biofilm [87];			
	Gas-lift	granular [88];			
	RBC	biofilm [89];			
	GSBR	granular [90];			

SBR – sequential bed reactor, CSTR – continuous stirred tank reactor, MBR - membrane bioreactor, FBR – fluidized bed reactor, RBC - rotating biological contactor, GSBR – granular sludge bed reactor.

In this work a two-reactor configuration is chosen, because of the easier process control.

In the first stage of partial nitritation biomass is often suspended, as dense aggregates are mostly only needed for the treatment of nitrogen-rich wastewater, such as effluent of anaerobic digester and source-separated urine [91]. Moreover, nitrifiers hardly form a biofilm or granules by self-immobilization due to relatively low growth rate and slow production of extracellular polymeric

substances (EPS), which are essential for biomass aggregation [92]. Despite relatively low growth rates of nitrifiers biomass retention is not crucial during this stage. For example, simple and inexpensive SHARON process has been successfully operated at a full scale at the Rotterdam Dokhaven wastewater treatment plant (WWTP), the Netherlands [93].

Regarding SHARON it should be noted, however, that despite this process was found to be the simplest and the most cost efficient solution for partial nitritation [93], very large reactors would be required to treat large flows. This is due to the fact that the system has no retention and HRT for partial nitritation is set at approximately 1 day, which is determined by microbial activity. In case if space for the reactor is limited, retention needs to be provided. The most cost efficient system with retention suitable for partial nitritation is MBR [93].

In the second stage the role of retention is higher. Biomass in Anammox reactors is often in the form of granules or biofilm. This is due to the fact that Anammox bacteria are very slow growers with the doubling time of 11 days [12], thus very efficient biomass retention is required, such as in granular sludge bed or biofilm reactors. However, an important problem has also been reported for the biofilm/granule based reactors [83, 84]. Nitrogen gas produced during the Anammox process is accumulated in the granules, which causes granule floatation and even breakage. This was only observed when total nitrogen loading rate exceeded maximum specific activity of the biomass, though [83].

Based on the information above the following reactor configurations have been chosen for this work: MBR with suspended sludge for partial nitritation and Fluidised Bed Reactor with granulated biomass for Anammox.

3.3.3. Process microbiology and physicochemical conversions

3.3.3.1. Partial Nitritation reactor

Nitrification is a two-stage process performed by different types of bacteria. In the first stage ammonia is oxidized to nitrite by ammonia oxidising bacteria (AOB), mainly *Nitrosomonas sp*. In the second stage nitrite is oxidized to nitrate by nitrite oxidising bacteria (NOB), mainly *Nitrobacter sp*. The retaining of AOB and suppressing of NOB is the desirable outcome of the partial nitritation process. Apart from nitrifiers heterotrophs can also be present in the reactor. These can be especially abundant if the influent is rich in organic carbon.

Interactions between bacteria and chemical species can be modelled in several ways. The most common and simple model available is a modified ASM1 that is expanded for two-step nitrification, taking into account nitrite intermediate. A more sophisticated ASM3 is more accurate in describing the microbial activity and provides a better fit to experimental data, but requires more computational time. Microbial interactions are also affected by the type of reactor. For example, in MBR higher biomass affinity for oxygen and ammonium was reported [94]. This is believed to be caused by the smaller floc size in MBR compared to conventional Activated Sludge systems (35 μm and 307 μm, respectively). The possible cause of this might be increased shear-rate conditions in MBR. Apart from that, soluble microbial products (SMP) were found to play a major role in MBR processes as these compounds contribute to membrane fouling. Despite the name “soluble”, SMP are in fact colloidal species (polysaccharides, proteins) and are partially retained by the membrane, thus, accumulating in the reactor [95]. The effect of SMP on MBR processes is acknowledged and

should not be neglected in the process modelling. This effect can be accounted for in two ways: by adding new states and new processes, which correspond to SMP conversions, or by recalibrating the model parameters. An example of the first approach can be found in a paper of Xie et al [96] where a model is proposed that accounts for SMP formation and two-step nitrification (crucial for partial nitrification modelling). However, because of the simplicity the second approach was chosen in this work. A simple ASM1 expanded for two-step nitrification and recalibrated for MBR according to Wyffels et al [9] is used in this work. According to this model the following species need to be considered.

Particulate species: **Biomass:** AOB (X_{AOB}), NOB (X_{NOB}), Heterotrophs (X_H);
Non-biomass: slowly biodegradable COD or biodegradable particulate COD (X_S), non-biodegradable particulate COD (inerts – X_I);

Soluble species: Ammonium species (S_{NH}), nitrite species (S_{NO2}), nitrate species (S_{NO3}), nitrogen gas (S_{N2}), dissolved oxygen (S_O), biodegradable soluble COD (S_S).

Interactions between these species are reflected in Peterson Matrix as given by [9] (see Appendix G). Bacterial growth and decay are modelled. Growth rate of any bacteria is assumed to be affected only by the availability of its electron donor and electron acceptor, as well as the concentration of bacteria itself, according to Monod kinetics. For AOB and NOB free ammonia (NH_3, FA) and free nitrous acid (HNO_2, FNA) are assumed to be the actual electron donors respectively, not total ammonia ($NH_3 + NH_4^+$) and total nitrite ($HNO_2 + NO_2^-$) [32]. Inhibition of AOB by FNA and NOB by FA is also considered [97]. The availability of FA and FNA is determined by the acid-base equilibrium that is controlled by temperature and pH. Thus, the effects of temperature and pH on the system are also considered (see below). Ammonium species apart from being electron donors for AOB are taken up by all bacteria to build up the biomass. Some of that ammonium is released during the biomass decay. Other products of biomass decay are non-biodegradable particulates (inerts X_I) and biodegradable particulates (X_S). In the presence of heterotrophic bacteria (X_H) biodegradable particulates are hydrolysed to biodegradable soluble species (S_S). The latter ones are used as an electron donor and a carbon source for heterotrophs. Electron acceptors for heterotrophs are oxygen (S_O), total nitrite (S_{NO2}) or total nitrate (S_{NO3}).

Kinetic and stoichiometric coefficients required in the model are given in Appendix G.

The effects of control handles (see Table 1) on the system are given below.

Temperature. The effect of temperature on the growth (and decay) rates of AOB and NOB **within a specific temperature range** is usually expressed via exponential Arrhenius function:

$$k(T) = k(T_r)e^{\Theta(T-T_r)} \quad (22)$$

Where $k(T)$ is a growth or decay rate at a temperature $\left[\frac{1}{d}\right]$; T_r is a reference temperature $[C]$(usually 30°C); Θ is Arrhenius constant, given by $\Theta = \frac{E_{act}}{R(T_r+273)(T+273)}$, where E_{act} is activation energy $[J]$. Values of E_{act} for AOB and NOB are 68 $\left[\frac{kJ}{mol}\right]$ and 44 $\left[\frac{kJ}{mol}\right]$, respectively [30].

The minimal time that bacteria needs to spend in the reactor to avoid washout (SRT_{min}) depends on the bacteria's growth and decay rates. These rates are in turn affected by temperature. Therefore, it

can be possible to selectively wash out some bacteria species by varying SRT at specific temperature. For a situation when all the substrates are abundant and both bacteria grow at maximal growth rate ($\frac{1}{SRT_{min}} = \mu_m - b$), the following graph can be obtained:

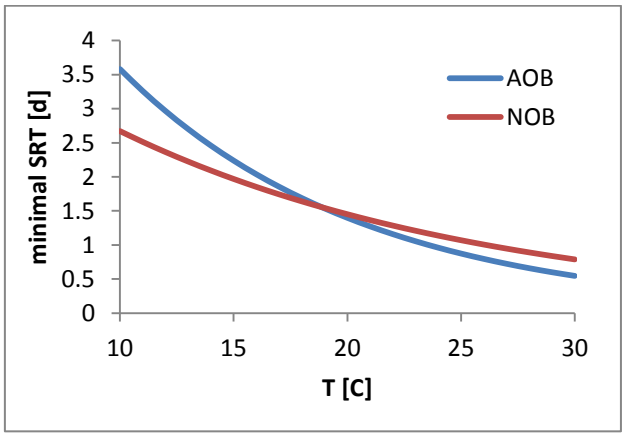

Figure 9. The effect of temperature on AOB and NOB.

It can be seen that at temperatures above 18°C AOB can grow at lower SRT, meaning that they can outcompete NOB at these conditions. This concept is used in SHARON process, which is normally operated at $HRT = SRT \approx 1$ day and high temperatures of around 30°C [98].

Dissolved oxygen (DO). However, even at temperatures below 18°C it is still possible to inhibit NOB growth in the reactor. The key factor to ensure the suppression of NOB growth at low temperatures is dissolved oxygen concentration (DO).

Oxygen acts as an electron acceptor for both AOB and NOB. AOB has a higher affinity for oxygen compared to NOB, which is characterized by a lower half saturation constant K_O value for AOB (see Appendix G). Figure 10 shows the effect of DO on the growth rate of AOB and NOB at different temperatures assuming that DO is the limiting substrate for both bacteria ($\mu = \mu_m e^{\Theta(T-T_r)} \frac{S_O}{K_O+S_O}$).

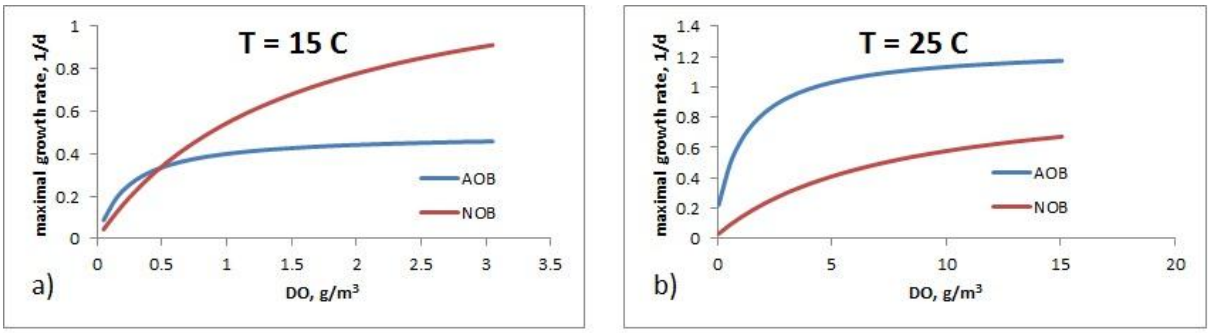

Figure 10. Effect of DO on AOB and NOB at a) 15°C and b) 25°C.

Figure 10 compares the maximal growth rates of AOB and NOB at temperatures above and below the crosspoint seen on Figure 9. It can be seen that AOB has the advantages at high temperatures but NOB at low ones. However due to the higher affinity for oxygen, AOB outcompetes NOB at low DO even at low temperatures.

Sludge retention time (SRT). See "Temperature".

pH. pH affects nitrifying bacteria in several ways [99] as described in the following paragraphs.

Activation-deactivation of AOB and NOB. H^+ and OH^- can bind to basic and acid groups of the enzymes. At extreme pH the effect of such binding can be irreversible which results in blocking the enzymatic acitivity and, as a consequence, disrupting the microbial activity. Dependence of bacteria growth rate on pH is normally given by a bell-shaped function,e.g. [32]:

$$\mu = \mu_m \frac{K_{pH}}{K_{pH}-1+10^{|pH_{opt}-pH|}} \quad (23)$$

Where K_{pH} – saturation constant for pH pH_{opt} – optimal pH for biomass.

Nutritional effect. Nitrifiers are autotrophs, meaning that they use carbonate species as C source. CO_2 is present in the reactor in three forms ($CO_3^{2-} \rightleftarrows HCO_3^- \rightleftarrows CO_2$) and the concentration of each form depends on pH. At low pH the dominant form is CO_2, which can be stripped away from the liquid phase leaving bacteria without the C source. At high pH the dominant form is CO_3^{2-} but it can be removed from the liquid phase by sedimentation if bivalent or trivalent ions are present. Nitrification reactors are normally operated at pH 7–8. In this pH interval bicarbonate is the dominant form. If it's supplied in excess, HCO_3^- also provides a buffering capacity against the proton production during ammonia oxidation. For that reason CO_2 species are assumed to be in excess in this work. Therefore, the growth rate of nitrifiers is not affected by those.

FA and FNA are the electron donors for AOB and NOB, respectively; appear in Monod terms $\frac{FA}{K_{NH}^{AOB}+FA}$ and $\frac{FNA}{K_{NO2}^{NOB}+FNA}$ in the expressions for growth rates. The availability of FA and FNA also depends on pH. This dependency is expressed as:

$$FA = \frac{S_{NH}}{1+\frac{10^{-pH}}{K_e^{NH}}}; \quad FNA = \frac{S_{NO2}}{1+\frac{K_e^{NO2}}{10^{-pH}}}^{4} \quad (24)$$

Where K_e^{NH} and K_e^{NO2} are the ionization constants for $NH_4^+ \rightleftarrows NH_3 + H^+$ and $HNO_2 \rightleftarrows H^+ + NO_2^-$ equilibria, and can be found according to [97]:

$$K_e^{NH} = e^{-\frac{6344}{T+273}}; \; K_e^{NO2} = e^{-\frac{2300}{T+273}}$$

Inhibition by FA and FNA. FA acts not only as a substrate for AOB and also as an inhibitor for NOB. SImilarily, FNA is a substrate for NOB and an inhibitor for AOB. The inhibiting effect is described with inhibition terms $\frac{K_{I,FA}^{NOB}}{K_{I,FA}^{NOB}+FA}$ for NOB and $\frac{K_{I,FNA}^{AOB}}{K_{I,FNA}^{AOB}+FNA}$ for AOB. The effect of pH on the concentration of FA and FNA has been described above.

[4] These expressions can be found from acid-base equilibria for ammonia and nitrite species:
For ammonia species: $NH_4^+ \rightleftarrows H^+ + NH_3$. This equilibrium is characterized by a constant $K_e^{NH} = \frac{[H^+][NH_3]}{[NH_4^+]}$. Considering that the total concentration of ammonia species is $S_{NH} = [NH_{tot}] = [NH_3] + [NH_4^+]$ and $[H^+] = 10^{-pH}$, the concentration of free ammonia can be expressed as $FA = [NH_3] = \frac{K_e^{NH}[NH_{tot}]}{[H^+]+K_e^{NH}} = \frac{S_{NH}}{\frac{10^{-pH}}{K_e^{NH}}+1}$.
Similarly the concentration of free nitrous acid (FNA) can be expressed.

Alkalinity/NH_3. Since it is assumed that bicarbonate is supplied in large excess to partial nitrification reactor (see "pH"), the effect of alkalinity-to-ammonia ratio can be neglected.

3.3.3.2. Anammox reactor

ANAMMOX (ANaerobic AMMonium OXidation) is a process for simultaneous ammonium and nitrite removal [10]. The process is performed by several bacteria genera that belong to the Brocadiales order (named after the place of discovery – a pilot plant at Gist-brocades) within the Plantomycetes phylum [74]. Anammox bacteria are obligate anaerobs and use nitrite as electron acceptor to oxidize ammonium to dinitrogen gas with hydrazine (N_2H_4) and hydroxylamine (NH_2OH) as intermediates [74]. Production of nitric oxide (NO), nitric dioxide (NO_2) and nitrous oxide (N_2O) has also been reported for Anammox bacteria (traces) [12]. Anammox bacteria has very high affinity towards the substrates but the growth rates of these bacteria are very low [100].

As for the partial nitritation system, a simple ASM1-based model is chosen in this work to simulate the microbiological processes taking place in anoxic ANAMMOX reactor. According to that model the following species are assumed to be present in the reactor:

Particulate species: Anammox bacteria (X_{AN}), Heterotrophs (X_H), slowly biodegradable particulate COD (X_S), non-biodegradable particulate COD (inerts – X_I);

Soluble species: Ammonium species (S_{NH}), nitrite species (S_{NO2}), nitrate species (S_{NO3}), nitrogen gas (S_{N2}), biodegradable soluble COD (S_S).

Interactions between bacteria and chemical species are reflected in Peterson Matrix as given by [31] (see Appendix H). It is taken into account that Anammox bacteria are autotrophic chemolithotrophs, which means that they utilize CO_2 species as a C-source and inorganic compounds for energy generation. The substrates are utilized according to a stoichiometric equation [12]:

$$NH_4^+ + 1.32NO_2^- + 0.066HCO_3^- + 0.13H^+ \rightarrow 1.02N_2 + 0.26NO_3^- + 0.066CH_2O_{0.5}N_{0.15} + 2.03H_2O \quad (25)$$

While all biocarbonate is used solely for biomass growth, the utilization of inorganic compounds (NH_4^+ and NO_2^-) is more complex. Large part of nitrite and ammonium are used for energy generation (catabolism) for which 1:1 ratio of these compounds is required. However, from stoichiometric equation it can be seen that the ratio of NO_2^-:NH_4^+ is different than 1:1. That is due to that fact that both nitrite and ammonia are also utilized for other purposes than energy generation [12]. Small part of the nitrite is used to donate electrons for CO_2 fixation since CO_2 needs to be reduced during this process. Nitrite itself is being oxidized to nitrate. Ammonia apart from being an energy source is also being assimilated to ensure biomass growth. During the biomass decay some of that ammonia is released (ammonification) and can be partially taken up by the inert sludge formed in the result of decay. Other products of the cell decay which are accounted for in the model are already mentioned inert sludge (X_I) and slowly biodegradable substrate (X_S). The latter can be hydrolysed to readily biodegradable substrate (S_S), which in turn can be taken up by the heterotrophic bacteria that are usually also present in the reactor.

Anammox bacteria are inhibited by oxygen, but since the reactor is assumed to be anoxic, no inhibition terms are included in the expressions for the growth rates of bacteria. Production of

intermediates (N_2H_4, NH_2OH, NO, NO_2 and N_2O) is not considered in the model. Temperature and pH effects are neglected as these control handles are assumed to be fixed during the Anammox process.

Apart from microbiology mass transfer plays a crucial role in the reactor since biomass is assumed to be forming granules in Anammox process. The effects of mass transfer on the process are described in the next section.

3.3.4. Model development

3.3.4.1. Partial Nitritation reactor

Partial nitritation is assumed to take place in MBR. The conversions of species inside the reactor are shown on Figure 11.

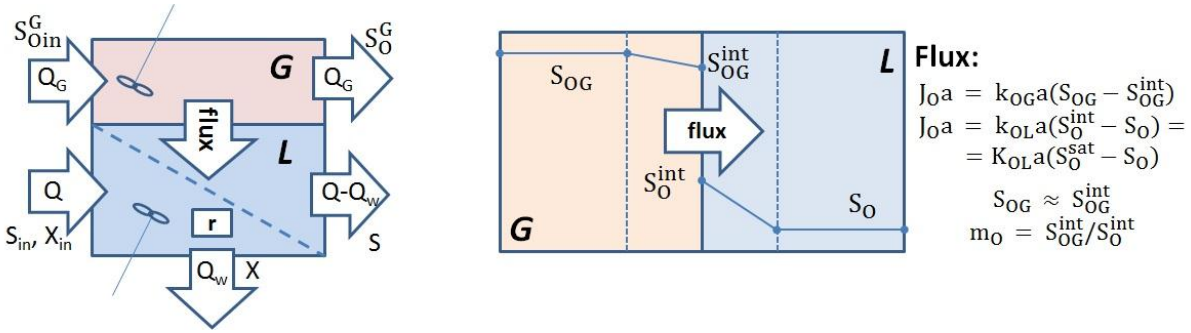

Figure 11. Partial nitritation in MBR.

Assumptions

- "Liquid" volume of MBR consists of two ideally mixed compartments at equilibrium;
- Suspended growth assumed for biomass;
- Membrane retains **ALL** the particulates (it has been shown that complete retention of biomass can be achieved with microfiltration membrane with pore diameter 0.6 μm [9]);
- Soluble species are not retained by the membrane;
- Reactions only take place in the liquid phase;
- pH can be controlled externally;
- Acid-base conversions of chemical species are much faster than microbiological conversions and mass transfer processes, so that (pseudo-)equilibrium can be assumed for different ionic forms of these species;
- Oxygen transfer: mass transfer resistance of the gas phase is negligible;
- Saturation concentration of oxygen (S_O^{sat}) is assumed to be constant, but the concentration of oxygen in the reactor is regulated by overall volumetric mass transfer coefficient of oxygen in the liquid phase (K_{OL} or $K_{OL}a$) so that $K_{OL}a(S_O^{sat} - S_O) = k_{OL}a\left(\frac{S_O^{int}}{m_O} - S_O\right)$ (S_O^{int} - concentration of oxygen on a gas-liquid interface).

Net reaction rates

Reaction rate for net production of specie i is calculated by multiplying the stoichiometric coefficients from column that characterizes specie i in Peterson matrix by the respective specific reaction rate expression. Reaction rates that characterize each process taking place in partial nitritation reactor are also given in Appendix G.

Mass balances

Taking into account the scheme on Figure 11 mass balances for any specie i in the reactor can be obtained. Due to the retention mass balances for soluble and particulate species are different. Since the membrane does not retain the soluble species one mass balance for the whole liquid phase is sufficient:

$$\textbf{\textit{Soluble}}: \quad \frac{dS_i}{dt} = \frac{Q}{V_r}S_{i,in} - \frac{Q_w}{V_r}S_i - \frac{Q-Q_w}{V_r}S_i + r_{Si} = \frac{Q}{V_r}S_{i,in} - \frac{Q}{V_r}S_i + r_{Si} \tag{26}$$

Particulates are retained by the membrane, so a mass balance for each compartment should be made. If f is a fraction of particulates that pass through the membrane, then:

$$\textbf{\textit{Particulates}}: \begin{matrix} 1st\ compartment: & \frac{dX_{i,w}}{dt} = \frac{Q}{V_r}X_{i,in} - \frac{Q_w}{V_r}X_{i,w} - f\frac{Q-Q_w}{V_r}X_{i,w} + r_{Xi,w} \\ 2nd\ compartment: & \frac{dX_{i,e}}{dt} = f\frac{Q-Q_w}{V_r}X_{i,w} - \frac{Q-Q_w}{V_r}X_{i,e} + r_{Xi,e} \end{matrix} \tag{27}$$

Since the complete retention of particulates by the membrane was assumed ($f = 0$) there cannot be any particulates in the second compartment ($X_{i,e} = 0$), thus, there can also be no conversion in this compartment ($r_{Xi,e} = r_{Xi,e}(X_{i,e}) = 0$). In this case the system is reduced to one balance:

$$\textbf{\textit{Particulates}}: \quad \frac{dX_{i,w}}{dt} = \frac{Q}{V_r}X_{i,in} - \frac{Q_w}{V_r}X_{i,w} + r_{Xi,w} \tag{28}$$

Oxygen balance differs from other balances for soluble species since it is transferred from the gas phase:

$$\textbf{\textit{Oxygen}}: \quad \frac{dS_O}{dt} = K_{OL}a(S_O^{sat} - S_O) - \frac{Q}{V_r}S_O + r_O \tag{29}$$

Here $K_{OL}a(S_O^{sat} - S_O) = k_{OL}a\left(\frac{S_O^{int}}{m_O} - S_O\right)$ is the term that describes oxygen flux from gas to liquid phase $\left[\frac{g}{m^3 d}\right]$, and r_{Si}, r_{Xi}, r_O – net reaction rates of species which can be found from Peterson Matrix $\left[\frac{g}{m^3 d}\right]$ [9] (see Appendix G).

3.3.4.2. Anammox reactor

Anammox process takes place in anoxic fluidized bed reactor where bacteria are present in the form of granules. The conversions of species are shown on Figure 12.

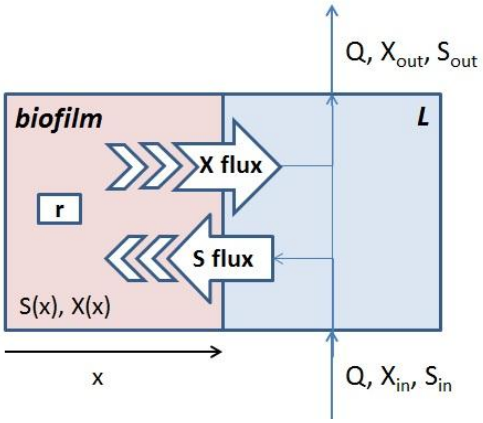

Figure 12. Biofilm system scheme.

As it has already been mentioned, the ANAMMOX reactor is considered as a biofilm system where mass transfer processes (convection and diffusion) play an important role. For such systems concentration of species is not only a function of time, but also a function of coordinate. Therefore, the system is described by partial differential equations, which makes modelling more difficult. For this reason, biofilm model is explained in more detail compared to other models described in this work.

3.3.4.3. Biofilm modelling

General information

A multispecies biofilm is a thin layer of fixed biomass composed of several microbial species which are subject to interactions, such as symbiosis, competition for space and, possibly, common substrates [39].

At the moment several biofilm models are available. A comparison of these models was performed by Morgenroth et al. [101], Eberl et al. [102] and Rittmann et al. [103] using benchmark problems - BM1, BM2 and BM3, respectively.

The models available are based on one of the two general approaches described below:

1. **Biofilm as a continuum**
   First detailed model of such kind was described by Wanner and Gujer [39] (commercially available software AQUASIM widely used for simulation of biofilm systems is based on such model);
   Transport of soluble and particulate species is described with physical laws for the conservation of mass and momentum;
   Most continuum models are 1D - only consider transport of species in a direction perpendicular to the film – support interface;
   Continuum models are believed to give adequate description of macroscopic conversions in biofilm systems as well as the layered structure of the biofilm [104].
2. **Biofilm as a collection of individual cells**

Such models were introduced recently: Individual Based Model [105] and Cellular Automata [106];
The appearance of these models was triggered by the introduction of powerful analytical tools for biofilm study (e.g. Confocal Laser Scanning Microscopy (CLSM)) and inability of the earlier models to describe the data obtained with these tools;
Interactions between individual cells are considered;
2D and 3D structure of the biofilm can be modelled.

The hybrid model that uses both approaches has also been proposed [107]. In this model the behaviour of cells is modelled with the individual based approach, but the behaviour of EPS - with continuum approach.
Obviously both approaches have their own advantages and disadvantages. These were discussed, for example, by Alpkvist et al [107] and are briefly summarized in Table 2.

Table 2. Comparison of two approaches that are used for the modelling of biofilm systems.

	Individual based	**Continuum**
Advantages	• Interactions at a level of individual bacterium can be studied; • Modifications of the model (addition of new local rules) is based on biological principles (instead of mathematical and physical analysis);	• Model formulation in a form of partial differential equations allows the use of well-developed tools for numerical analysis;
Disadvantages	• The output of the model can be stochastic; • Error analysis is non-trivial;	• Microbial ecology cannot be studied;

The choice of the modelling approach generally depends on the purpose of modelling. As it was noted by Morgenroth et al. [108], the main challenge at this stage is to determine the relevant scale of the model for the system of interest. For example, for studying a dental plaque development, biofilm structure (microscale) is of a high importance, and individual based approach seems more appropriate. However, in this work the main important output of the model is the reactor effluent quality (macroscale). Thus, the **continuum** approach is preferred.

Model derivation

The system is characterized by the set of assumptions. Despite some simplifying assumptions are quite unrealistic, they are justified since the only significant output of the model within this work is the reactor effluent quality.

Assumptions:

- Reactor – FBR (biomass forms granules);
- Granules are non-overlapping spheres;
- Fraction of the reactor volume occupied by granules is constant;
- Biofilm is considered to be a continuum;

- Biofilm has a constant density over its thickness;
- Biofilm is one-dimensional in space - all the spatial gradients are considered only in the direction perpendicular to the biofilm-support interface;
- Biofilm thickness (R) is assumed constant (detachment velocity form the biofilm is assumed to be the same as growth velocity at the biofilm-liquid interface);
- Boundary layer around granules is neglected;
- No attachment onto biofilm is considered;
- Particulate components do not diffuse and their transport in biofilm is only governed by convection;
- For soluble components convection is neglected and their transport in biofilm is only governed by diffusion;
- Net reaction rates are modelled with ASM1-based model [31];
- Reactions only take place in the biofilm (no reaction in the bulk);
- Bulk is modelled as one CSTR.

Net reaction rates

Reaction rate for net production of specie i is calculated by multiplying the stoichiometric coefficients from column that characterizes specie i in Peterson matrix by the respective specific reaction rate expression. Reaction rates that characterize each process taking place in ANAMMOX reactor are also given in Appendix H.

Mass balances

As it was already mentioned, continuum models are based on a 1D model first described by Wanner and Gujer [39]. The model derivation shown below is majorly based on this first work. Just like in Activated Sludge Models, soluble (S) and particulate (X) species are treated separately. The difference in size between solutes and particulates has a significant effect on modelling [107]: (i) the transport processes in the biofilm are different (particulates do not diffuse, while solutes – do), (ii) the characteristic times of the processes associated with solutes and particulates are different. Because of this, different balances are given for soluble and particulate species.

Soluble species

The first step is to set up the microbalance for soluble species at any point inside the biofilm. The basic scheme of conversions of a single soluble species is shown on Figure 13a.

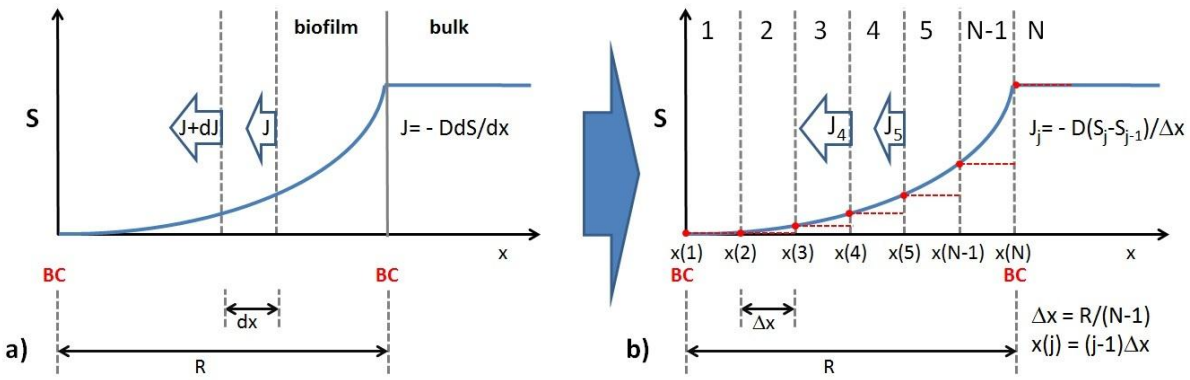

Figure 13. Conversions of a single soluble specie S_i inside the biofilm.

Since the accumulation of specie j at point x depends on a flux of the specie from/to the surrounding points and on the net production rate of the specie at point x ($r_{Si}(x)$), it is possible to write:

$$\frac{\partial S_i(t,x)}{\partial t}Adx = -\left[J_i^{Diff}(t,x)A - \left(J_i^{Diff}(t,x) + dJ_i^{Diff}(t,x)\right)A\right] + r_{Si}(t,x)Adx \quad (30)$$

Where A is the surface area of the biofilm $[m^2]$, J_i^{Diff} - diffusive flux of a specie i $\left[\frac{g}{m^2 d}\right]$ (negative sign in equation (30) indicates that the direction of the flux is opposite to that of x-axis). It can be found according to $J_i^{Diff} = -D_i\frac{\partial S_i(t,x)}{\partial x}$, where D_i is a diffusion coefficient of specie i. Including this in (30) after simplifications yields:

$$\frac{\partial S_i(t,x)}{\partial t} = -D_i\frac{\partial^2 S_i(t,x)}{\partial x^2} + r_{Si}(t,x)$$

In order to further simplify the system to allow a numerical solution, the biofilm can be represented as a series of $(N-1)$ film segments. Each segment is characterized by a finite thickness Δx and a constant concentration of S within the segment, as shown in red dashed line on Figure 13b. In this case it is possible to rewrite equation (30) for a segment i **inside the biofilm**:

$$\boldsymbol{for\ j} = [\mathbf{2}; (\boldsymbol{N}-\mathbf{1})]: \ \frac{dS_{i,j}}{dt}A\Delta x = -\left[J_{i,j+1}^{Diff}A - J_{i,j}^{Diff}A\right] + r_{Si,j}A\Delta x \quad (31)$$

Considering that $J_{i,j}^{Diff} = -D_i\frac{S_{i,j}-S_{i,j-1}}{\Delta x}$, after all the simplifications equation (31) yields:

$$\frac{dS_{i,j}}{dt} = D_i\frac{\left(S_{i,j+1}-2S_{i,j}+S_{i,j-1}\right)}{\Delta x^2} + r_{Si,j}$$

The expressions for the 1st and Nth film segment, however, would be different because of the boundary conditions.

From Figure 13b it can be seen that there is no flux out of the 1st segment. In this case we can write:

$$\boldsymbol{for\ j} = \mathbf{1}: \ \frac{dS_{i,j}}{dt}A\Delta x = -\left[J_{i,j+1}^{Diff}A - 0\right] + r_{Si,j}A\Delta x \quad (32)$$

After simplifications this yields:

$$\frac{dS_{i,1}}{dt} = D_i\frac{S_{i,2}-S_{i,1}}{\Delta x^2} + r_{Si,1} \quad (33)$$

For Nth segment the situation is different since the Nth segment is the bulk. It was assumed that there is no reactions taking place in the bulk. Thus bulk mass balance only consists of inflow, outflow and flux terms. The latter is the sum of all fluxes from bulk to biofilms on top of granules. This sum depends on the number of granules in the reactor (n). If the fraction of reactor volume occupied by granules is f_G, the number of granules can be found according to $n = \frac{fV_r}{\frac{4}{3}\pi R^3}$. The resulting bulk balance is:

$$\boldsymbol{for\ i} = \boldsymbol{N}: \ \frac{dS_{i,j}}{dt}(1-f_G)V_r = Q\left(S_{i,in}-S_{i,j}\right) - \left(-J_{i,j}^{Diff}A\cdot n\right) \quad (34)$$

After simplifications this yields:

$$\frac{dS_{i,N}}{dt} = \frac{Q}{(1-f_G)V_r}\left(S_{i,in} - S_{i,N}\right) - D_i \frac{S_{i,N}-S_{i,N-1}}{\Delta x}\frac{4\pi R^2}{(1-f_G)V_r}n \quad (35)$$

In case if it is necessary to simulate a system where granules do not fully consist of biomass but instead are formed by the inert support and a biofilm growing on it, in equation (35) R should be replaced with $(R - R_{inert})$, where R is the total radius the granule $[m]$, and R_{inert} – radius of the inert support – a core of the granule $[m]$.

Initial conditions for such system:

$$\boldsymbol{for\ j = N}:\ S_{i,j} = S_{i,in}$$

$$\boldsymbol{for\ j} = [\mathbf{1}; (\boldsymbol{N-1})]:\ S_{i,j} = any\ relatively\ small\ value, e.g., 1\left[\frac{g}{m^3}\right]$$

Particulate species

Just like in the previous section, modelling the changes of particulate species in time and space starts with setting up the microbalance for particulates at any point in biofilm. The basic scheme of conversions of single particulate specie is shown on Figure 14a.

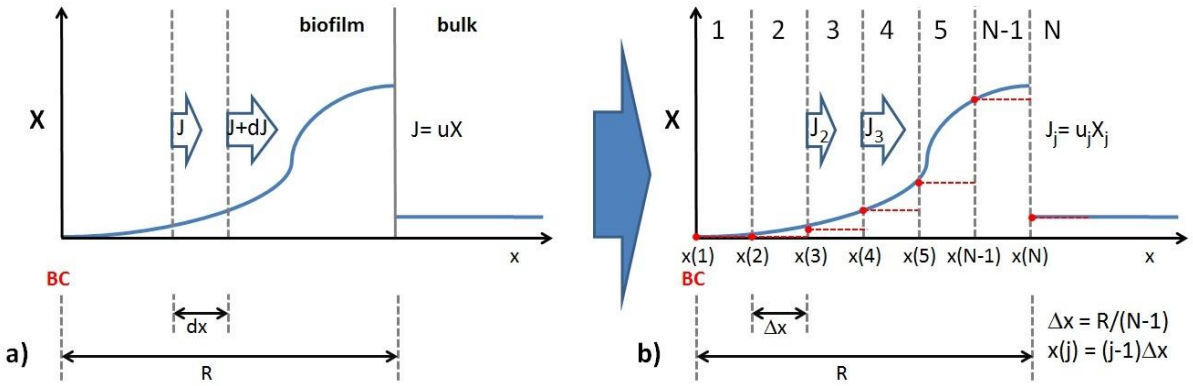

Figure 14. Conversions of single particulate specie X_i inside the biofilm.

The accumulation of specie i at point x depends on a flux of the specie from/to the surrounding points and on the net production rate of the specie at point x ($r_{Xi}(x)$). Since we assume that the density of the biofilm is constant over its thickness, it might be convenient to express concentration of particulates in terms of volume fractions (f_i), so that $X_i(t,x) = f_i(t,x)X_T$, with X_T being the biofilm density $\left[\frac{g}{m^3}\right]$. Considering this the microbalance for particulate specie would be:

$$\frac{\partial(f_i(t,x)X_T)}{\partial t}Adx = \left[J_i^{conv}(t,x)A - \left(J_i^{conv}(t,x) + dJ_i^{conv}(t,x)\right)A\right] + r_{Xi}(t,x)Adx \quad (36)$$

Where A is the surface area of the biofilm $[m^2]$, J_i^{conv} is convective flux of specie i $\left[\frac{g}{m^2 d}\right]$. Convective flux depends on the displacement velocity $u(x)$ at which the microbial mass is displaced with respect to the film-support interface: $J_i^{conv} = uf_iX_T$. The expression for displacement velocity u can be found by summation of equation (36) over all particulate species. After simplifications the resulting equation is:

$$\sum\frac{\partial f_i}{\partial t} = -\sum\frac{\partial(uf_i)}{\partial x} + \sum\frac{r_{Xi}}{X_T} \quad (37)$$

After applying the chain rule and noticing that $\Sigma f_i = 1$ and $\sum \frac{\partial f_i}{\partial t} = \sum \frac{\partial f_i}{\partial x} = 0$ the expression above becomes:

$$\frac{\partial u}{\partial x} = \sum \frac{r_{Xi}}{X_T} \tag{38}$$

The final version of expression (36) is now

$$\frac{\partial f_i}{\partial t} = -\frac{\partial (f_i u)}{\partial x} + \frac{r_{Xi}}{X_T} \tag{39}$$

Where u can be found from (38).

Now just like in the case with soluble species, partial differential equations can be converted into a set of ordinary differential equations. Biofilm is considered to be a series of segments with finite thickness and constant concentration of X_T in each segment (see Figure 14b). For the segments inside biofilm it is possible to write:

$$\boldsymbol{for\ j} = [\mathbf{2}; (\boldsymbol{N} - \mathbf{1})]: \quad \begin{matrix} u_j = u_{j-1} + \sum \frac{r_{Xi,j}}{X_T} \Delta x \\ \frac{d(f_i X_T)}{dt} A \Delta x = \left[J_{i,j-1}^{conv} A - J_{i,j}^{conv} A \right] + r_{Xi,j} A \Delta x \end{matrix} \tag{40}$$

After simplifications:

$$\begin{matrix} u_j = u_{j-1} + \sum \frac{r_{Xi,j}}{X_T} \Delta x \\ \frac{df_i}{dt} = \frac{u_{j-1} f_{i,j-1}}{\Delta x} - \frac{u_j f_{i,j}}{\Delta x} + \frac{r_{Xi,j}}{X_T} \end{matrix} \tag{41}$$

Again, the expressions for the 1st and the last (Nth) segment are different from that above.

In case of the 1st segment it should be considered that there is no displacement in the centre of the granule, thus, it is possible to write:

$$\boldsymbol{for\ j} = \mathbf{1}: \quad \begin{matrix} u_j = 0 + \sum \frac{r_{Xi,j}}{X_T} \Delta x \\ \frac{d(f_i X_T)}{dt} A \Delta x = \left[0 - J_{i,j}^{conv} A \right] + r_{Xi,j} A \Delta x \end{matrix} \tag{42}$$

After simplifications:

$$\begin{matrix} u_1 = 0 + \sum \frac{r_{Xi,1}}{X_T} \Delta x \\ \frac{df_i}{dt} = 0 - \frac{u_j f_{i,1}}{\Delta x} + \frac{r_{Xi,1}}{X_T} \end{matrix} \tag{43}$$

Nth segment is bulk. The only input of particulate species in the bulk is the detachment flux from the granules (number of granules n needs to be considered) and the only output – outflow from the reactor. Detachment velocity for the constant-thickness biofilm can be assumed to be the same as displacement velocity in the (N-1)th segment.

$$\boldsymbol{for\ j} = \boldsymbol{N}: \quad \begin{matrix} u_j = u^{detach} = u_{N-1} \\ \frac{d(f_i X_T)}{dt} (1 - f_G) V_r = J_{i,detach}^{conv} A \cdot n - Q X_{i,j} \end{matrix} \tag{44}$$

After simplifications:

$$u_N = u_{N-1}$$
$$\frac{df_i}{dt} = u_N f_{i,N} \frac{4\pi R^2}{(1-f_G)V_r} N_{gr} - \frac{Q}{(1-f_G)V_r} f_{i,N} \quad (45)$$

3.4. Integrated system

To fulfil the main objective of this work it is necessary to combine the individual models described in the previous sections in a single system. Picture below shows which models were chosen for the processes simulation in this work:

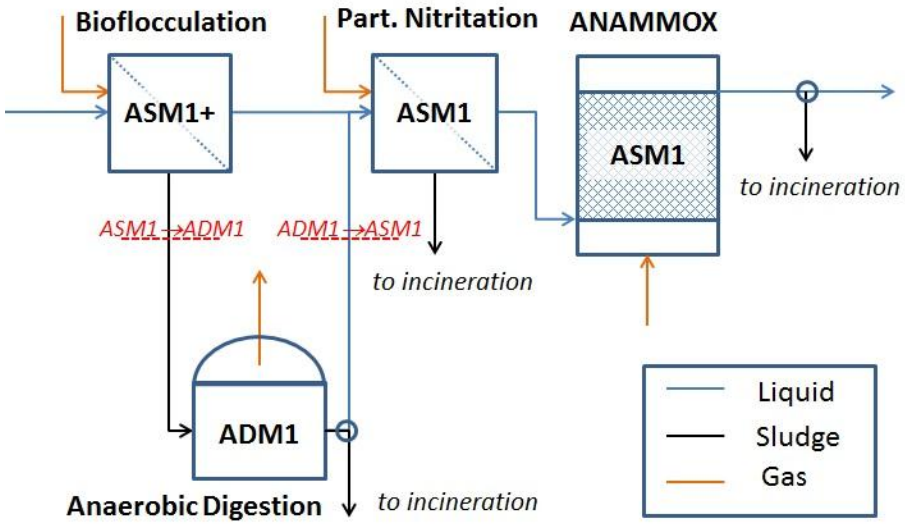

Figure 15. Models used to simulate the individual processes.

It can be seen that bioflocculation, partial nitritation and ANAMMOX models are based on ASM1, so they can be considered "compatible" (use the same set of state variables); however anaerobic digestion model is based on ADM1 which uses completely different state variables than ASM1.

Combining individual models in a single system is a simple task as long as these models are "compatible", but can be non-trivial for other cases. Vanrollenghem et al [38] pointed out the following problems that are likely to occur when it is necessary to combine the individual models that were developed in isolation into a single system:

- *Some state variables used in one model do not exist in the connected model.*
- *The "meaning" of a state variable in one system may not hold for the other system (e.g. components can be considered as inert in one system but may be biodegradable in another).*
- *The elemental composition of a component in one model may not be identical for the connected model and in some instances, the elements considered are not the same (e.g. in ASM3 COD, N and charge are considered whereas in ADM1 COD, C and N are taken into account).*

If these problems are not tackled the overall system might turn out to be inconsistent. There are generally two approaches to avoid this inconsistency [37]:

- **The supermodel approach:** the same state variables are defined for every individual model in the system. Such approach was used e.g. by Young et al [109] who proposed the Combined Activated Sludge – Anaerobic Digestion Model (CASADM). The model includes the following processes: nitrification (with nitrite intermediate), denitrification, hydrolysis, fermentation,

methanogenesis, and production/utilisation of SMP and EPS. The model simulates the production/utilisation of eight particulates (heterotrophs, AOB, NOB, fermenting bacteria, methanogenic Anchaea, EPS and inert biomass), eight solubles (acetate, soluble COD that is not acetate, dissolved oxygen, UAP, BAP, ammonium, nitrite and nitrite) and two gaseous species (nitrogen and methane). The obvious advantage of such approach is the compatibility of all the individual models of the integrated system. However in order to track down the specific species in every individual reactor some other species/ processes have to be lumped together or omitted in order to avoid excessive model complexity. Such simplifications might decrease the model accuracy.

- **The interface approach:** individual models use different set of state variables but the mapping of compounds between these models is clearly defined. Such approach was used by the number of authors [37, 38, 110] who defined the interface for state conversion from ASM1 to ADM1 and from ADM1 to ASM1.

A second approach is used in this work, and the following interface was used for component mapping from ASM1 to ADM1:

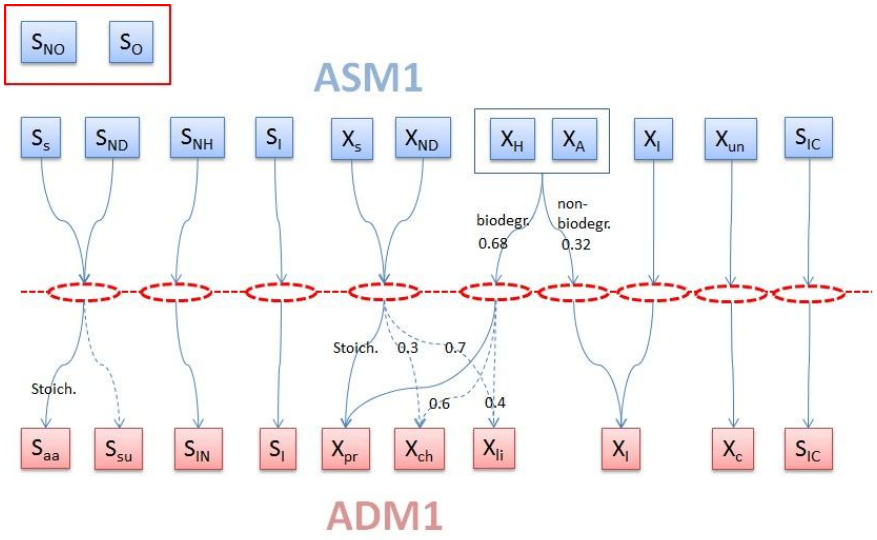

Figure 16. ASM1 - ADM1 model interface (adopted from Nopens et al [37]).

Twelve state variables of bioflocculation model are mapped on some of the state variables of anaerobic digestion model according to the procedure similar to that suggested by Nopens et al [37]:

1. All the negative COD (oxygen and nitrate) is subtracted from the total COD pool with the loss of substrate in the following order: S_s, X_s, X_H, X_A.
2. Readily biodegradable COD (S_s) and organic nitrogen (S_{ND}) are converted into amino acids (S_{aa}). Nitrogen content in amino acids should be in agreement in the value used in ADM1[29]. Any remaining S_s is mapped into sugars (S_{su}).
3. Soluble inerts (S_I) are mapped into soluble inerts (S_I).
4. Slowly biodegradable COD (X_s) and particulate organic nitrogen (X_{ND}) are converted into proteins similarly as it was done in step 2. Any remaining X_s is mapped into carbohydrates (X_{ch}) and long chain fatty acids (X_{li}) according to the ratio X_{ch}:X_{li} = 0.3:0.7. This choice of this ratio is based on the values reported by Siegrist et al [111].

5. Biomass (X_H + X_A) is converted to biodegradable (0.68) and non-biodegradable (0.32) part. Biodegradable part is a mix of proteins, carbohydrates and lipids, while non-biodegradable – particulates inerts (X_I). Fraction of proteins is calculated from comparing the nitrogen content in biomass (i_{NBM} = 0.088 [gN/gCOD]) to that in proteins (i_{Npr} = N_{aa} = 0.007·14 [gN/gCOD]) and in carbohydrates and lipids (i_{Nch} = i_{Nli} = 0 [gN/gCOD]). From the nitrogen balance [5] it can be seen that the fraction of proteins is i_{NBM}/i_{Naa}. The remaining fraction of biomass is assigned to carbohydrates (0.6) and lipids (0.4). This way distinction can be made between anaerobic digestion of primary and secondary sludge.
6. Particulates inerts (X_I) are mapped inot particulate inerts (X_I).
7. Mapping unflocculated particulates (X_{un}) is quite difficult since this specie is not traced down in the standard models. On one hand, it can be mapped into carbohydrates and lipids, but not to proteins since it doesn't contain any nitrogen, in a similar way as it was done for X_s. But in that case no distinction between unflocculated and flocculated particulates can be made. On the other hand, it can be mapped into complex particulates (X_c) to account for the fact that it can't be directly hydrolysed. But in that case the model would be inconsistent in terms of nitrogen, since X_{un} does not contain any N but X_c – do (during the disintegration of X_c proteins are formed among other, and proteins release nitrogen when hydrolysed).
8. The best way to find a compound that can be mapped to inorganic carbon (S_{IC}) in ADM1 is to keep track of it in ASM1 and then map it directly. For this reason additional state variable representing inorganic carbon was included in ASM1, and its stoichiometry was tackled using the carbon balances the same way as it was done for ADM1.

The scheme to map components from ADM1 to ASM1 that was used in this work is also similar to the one suggested by Nopens et al [37]. Although since in partial nitritation model such components as particulate organic nitrogen (X_{ND}) and soluble organic nitrogen (S_{ND}) are not considered, these compounds are replaced by ammonia species (S_{NH}) in the scheme:

[5] $1 \cdot i_{NBM} = f_{pr} \cdot i_{Npr} + (1 - f_{pr}) \cdot 0$,
where f_{pr} – fraction of proteins in the biomass (secondary sludge), $(1 - f_{pr})$ – fraction of carbohydrates and lipids in biomass, i_{NBM} – nitrogen content of the biomass, i_{Npr} – nitrogen content of the proteins.

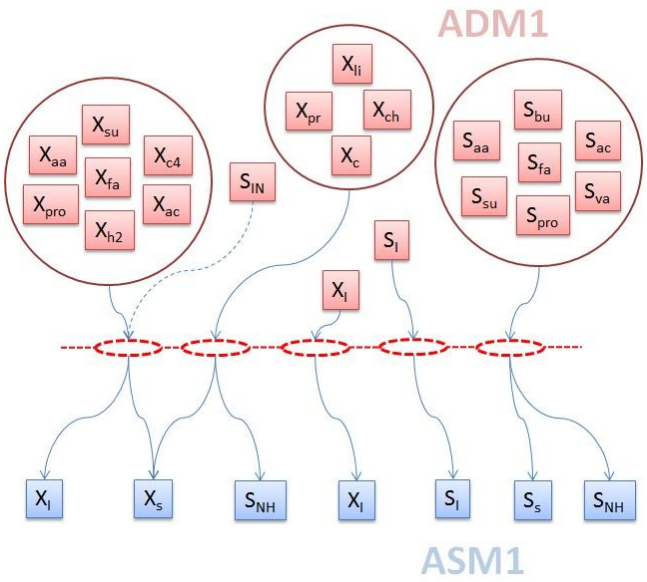

Figure 17. ADM1 - ASM1 model interface (adopted from Nopens et al [37])

1. All active biomass from ADM1 is mapped to slowly biodegadable COD (X_s) and particulate inerts (X_I) taking into account the nitrogen content of the components. Biomass serves as a nitrogen source. If nitrogen in biomass is insufficient inorganic nitrogen (S_{IN}) is used as additional source.
2. Remaining particulate COD (X_c, X_{pr}, X_{li}, X_{ch}) is mapped to slowly biodegradable COD (X_s) and ammonia species according to the nitrogen content of the species.
3. Particulate inerts (X_I) are mapped to particulate inerts (X_I).
4. Soluble inerts (S_I) are mapped to soluble inerts (S_I).
5. Soluble species (S_{aa}, S_{fa}, S_{su}, S_{ac}, S_{pro}, S_{bu}, S_{va}) are mapped to readily biodegradable COD (S_s) and ammonia species according to the nitrogen content of the components.

4. Results and Discussion

In this work a plant-wide simulation was carried out. The basic scheme of the plant is shown on Figure 18. Each operational unit of the plant is simulated using the standard model, with the only exception being a bioflocculation unit, for which no standard model is available at the moment. Individual models that describe each of the plant units are incorporated in an overall model. Each unit is simulated for sufficiently large time to ensure that the steady-state is reached. The steady-state output of one individual model is used as an input for the next model according to a scheme on Figure 18. Internal loops are avoided in the simulation.

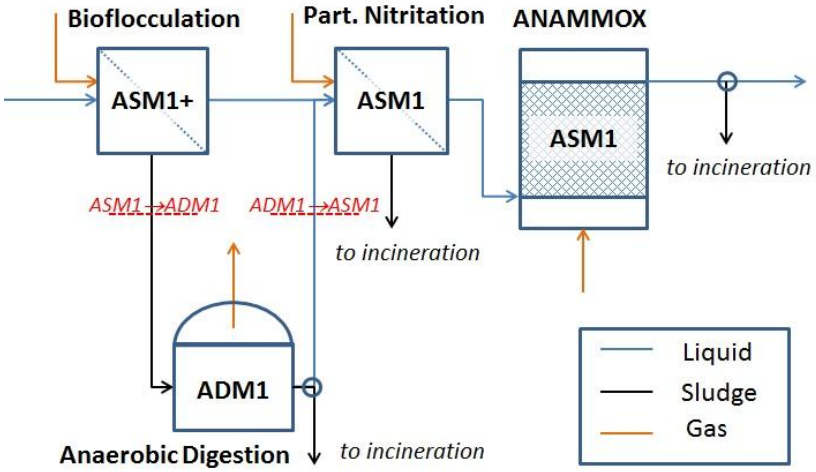

Figure 18. Overall process scheme.

The overall system consists of two big blocks: carbon removing block (Bioflocculation and Anaerobic Digestion) and nitrogen removing block where remaining carbon is removed in aerobic and anoxic environment (Partial nitritation and Anammox). It is more convenient to discuss these blocks separately.

4.1. Anaerobic carbon removal

4.1.1. System inflow

The main goal of bioflocculation within this work is to provide optimal concentrate for the anaerobic digestion step. Performance of anaerobic digestion can be evaluated by the methane production. The operating conditions in bioflocculation reactor can be chosen such, that its effluent would ensure higher CH_4 production. There are several factors that affect the effluent and concentrate quality in bioflocculation reactor: HRT, SRT, $K_{OL}a$ (affects concentration of dissolved oxygen in the reactor), organic loading rate (depends on the influent concentration and flow rate) and temperature.

In this work SRT and $K_{OL}a$ are chosen as the main controls, and slowly biodegradable COD concentration in the influent $X_{un}(in)$ – as the main disturbance for the bioflocculation step.

The characteristics of the modelled system are shown in Table 3.

Table 3. System characterization for carbon removal block simulation.

Name	Value/Range	Unit	Comments
Influent wastewater			
Flow rate (Q)	13000	m^3/d	
Soluble biodegradable COD (S_s)	100	$gCOD/m^3$	
Slowly biodegradable COD (X_s)	200 - 500	$gCOD/m^3$	
Total nitrogen (in the form of ammonia species S_{NH})	40	gN/m^3	AD model appeared unstable at S_{NHin} below 40 gN/m^3
Bioflocculation reactor			
Sludge retention time (SRT)	1.5 - 5	d	
Hydraulic retention time (HRT)	1.5/24	d	Lower HRT is preferable as it corresponds to lower reactor volume and lower process costs as well as higher sludge concentration;
Overall volumetric oxygen mass transfer coefficient ($K_{OL}a$)	60 - 180	1/d	Low $K_{OL}a$ to suppress excessive microbiological activity in order to avoid excessive carbon mineralization;
Temperature (T)	20	^oC	
Anaerobic Digester			
Hydraulic retention time (HRT)	20	d	
Temperature (T)	35	^oC	Mesophilic microorganisms assumed;
Partial Nitritation			
To be specified			
Anammox			
To be specified			

HRT value is chosen to be minimal: low HRT is needed to ensure low reactor volume that would result in lower process costs, as well as high sludge concentration in the rejected stream that is expected to result in better performance of AD step [8]. HRT value of 1.5 h is chosen in this work. Reported HRT values used for bioflocculation process range from 1.2 to 6 h [4, 45, 46].

4.1.2. Bioflocculation

Bioflocculation process was simulated using the original ASM1 [25] expanded for an extra state variable X_{un} (unflocculated biodegradable particulate COD or slowly biodegradable COD) and for an extra process of bioflocculation, as it was done in a paper of Dold et al [24]. The simulation was carried out for 200 days to ensure that the steady-state is reached.

Concentrate of bioflocculation reactor and corresponding methane production in anaerobic digester was evaluated as a function of SRT, overall mass transfer coefficient $K_{OL}a$ and the concentration of slowly biodegradable unflocculated COD in the system influent $X_{un}(in)$.

Figure 19 shows how the concentrate of the bioflocculation reactor is affected by SRT and overall oxygen mass transfer coefficient ($K_{OL}a$) for different particulate COD concentrations in the inlet ($X_{un}(in)$)

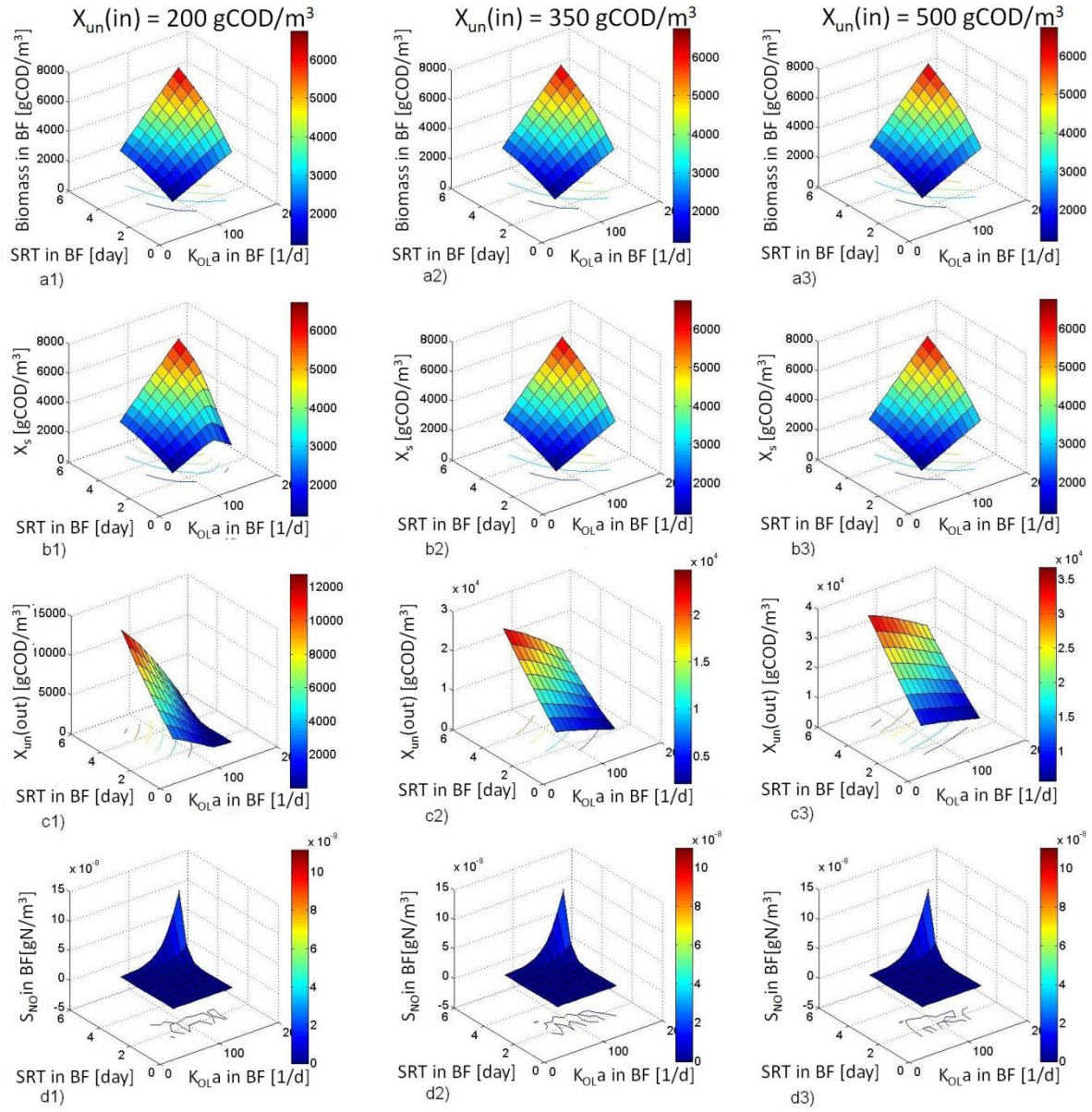

Figure 19. Bioflocculation reactor concentrate quality as a function of SRT and $K_{OL}a$ at different influent particulate biodegradable COD $X_{un}(in)$ concentrations.

It can be seen that increase in any of SRT, $K_{OL}a$ or $X_{un}(in)$ leads to the increase of active biomass concentration (Figure 19a). The amount of flocculated particulate COD is limited by the active biomass concentration – the surfaces that characterize these two state variables nearly coincide. This is because the expression for bioflocculation rate contains the term which acts as a switching function $\left(f_{ma} - \frac{X_s}{X_H}\right)$, where X_s is flocculated particulate COD $\left[\frac{gCOD}{m^3}\right]$, X_H is active heterotrophic biomass $\left[\frac{gCOD}{m^3}\right]$, f_{ma} is a maximal ratio between particulate COD and active biomass in a floc $[-]$. It can be seen that the bioflocculation rate decreases as the X_s/X_H ratio gets closer to f_{ma} value, and at the moment when X_s/X_H becomes equal f_{ma} bioflocculation process terminates. In a paper of Dold et al [24] f_{ma} value of 1 was used, meaning the concentration of X_s would never exceed the concentration of X_H in terms of COD, which is also seen on the graphs (Figure 19 a and b). A sharp decrease of X_s at high $K_{OL}a$ and low inlet particulate concentrations (Figure 19b1) is due to the lack of unflocculated particulates in the reactor at these conditions, as it can be seen from Figure 19c1.

As it was shown, the amount of the flocculated biodegradable particulate COD (X_s) is controlled by the active biomass concentration, which is in turn controlled by SRT, $K_{OL}a$ and $X_{un}(in)$. Excessive biomass production should be avoided during the bioflocculation process because it is associated with carbon mineralization to CO_2. This is undesirable for two reasons: (i) CO_2 is a greenhouse gas and (ii) carbon of CO_2 is removed from the COD pool and can no longer be recovered as methane during the Anaerobic Digestion step [4].

While heterotrophic activity is necessary for the bioflocculation process (even though the excessive activity should be avoided for the reasons described above), autotrophic activity should be avoided completely. That is due to the fact that nitrate species produced by autotrophs cannot be removed from the system in the proposed scenario, since the removal of nitrogen takes place in Anammox stage which implies that only ammonia and nitrite species can be removed. Autotrophic activity can be tracked down for example by accessing the amount of nitrate produced in the process (Figure 19d). It can be seen that nitrification starts at SRT above 5 d and $K_{OL}a$ above 120 1/d, although the maximal concentration of the nitrate species in the selected range is still negligible. This means that in the selected region no significant autotrophic activity occurs.

*****

It might also be interesting to see more detailed picture of what happends in the reactor at specific conditions. Four points have been selected to characterize the system at the extreme conditions within the chosen range for $X_{un}(in) = 200\ [gCOD/m^3]$. Low $X_{un}(in)$ concentration has been chosen because more diversity can be seen for this concentration in the selected range of conditions. Range of conditions was limited to a region where anaerobic digestion model is stable. Numerical issues associated with implementation of anaerobic digestion model will be discussed further. Apart from that it might also be interesting to see if it would be possible to perform efficient digestion of relatively dilute wastewater stream that is pre-concentrated in bioflocculation.

	A	**B**	**C**	**D**
X_{un}(in), [gCOD/m^3]	200	200	200	200
SRT, [d]	1.5	1.5	5	5
K_{OL}a, [1/d]	60	160	60	160

Concentrations of different species in bioflocculation reactor operated at conditions characterized by these points are shown on Figure 20.

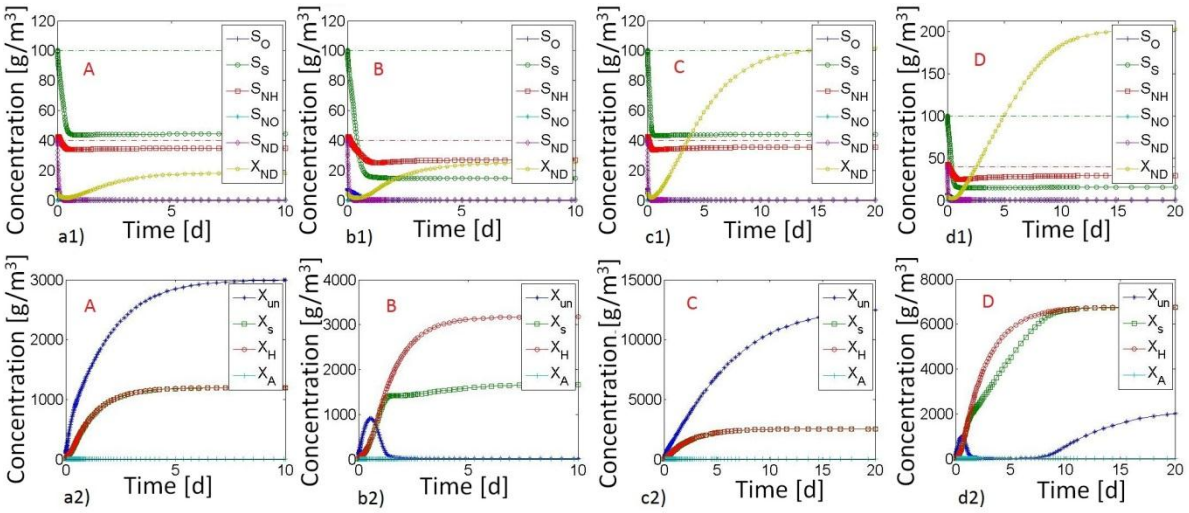

Figure 20. Bioflocculation process at different operating conditions: a) SRT = 1.5 d, $K_{OL}a$ = 60 1/d (point A); b) SRT = 1.5 d, $K_{OL}a$ = 160 1/d (point B); c) SRT = 5 d, $K_{OL}a$ = 60 1/d (point C); d) SRT = 5 d, $K_{OL}a$ = 160 1/d (point D). X_{un}(in) for all cases 200 gCOD/m^3.

First row of the Figure 20 shows concentrations of soluble components as well as particulate organic nitrogen in the reactor at the conditions characterized by the points A, B, C and D. The second row shows concentrations of some particulate species at the same conditions. The time required for soluble and particulate species to achieve equilibrium differs significantly as it can be seen from the graphs. This clearly shows that the system is stiff and the use of stiff solver ODE15s is justified. The stiffness problem will be discussed in more detailes in an "Anaerobic Digestion" section.

It can be seen that already at short SRT concentration of soluble COD S_s drops quickly as it is utilised by heterotrophic bacteria to build biomass and produce energy. The extent at which S_s is utilised depends on the amount of dissolved oxygen S_O in the system that is controlled by $K_{OL}a$. Oxygen is clearly the limiting compound for heterotrophic biomass growth: its concentration quickly drops to nearly zero for all cases (Figure 20 a1, b1, c1 and d1).

$K_{OL}a$ limits the biomass growth, and biomass concentration in turn is one of factors controlling the extent of bioflocculation. For this reason it can be expected that at very low $K_{OL}a$ not all the biodegradable particulates would be flocculated, as seen on Figure 20 a2 and c2. At high $K_{OL}a$ more biomass can grow and consequently more biodegradable particulates X_s become flocculated: at short SRT no more X_{un} is left in the reactor at the steady state (Figure 20b2). At high SRT however X_{un} is at first completely converted into X_s, but later on it "reappears" in the reactor (Figure 20d2). This "reappearance" is due to the formation of new unflocculated particulates during the biomass decay, which is more pronounced at higher $SRTs$ than at short ones.

The concentration of flocculated slowly biodegradable COD (X_s) depends on the concentration of heterotrophic biomass X_H, unflocculated particulate biodegradable COD X_{un}, and the X_s/X_H ratio. As it was already mentioned, maximal concentration of X_s at any point in time is equal to the biomass concentration at the same time. The depletion of X_{un} results in X_s concentration being below its maximal value.

Apart from oxygen and the carbon source, nitrogen is also needed for the biomass growth. Heterotrophs only utilise it as a nutrient, but autotrophs – as both nutrient and energy source. No

significant autotrophic activity however takes place at the selected conditions – the concentration of autotrophic biomass is negligibly low on all graphs (Figure 20 a2, b2, c2 and d2). This means that all the removal of nitrogen is the result of heterotrophic activity. Ammonia nitrogen S_{NH}, being a soluble specie, quickly reaches the equilibrium value at short SRT. However at long SRT slow increase in S_{NH} concentration can be observed after the initial quick drop. This slow increase takes place due to biomass decay which is more pronounced at high SRT. In ASM1 it is assumed that during the biomass decay particulate organic nitrogen X_{ND} is released from cells [25]. This nitrogen accumulates in the reactor due to the membrane retention and is slowly hydrolysed to soluble organic nitrogen S_{ND}, which is quickly converted into the ammonia species S_{NH} in a process of ammonification. Since ammonification is much quicker than hydrolysis the concentration of S_{ND} is very low at all times.

*****

Tendencies predicted by the model seem reasonable; however, the absolute values obtained during the simulation should be treated with caution. As it was already discussed before, no standard model exists at the moment that would accurately describe the bioflocculation process. Standard activated sludge models cannot be used to model bioflocculation process for two reasons: (i) they assume that the bioflocculation is an instantaneous process [25], and (ii) use the set of parameters calibrated for the systems which are operated at $HRTs$ and $SRTs$ that significantly exceed those used for bioflocculation.

Attempt to tackle the first problem was made in this work by extending the standard ASM1 with the adsorption/bioflocculation step as suggested by Dold et al [24]. The second problem, however, requires the experimental data in order to recalibrate the model, which is outside the scope of this work.

Despite it is a common practice to adapt parameter values from another researches, attention must be paid when doing so. For example, if the processes in MBR are simulated using the default ASM1 parameters values, the simulation results can be inconsistent with the observations [47].

Sperandio and Espinosa [112] collected a dynamic data in aerobic submerged MBR at a wide range of SRT (from 10 to 110 days) and found the discrepancies between the model output (ASM1 and ASM3) and the experimental data, especially at high $SRTs$. For example, it was shown that the default values for kinetic parameters for nitrification were not exact and a new set of parameters was proposed. New values of maximal growth and decay rate of nitrifying bacteria were found to be 0.45 1/d and 0.04 1/d, respectively (compare with 0.8 1/d and 0.04 1/d in ASM1). The half saturation constant was found to be a function of the operating conditions in MBR.

Jiang et al [94] also reported lower maximal growth rates of nitrifiers in MBR, as well as higher affinity of the MBR biomass to oxygen and ammonia, which may be caused by the smaller size flocs that develop in MBR and corresponding smaller mass transfer limitations.

Other reasons why parameter values differ in CAS and MBR systems were summarized in a review of Fenu et al [47] and are the following:

- Specific biomass selection due to high SRT (not relevant for bioflocculation) and the retention of free biomass. In the settler only the floc forming bacteria can be retained, while

MBR retains all the bacteria species, which obviously has an effect on the overall kinetics of the microbial community.

- High biomass concentration in MBR.
- Different hydrodynamic conditions: while the conditions in a settler are quite tranquil, in MBR continuous or cyclic air flow that scours the membrane element creates a lot of turbulence.

Similarly it might be expected that the extreme conditions at which bioflocculation process is operated would have an effect on the microbial community, and consequently – on the kinetic parameters that are used to describe such community.

Apart from that, the structure of the model used in this work might appear to be insufficient to accurately describe bioflocculation. As it was already mentioned in the "Bioflocculation" section, a perfect model to describe this process might need to consider the formation of SMP and EPS. These compounds are believed to be important for the membrane processes in general and bioflocculation process in particular. Floc size distribution might also be considered. However a care should be taken to avoid making the model too complex and thus impractical.

Both changing the structure of the model and its recalibration is a challenge for further research, and extensive experimental data would be needed to conduct it.

4.1.3. Anaerobic Digestion

Anaerobic Digestion process was simulated according to the standard IWA model ADM1 [29] with modifications suggested by Rosen and Jeppsson [63]. The aim of the modifications was to deal with some inconsistencies noticed in the original paper of Batstone et al [29]. The list of modifications to ADM1 used in this work as proposed by Rosen and Jeppsson [63] is given below:

- *Extended stoichiometry to guarantee mass balances for nitrogen and carbon in AD;*
- *Modification of default values for $f_{xI,xc}$, $f_{li,xc}$, N_I, N_{bac} and N_{xc} to correct an inherent nitrogen unbalance in the ADM1 and to add consistency with the ASM1 model [25];*
- *Modification of default value for C_{xc} (carbon content of composite material) to correct and inherent carbon unbalance in the ADM1;*
- *Use of the second alternative in the ADM1 report for calculation of the gas flow rate to avoid numerical problems and possible multiple steady states.*

The simulation of Anaerobic Digestion process was carried out for 200 days to ensure that the steady state is reached.

To avoid making the simulation overly complicated the controls of Anaerobic Digester were set to fixed values. The values of control handles were chosen to be the same as in the paper of Rosen and Jeppsson [63]. These control handles include sludge retention time SRT, volume of the head space V_G, volumetric mass transfer coefficient $k_L a$, temperature T.

To find out which compositions of the rejected stream of bioflocculation step are the most favourable for the next step, the AD process was simulated on the same grid as bioflocculation using

the output steady-state concentrations of the rejected stream as the new inputs. The simulation results are shown on Figure 21.

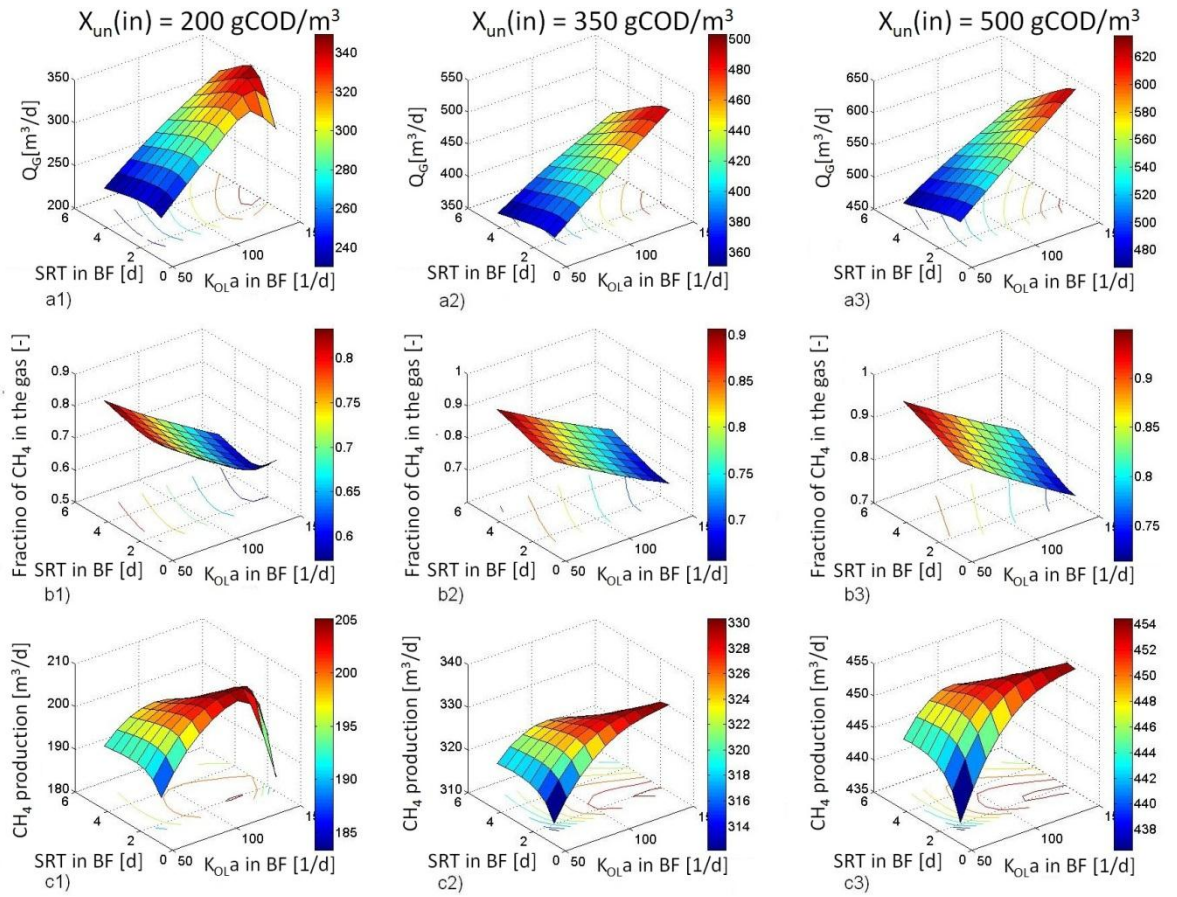

Figure 21. Total gas production (a), fraction of methane in the gas (b) and methane production (c) in anaerobic digester as a function of SRT and $K_{OL}a$ in bioflocculation reactor, as well as influent particulate biodegradable COD X_{un}(in).

Effect of $X_{un}(in)$. Higher concentration of particulates in the system inflow $X_{un}(in)$ results in a higher gas production in the Anaerobic Digestion step. It can also be seen that the surfaces characterizing the system with higher X_{un} in the inflow are somewhat shifted to the right along the $K_{OL}a$ axis. This reflects the fact that more oxygen is needed when treating high concentrated influents to achieve the same concentrate quality as in case of influents with lower COD concentration.

Effect of $K_{OL}a$ in bioflocculation reactor. For system with low strength influent it can be observed that initially raise of $K_{OL}a$ in a bioflocculation reactor leads to an increase in gas production. However, further $K_{OL}a$ increase has an opposite effect. A maximum gas production can be observed at $K_{OL}a > 110\ [1/d]$ (depends on SRT), which correlates well with the formation of X_s in the bioflocculation reactor (Figure 20). This correlation suggests that flocculation favours gas production in digester. This is in the agreement with the general idea behind using bioflocculation as a pre-treatment before AD.

It is interesting to note that the maximum of total gas and methane production also correlates with the minimum of methane fraction in the gas produced. This means that despite increasing $K_{OL}a$ till some threshold has positive effect on gas production, the increase of gas flow rate is majorly due to production of CO_2.

Low $K_{OL}a$ in bioflocculation reactor favours high methane fraction in the gas, but higher $K_{OL}a$ – high methane production. But since the maximal methane production can be obtained at rather wide $K_{OL}a$ range (from 100 to 140 $[1/d]$ at $X_{un}(in) = 200\ [kgCOD/m^3]$) it might be suggested that "optimal" $K_{OL}a$ value in bioflocculation reactor is around 100 $[1/d]$. At this value both sufficiently high methane production and methane fraction in the gas can be achieved.

Effect of SRT in bioflocculation reactor. Results of the simulation indicate that the optimal SRT value exists at which the total gas and methane production is maximal. The position of the maximum depends on $K_{OL}a$ in bioflocculation reactor and influent particulates concentration $X_{un}(in)$. The absolute maximum however situated around $SRT = 2\ [d]$ for all $X_{un}(in)$.

Lower gas production at low SRT values might be related to high fraction of X_{un} in the concentrate that goes to anaerobic digester. The negative effect of high X_{un} fraction in the concentrate on methane production might be caused by the longer time it takes to digest X_{un} compared to biomass or X_s.

Poor system performance at higher SRT might be related to secondary sludge (biomass) production. Biomass growth is associated with carbon mineralisation and on the ASM1-ADM1 interface 32% of biomass from bioflocculation reactor is mapped to inert particulates X_I [37]. COD incorporated in X_I can no longer be used as a substrate for anaerobic microorganisms and is "removed" from the COD pool. Less COD that is available as a substrate results in lower gas production.

Thus the optimal values for SRT and $K_{OL}a$ in bioflocculation reactor can be chosen: $SRT_{opt} = 2[d]$ and $K_{OL}a_{opt} = 100\ [d]$.

Figure 22 and Figure 23 show a more detailed picture of the system operated at optimal SRT and $K_{OL}a$ for $X_{un}(in) = 200\ [gCOD/m^3]$. Important information that characterizes the system is given in Table 4.

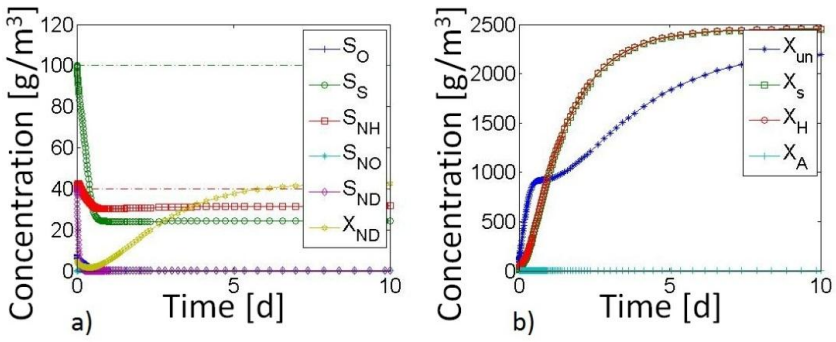

Figure 22. Concentration of a) soluble b) particulate species in bioflocculation reactor at the optimal conditions (HRT(bf) = 1,5 h; SRT(bf) = 2 d, $K_{OL}a$(bf) = 100 1/d); X_{un}(in) = 200 gCOD/m^3.

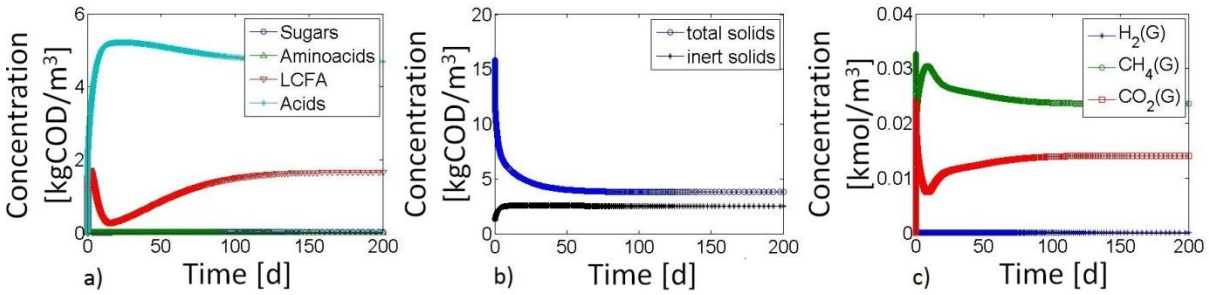

Figure 23. Concentration of a) soluble, b) particulate and c) gaseous species in anaerobic digester at the optimal conditions.

Table 4. Bioflocculation and Anaerobic Digestion simulation results (HRT(bf) = 1.5 h, SRT(bf) = 2 d, $K_{OL}a$(bf) = 100 1/d; X_{un}(in) = 200 gCOD/m^3).

BIOFLOCCULATION			ANAEROBIC DIGESTION		
Name	**Value**	**Unit**	**Name**	**Value**	**Unit**
Concentrate flow rate	406.25	m^3/d	S_s out	4057.58	gCOD/m^3
Total biomass in concentrate	2456.36	gCOD/m^3	Total N out	217.95	gN/m^3
X_s in concentrate	2449.40	gCOD/m^3	Total gas production	272.09	m^3/d
X_{un} in concentrate	2191.94	gCOD/m^3	Methane fraction in gas	0.6036	[-] (mol)
Nitrogen species out:			Methane production	164.24	m^3/d
S_{NH}	31.62	gN/m^3	Equilibrium pH	4.43	[-]
S_{NO}	0.00	gN/m^3	Methane yield	0.2292	gCOD(CH_4)/gCOD$_{in}$(tot)
S_{ND}	0.11	gN/m^3		0.0638	m^3(CH_4)/kgCOD$_{in}$(tot)
X_{ND}	42.58	gN/m^3			

It can be seen that at the conditions chosen for the operation of bioflocculation reactor efficient sludge removal can be carried out in anaerobic digester (Figure 23b). Part of the COD released during the sludge digestion is utilized for biogas formation, which mainly consists of methane and CO_2 (Figure 23c). However, it can also be seen that rather big fraction of COD is converted into Short Chain Fatty Acids that accumulate in the reactor (Figure 23a). Due to the accumulation of acids pH in the reactor reduces. At low pH acidification is enhanced but methanogenesis is dampened [7]. At such conditions methane yield is very low: 0.0638 m^3 of methane produced per kg of total biodegradable COD in AD influent against 0.35 m^3(CH_4)/kgCOD(in) that is expected in AD process (standard conditions) [8]. Furthermore accumulation of Long Chain Fatty Acids (LCFA) in the reactor has an impact on AD process. LCFA were reported to inhibit methanogenic activity of anaerobic microorganisms [69]. This inhibition was not included in original ADM1 [29] and is not considered in this work. ADM1 expansion to account for LCFA inhibition was performed for example by Zonta et al [70].

One of the causes of digester failure is reactor overloading, which implies that the problem might be solved by decreasing the organic loading rate. Organic loading rate depends on the flow rate and concentration of membrane rejected stream coming from bioflocculation reactor. Inlet flow rate in

the system cannot be controlled and flow rate in digester is controlled by SRT in bioflocculation reactor, which was chosen to be "optimal". However, COD load to digester can still be regulated by HRT in bioflocculation reactor. Increasing HRT should result in decreasing COD content of concentrate. Below are the results of simulation for the same system operated at $HRT(bf)$ = 3 h.

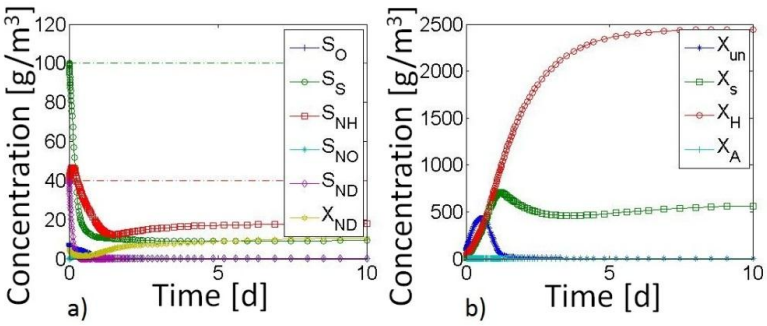

Figure 24. Concentration of a) soluble b) particulate species in bioflocculation reactor at the new conditions (HRT(bf) = 3 h; SRT(bf) = 2 d, $K_{OL}a$(bf) = 100 1/d); X_{un}(in) = 200 gCOD/m^3.

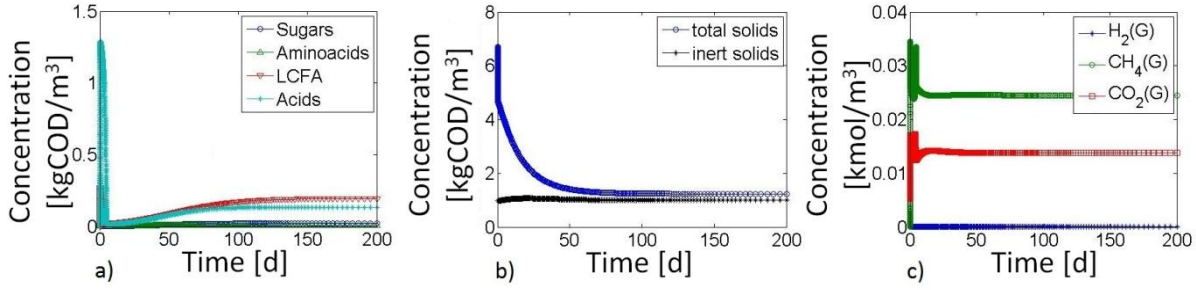

Figure 25. Concentration of a) soluble, b) particulate and c) gaseous species in anaerobic digester at new conditions.

Table 5. Bioflocculation and Anaerobic Digestion simulation results (HRT(bf) = 3 h, SRT(bf) = 2 d, $K_{OL}a$(bf) = 100 1/d; X_{un}(in) = 200 gCOD/m^3).

BIOFLOCCULATION			ANAEROBIC DIGESTION		
Name	**Value**	**Unit**	**Name**	**Value**	**Unit**
Concentrate flow rate	812.50	m^3/d	S_s out	383.92	gCOD/m^3
Total biomass in concentrate	2448.04	gCOD/m^3	Total N out	158.59	gN/m^3
X_s in concentrate	489.39	gCOD/m^3	Total gas production	738.26	m^3/d
X_{un} in concentrate	6.07	gCOD/m^3	Methane fraction in gas	0.6711	[-] (mol)
Nitrogen species out:			Methane production	495.41	m^3/d
S_{NH}	25.25	gN/m^3	Equilibrium pH	6.36	[-]
S_{NO}	0.00	gN/m^3	Methane yield	0.7508	gCOD(CH_4)/gCOD$_{in}$(tot)
S_{ND}	0.19	gN/m^3		0.2809	m^3(CH_4)/kgCOD$_{in}$(tot)
X_{ND}	10.48	gN/m^3			

It can be seen that decreasing organic loading rate via HRT significantly improves methane yield, indicating that the poor performance of AD at the conditions selected above was indeed caused by reactor overloading. It seems to be interesting to investigate the effect $HRT(bf)$ on methane

formation in more details. However, model instability at higher $HRT(bf)$ limits further research (see "Numerical Issues" below).

*****

It might seem that another way to stabilize the system on Figure 23 would be through pH control: setting pH around 7 should favour methanogenesis. However, neutral pH inhibits the activity of acidogenic microorganisms that supply substrate for methanogens. Such different pH preferences of microorganisms in digester suggest that separating these microorganisms in space and providing optimal conditions for each of these might help to overcome inhibitory effect of intermediates and result in a better overall performance. This concept is known as a two-stage or two-phase AD. The two-phase anaerobic digestion concept was first introduced in 1971 by Pohland and Ghosh [113]. Successful implementations of the concept have been reported by the number of authors [114-116]. A major advantage of two-stage AD is the buffering capacity against overloading provided by the first hydrolysis/acidogenesis stage [117].

This suggests that introducing one more digester in the system should help to improve methane production. Figure 26 shows results of the simulation for the system where two anaerobic digesters are put in series. Reactors are chosen to be identical with the only exception being the pH control provided in the second reactor; pH is set at 7 for acetogenesis/methanogenesis.

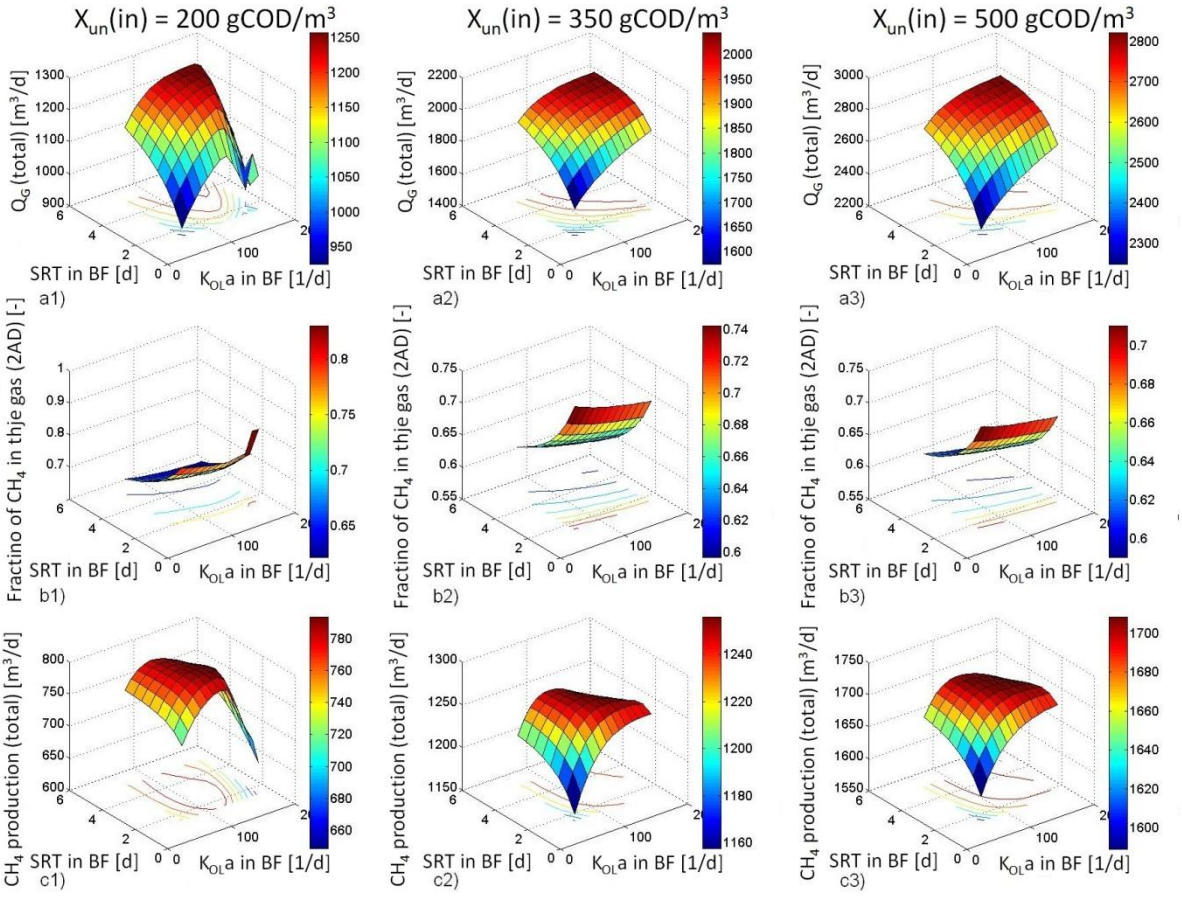

Figure 26. Total gas production in two digesters (a), fraction of methane in the gas cpming from the second digester (b) and total methane production in two digesters (c) as a function of SRT and $K_{OL}a$ in bioflocculation reactor, as well as influent particulate biodegradable COD X_{un}(in).

A more detailed picture of the conversions taking place in the second digester is shown on Figure 27. Concentration of a) soluble, b) particulate and c) gaseous species in second anaerobic digester for two-stage configuration..

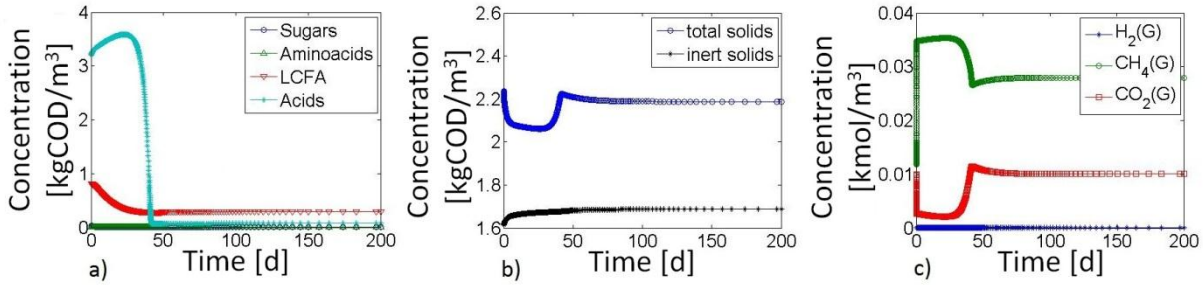

Figure 27. Concentration of a) soluble, b) particulate and c) gaseous species in second anaerobic digester for two-stage configuration.

Table 6. Anaerobic Digestion simulation results for a system with 2 digesters in series (HRT(bf) = 1.5 h, SRT(bf) = 2 d, $K_{OL}a$(bf) = 100 1/d; X_{un}(in) = 200 gCOD/m^3).

ANAEROBIC DIGESTION (2nd reactor)			ANAEROBIC DIGESTION (2 reactors)		
Name	**Value**	**Unit**	**Name**	**Value**	**Unit**
S_s out	373.53	gCOD/m^3	S_s out	373.53	gCOD/m^3
Total N out	205.93	gN/m^3	Total N out	205.93	gN/m^3
Total gas production	836.78	m^3/d	Total gas prod.	1108.87	m^3/d
Methane fraction in gas	0.7355	[-] (mol)	Methane fraction in gas	0.7031	[-] (mol)
Methane production	615.45	m^3/d	Methane production	779.69	m^3/d
Equilibrium pH	7.00	[-]	Equilibrium pH	-	[-]
Methane yield	0.3824	gCOD(CH_4)/gCOD$_{in}$(tot)	Methane yield	0.6927	gCOD(CH_4)/gCOD$_{in}$(tot)
	0.3237	m^3(CH_4)/kgCOD$_{in}$(tot)		0.3029	m^3(CH_4)/kgCOD$_{in}$(tot)

Simulation results of one-stage system (Figure 23) and two-stage system (Figure 27) clearly show that introducing one more digester in the system not only significantly improves methane production but also helps to negate the consequences of overloading. Safer operation means that the system can be operated at maximum capacity. Normally it is not done and reactors are operated far below their maximum capacity in order to reduce the risk of system overload [115]. Two-stage configuration seems more advantageous than more common one-stage AD in terms of operation. The disadvantages of such system are associated with high investment and operating costs due to the necessity to install additional digester.

More common way of promoting acidification in the first digester in two-stage systems is decreasing SRT rather increasing of organic loading rate that is shown in this work. Optimization of anaerobic digestion performance by varying the conditions in digester(s) is not studied in this work, but can be recommended as a topic for further research.

4.2. Nitrogen removal

4.2.1. System characterization

To simulate nitrogen removal block controls characterizing anaerobic carbon removal were set to fixed values and new controls characterizing nitrogen removal were specified. The extended characteristics of the modelled system are given in Table 7.

Table 7. System characteristics for nitrogen removal block simulation.

Name	Value/Range	Unit	Comments
Influent wastewater			
Flow rate (Q)	13000	m^3/d	
Soluble biodegradable COD (S_s)	100	$gCOD/m^3$	
Slowly biodegradable COD (X_{un})	200-500	$gCOD/m^3$	
Total nitrogen (in the form of ammonia species S_{NH})	40	gN/m^3	AD model appeared unstable at S_{NHin} below 40 gN/m^3
Bioflocculation reactor			
Sludge retention time (SRT)	2	d	Value selected based on the analysis of AD simulation;
Hydraulic retention time (HRT)	1.5/24	d	Such low HRT was found to cause digester overload; for two-stage AD overloading of the 1st digester is intentional;
Overall volumetric oxygen mass transfer coefficient ($K_{OL}a$)	100	1/d	Value selected based on the analysis of AD simulation;
Temperature (T)	20	^oC	
Anaerobic Digester (1)			
Hydraulic retention time (HRT)	20	d	
Temperature (T)	35	^oC	Mesophilic microorganisms assumed;
pH	-	-	Not controlled in the first digester;
Anaerobic Digester (2)			
Hydraulic retention time (HRT)	20	d	
Temperature (T)	35	^oC	Mesophilic microorganisms assumed;
pH	7	-	Optimal pH for methanogenesis;
Partial Nitritation			
T	20-30	^oC	
HRT	0.3	d	
SRT	2-23	d	
$K_{OL}a$	30-150	1/d	
Anammox			
T	30	^oC	
HRT	0.2	d	
Fraction of “liquid” reactor volume occupied by granules	0.4	-	
Granule radius	0.001	m	Average granule diameter was found to fluctuate between 1 and 4.5 mm. No significant improvement of N removal can be achieved if granule diameter is above 1 – 1.3 mm [31].

4.2.2. Partial Nitritation

Partial nitritation was simulated according to standard IWA ASM1 expanded for 2-step nitrification but lacking particulate organic nitrogen X_{ND} and soluble organic nitrogen S_{ND} states, according to Wyffels [9]. The model was implemented for MBR and the parameters specifically calibrated for MBR were used. The simulation of partial nitritation was carried out for 200 days to ensure that the steady-state is reached. The effluent of bioflocculation and soluble fraction of anaerobic digestion were used as the model input.

The main desirable output of partial nitritation step is to ensure optimal NO_2^-/NH_4^+ ratio for Anammox process and to avoid nitrate formation which cannot be removed in the next stage.

In order to better see the correlation of the outputs of partial nitritation and Anammox models the simulation results are placed together in the "Anammox" section.

4.2.3. Anammox

Anammox process was assumed to take place in fluidized bed reactor. Bacteria were assumed to be in the form of granules. Body of the reactor was modelled as a single CSTR.

Simulation of Anammox process consists of mass transfer modelling and reaction modelling. Mass transfer of species inside the biofilm was modelled according to a 1D multispecies biofilm model proposed by Wanner and Gujer [39] assuming the constant biofilm thickness. Reactions taking place inside the biofilm were simulated according to a model used by Ni et al [31], which is based on a standard ASM1.

The results of the modelling of nitrogen removal in partial nitritation and Anammox processes are shown on Figure 28.

As it has been mentioned the main goal of the partial nitritation step is to provide optimal nitrite-to ammonia ratio necessary for Anammox process and to avoid nitrate formation. Figure 28 a and b shows how nitrite-to ammonia ratio and nitrate production in partial nitritation reactor are affected by $K_{OL}a$, SRT and particulate biodegradable COD concentration in the system inlet $X_{un}(in)$. Figure 28c shows how the same controls/disturbances affect total nitrogen concentration in the system outlet.

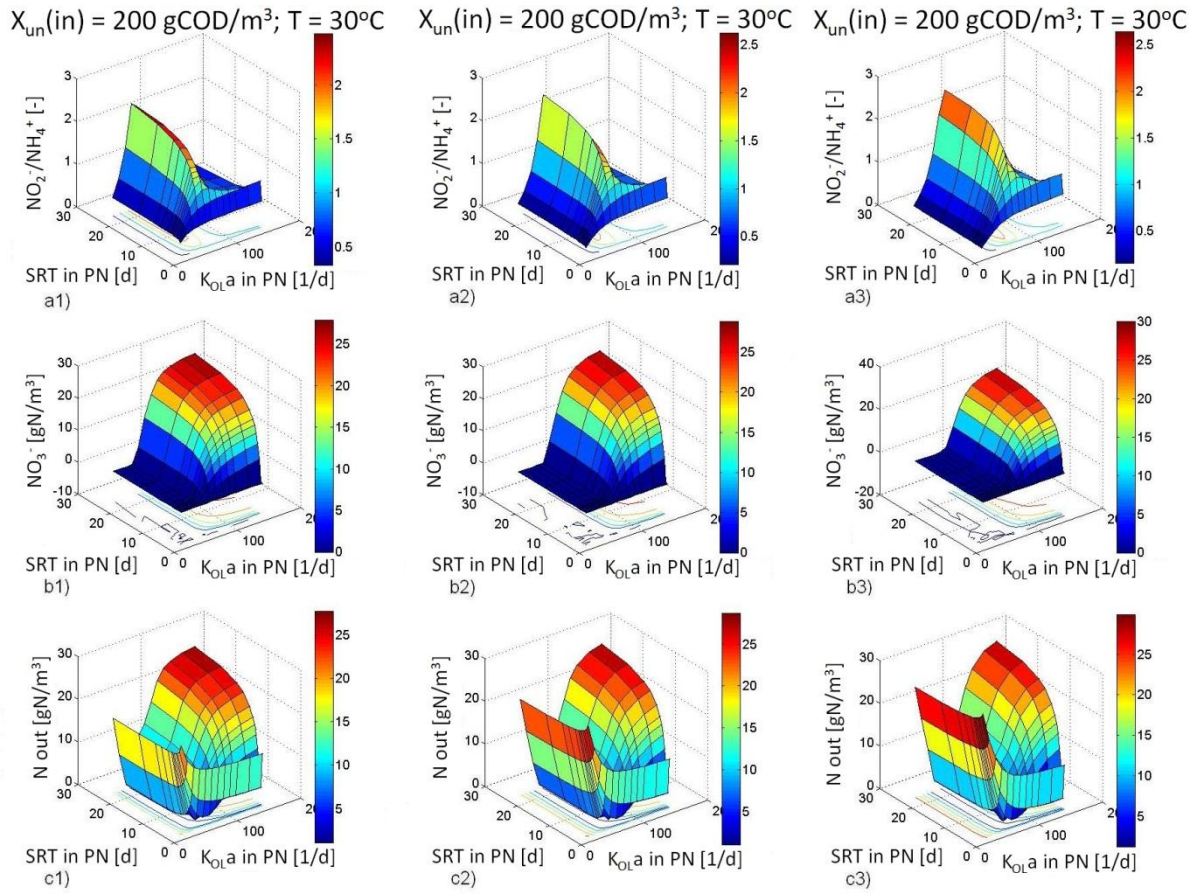

Figure 28. Nitrite-to-ammonia ratio in partial nitritation reactor (a), nitrate production in partial nitritation reactor (b) and total nitrogen in the outlet of Anammox reactor (c) as a function of SRT(pn) and $K_{OL}a$(pn) at different inlet particulate biodegradable COD concentrations X_{un}(in). Temperature in partial nitritation reactor T(pn) = 30°C.

Effect of $K_{OL}a$ in partial nitritation reactor. It can be seen that initially raising $K_{OL}a$ results in higher nitrite production, which causes the increase in NO_2^-/NH_4^+ ratio. However rising $K_{OL}a$ above specific value causes the opposite effect. Nitrite-to-ammonia ratio starts to decrease and nearly reaches zero. Figure 28b provides the explanation for this phenomenon. At 30°C ammonia oxidizers (AOB) have higher affinity for oxygen than nitrite oxidizers (NOB), meaning that AOB would outcompete NOB at low dissolved oxygen concentrations. But at high $K_{OL}a$ the amount of dissolved oxygen in the reactor becomes sufficiently high for both AOB and NOB to become active. Thus nitrite is being oxidized to nitrate (Figure 28b) and nitrite-to-ammonia ratio decreases. Nitrate produced by NOB can no longer be removed from the system and passes the Anammox stage without any conversions. High amount of total nitrogen in the system outlet (Figure 28c) at high SRT and $K_{OL}a$ is mainly due to the nitrate produced in partial nitritation reactor.

Effect of SRT in partial nitritation reactor. SRT regulates biomass concentration in the reactor. At higher SRT concentration of AOB and NOB is high, and consequently ammonia and nitrite oxidation rates are higher as well. This results in higher oxidation products concentration: as SRT rises nitrate concentration increases until nearly all nitrogen is oxidized to NO_3^-. Increase of nitrite concentration is not as pronounced because both its production and consumption rates increase with SRT. It can also be seen that at very low SRT, concentrations of nitrite and nitrate are nearly zero. This is because at such $SRTs$ both AOB and NOB are washed out from the reactor and no ammonia or nitrite oxidation can take place.

Effect of $X_{un}(in)$. Heterotrophs that are responsible for removal of remaining COD in partial nitritation reactor have higher affinity for oxygen compared to autotrophic microorganisms. This means that dissolved oxygen in the reactor would first be consumed by heterotrophs to oxidize COD to CO_2. Then the remaining oxygen would be used by autotrophs to oxidize ammonia to nitrite and nitrite to nitrate. Due to this the surfaces that describe ammonia-to-nitrite ratio and nitrate production are shifted to the right along the $K_{OL}a$ axis for higher $X_{un}(in)$.

It can be seen by comparing Figure 28 a, b and c that amount of total nitrogen in the system outlet correlates well with the ammonia-to-nitrite ratio in partial nitritation reactor. Lowest total nitrogen concentrations in the Anammox reactor are obtained for the cases when NO_2^-/NH_4^+ ratio in the effluent of partial nitritation reactor is close to 1.32. Minimal total nitrogen in the system outlet can be achieved either by accurately regulating $K_{OL}a$ and allowing SRT vary in a wide range, or by precisely regulating SRT and allowing $K_{OL}a$ vary in a wide range. Considering that $K_{OL}a$ cannot be controlled directly while controlling SRT can be done rather easy, the second option seems to be a better choice. However, in that case minimal nitrogen concentration in the system outlet would range from 1.1 to 10 [gN/m^3] depending on $K_{OL}a$ (for $X_{un}(in)$ = 350 [gCOD/m^3], SRT = 5 [d], $T(pn)$ = 30^{o}C). In case if precise $K_{OL}a$ control would be possible, stable effluent nitrogen concentration of 1.1-1.4 [gN/m^3] would be ensured (for $X_{un}(in)$ = 350 [gCOD/m^3], $K_{OL}a$ = 50 [1/d], SRT = 5-10 [d], $T(pn)$ = 30^{o}C).

The mentioned results have been obtained for a system in which partial nitritation reactor is operated at $T(pn)$ = 30^{o}C. High temperature in partial nitritation reactor is necessary to suspend nitrate formation since maximal growth rate of AOB is higher than that of NOB at high temperatures (see "Partial Nitritation and Anammox"). Maintaining such temperature, however, might not be economically attractive. Thus it would be interesting to see how the system would perform at lower temperatures and how the conditions would need to be adjusted to achieve the same nitrogen removal.

According to Urban Wastewater Treatment Directive 91/271/EEC [1] maximal total nitrogen concentration in dischargeable effluent is 10 [gN/m^3]. It is known however that the legislation regulating concentration of nitrogen in the dischargeable effluent will become more stringent in the near future. New maximal effluent nitrogen concentration would be 2.2 [gN/m^3] [2]. Such low nitrogen concentration in the system outlet is still obtainable according to the model, but more accurate control would be required to achieve it. Figure 29 shows how the process controls should be adjusted so that the nitrogen content of the effluent would to meet the requirements of existing and new legislation.

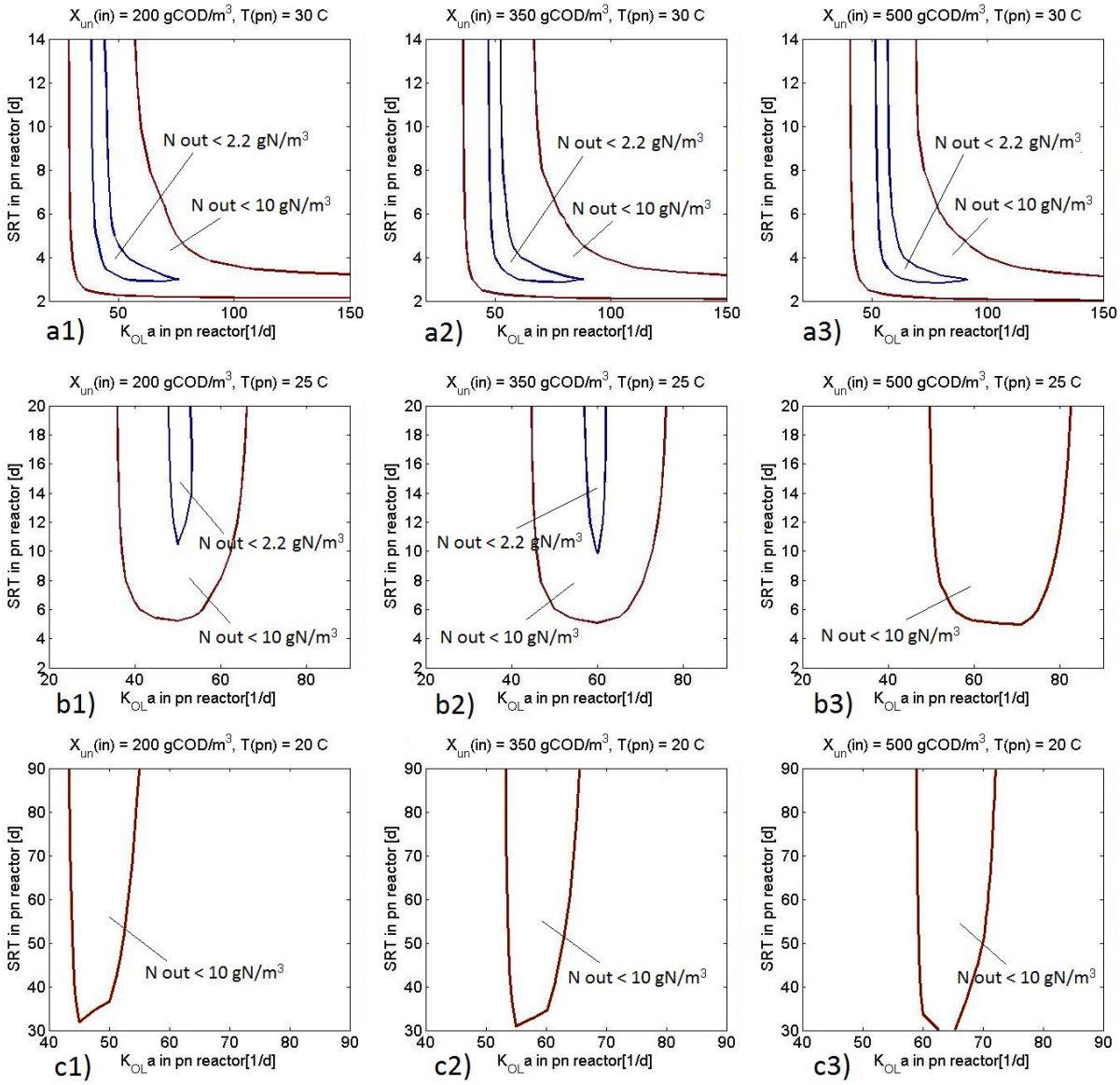

Figure 29. Total nitrogen in the system outlet at different temperatures in partial nitritation reactor.

Important conclusion that can be drawn with the help of Figure 29 is that for the selected conditions (Table 7) system effluent will not meet the requirements of new EU legislation in regards of N concentration if partial nitritation reactor would be operated at 20°C or lower.

It is also crucial to stress that to ensure that the effluent quality would meet the new EU legislation standards, the range in which $K_{OL}a$ may vary should be very narrow, especially for lower temperatures. Maintaining $K_{OL}a$ within the narrow range might be problematic from practical point of view, since $K_{OL}a$ cannot be controlled or measured directly. Operating the partial nitritation reactor at higher temperatures seems safer, since allowed $K_{OL}a$ range is wider at high T. This, however, comes at a cost of energy that needs to be provided to maintain the temperature needed.

Apart from that it can also be seen that allowed $K_{OL}a$ range depends on the system influent quality. Allowed $K_{OL}a$ ranges for lowest and highest $X_{un}(in)$ considered in this work do not overlap. This means that there is no "safe $K_{OL}a$ range" that can ensure needed effluent quality independently on

system influent composition, and continuous adjustment of the controls depending on the system influent would need to be provided.

Figure 29 helps to select optimal operational conditions for partial nitritation reactor which should ensure that the effluent from the plant meets the discharge criteria of the new EU legislation. For example for combined effluents from bioflocculation reactor (Table 4) and 2nd anaerobic digester (Table 6) efficient nitrogen removal can be achieved if partial nitritation reactor is operated at 30°C, $SRT(pn)$ = 4 [d] and $K_{OL}a(pn)$ = 50 [1/d]. Simulation results for such system are shown on Figure 30.

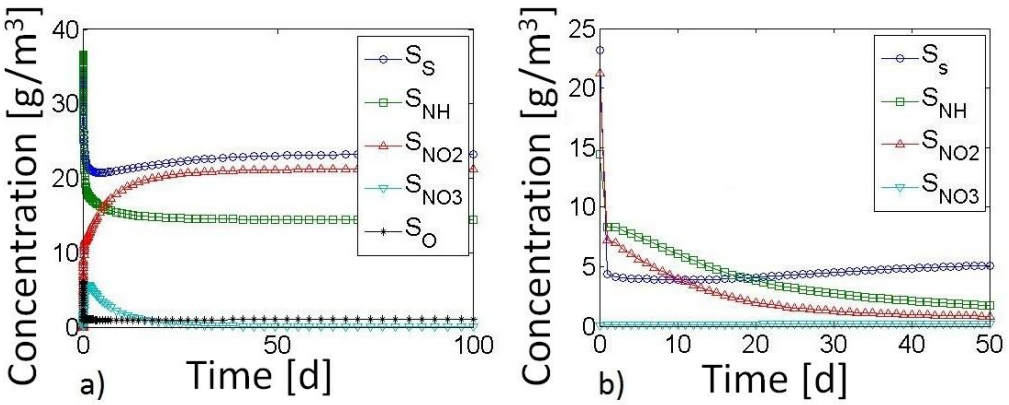

Figure 30. Concentration change of soluble species in partial nitritation (a) and Anammox (b) reactor; X_{un}(in) = 200 gCOD/m^3, SRT(pn) = 4 d, K_{OL}a(pn) = 50 1/d, T(pn) = 30°C.

Table 8. Outlet concentrations of soluble species in partial nitritation and Anammox reactor.

PARTIAL NITRITATION			ANAMMOX		
Name	**Value**	**Unit**	**Name**	**Value**	**Unit**
S_s out	23.21	gCOD/m^3	S_s out	6.45	gCOD/m^3
S_{NH} out	14.41	gN/m^3	S_{NH} out	0.40	gN/m^3
S_{NO2} out	21.25	gN/m^3	S_{NO2} out	0.48	gN/m^3
S_{NO3} out	0.00	gN/m^3	S_{NO3} out	0.19	gN/m^3
S_{NO2}/S_{NH4} at steady state	1.47	[-]	Total N out	1.07	gN/m^3

It is interesting to note that initial ammonia concentration in partial nitritation reactor is almost as high as it was in the overall system inflow, despite ammonia concentration dropped to 25.2 gN/m^3 during bioflocculation process. This is because ammonia nitrogen incorporated in cell biomass during bioflocculation got released during the biomass digestion in AD step. Therefore, most of the ammonia nitrogen, which was present in the system inflow returns to the partial nitritation reactor. Only small amount of nitrogen is wasted from the system with the anaerobic biomass formed in digesters.

In partial nitritation reactor soluble biodegradable COD (S_s) is partially removed by heterotrophs and ammonia species (S_{NH}) are partially converted to nitrite (S_{NO2}). No further oxidation to nitrate (S_{NO3}) takes place. In regard to S_s it can be seen that concentration of this specie first drops but later slowly increases until the steady state is reached. This later increase is due to the hydrolysis of biodegradable products of bacteria decay X_s.

Nitrite-to-ammonia ratio in the effluent of partial nitritation reactor is 1.47, which is not stoichiometric ratio necessary for Anammox but it still results in a good performance of Anammox reactor. Such inconsistency with theoretical expectations might be caused by the heterotrophic activity during Anammox process. Since S_s is not completely removed in partial nitritation reactor, it can be expected that heterotrophs who use it as a carbon and energy source will grow in Anammox reactor. These bacteria can grow in anoxic environment by utilizing nitrite or nitrate as an electron acceptor. To compensate for this nitrite removal by heterotrophs nitrite-to-ammonia ratio in the outlet of partial nitritation step needs to be corrected.

Another indicator of heterotrophic activity in the Anammox reactor is the difference in ammonia (S_{NH}) and nitrite (S_{NO2}) initial utilisation rates. It can be expected that Anammox bacteria would simultaneously utilize ammonia and nitrite, however it can be seen that the concentration of nitrite initially decreases at a higher rate than the concentration of ammonia. This is due to anoxic growth of heterotrophs which are present in Anammox reactor. Using nitrite as electron acceptor heterotrophic bacteria also ensure removal of remaining soluble biodegradable COD S_s that was not completely removed in partial nitritation step. Apart from nitrite heterotrophs can also use nitrate as an electron acceptor. Nitrate is produced in the reactor by Anammox, but its concentration remains low due to heterotrophic activity.

Even better understanding of the processes taking place in Anammox reactor can be provided by analysis of different species distribution in a biofilm (Figure 31). The simulation results show that fast growing heterotrophs are the first to develop in a biofilm. These bacteria form a thin layer on the biofilm-bulk interface where the substrates are the most abundant. Fast removal of S_s and S_{NO2} is associated with the growth of heterotrophs. Ammonia S_{NH} is also utilized by heterotrophic bacteria but at a lesser extent. Effective removal of ammonia starts after the first few months when slow growing Anammox bacteria develop. Anammox occupy a specific niche in the inner layers of biofilm. In this niche concentration of substrates is normally lower, but Anammox cannot outcompete heterotrophs due to lower growth rates and slightly lower affinity for substrates. Slow growth rate of Anammox results in a long time necessary to reach steady state. Simulation showed that the bulk concentration of soluble species practically did not change after 200 days, while some changes for particulates could still be observed even after 2000 days of simulation.

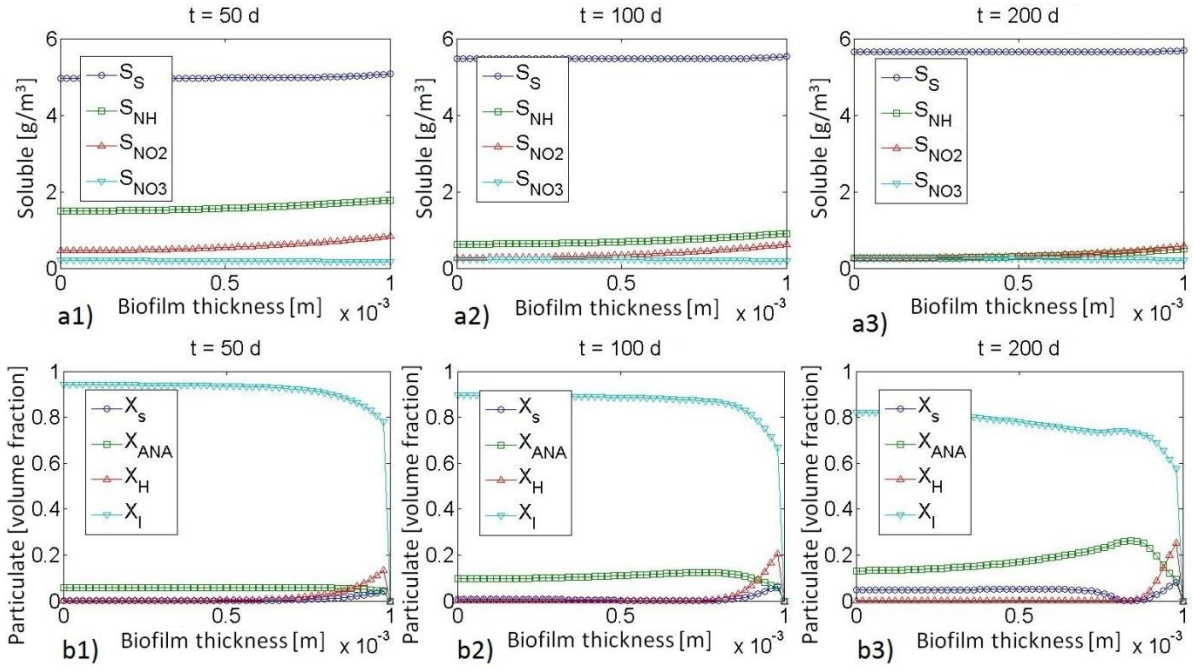

Figure 31. Soluble (a) and particulate (b) species distribution in biofilm in time.

Although heterotrophs force out Anammox to occupy the inner biofilm layers that are less rich with substrate, advantage can be taken from this bacteria distribution. Since heterotrophs would always grow on a biofilm-bulk interface they can be used as a buffer to protect Anammox from inhibiting compounds, such as oxygen. If the amount of oxygen can be controlled precisely so that it does not fully penetrate the granule, a very unique microbial community can develop where heterotrophs, AOB, NOB and Anammox coexist. In such system partial nitritation and Anammox processes can happen in the same reactor. This concept is implemented in CANON [75, 76] and OLAND [77] processes. A lot of literature is available both on practical implementation [86, 88, 89] and on simulation [30, 118] of these processes. In this work only the simulation of two-reactor configuration of partial nitritation and Anammox processes has been performed. Comparison of simulation results for one- and two-reactor configurations might be an interesting topic for further research.

4.3. Phosphorus removal

Along with nitrogen, phosphorus is an important nutrient for different types of organisms. The excessive amount of phosphorus in water can lead to eutrophication and oxygen depletion in water reservoirs. To avoid it phosphorus concentration in the dischargeable effluent is regulated by legislation [1].

In this work phosphorus removal and/or recovery is not considered, and it is assumed that phosphorus does not become a limiting nutrient in any of the processes. In a real plant however due to the strict effluent quality requirements a special operational unit for phosphorus removal and/or recovery needs to be provided.

Introducing a new operational unit in a system would induce several changes in the process modelling as well. First, new individual model for phosphorus removal/recovery unit would need to be provided. Second, all the individual models used for the simulation would need to be completely

rewritten or expanded for an extra state variable. ASM1-based models used in this work would need to be replaced by ASM2-based models [25] where phosphorus removal is already considered. ADM1 would require an extension to account for phosphorus removal. To our knowledge such extension has not been yet described in the literature, but according to Batstone et al [119] ADM1 extension that would account for phosphorus removal is going to be relatively simple. Third, new interfaces between ASM2 and ADM1 would need to be defined. Example of combining ADM1 and ASM2d models can be found in a paper of Kauder et al [120].

4.4. Overall system

Table below shows how the effluent characteristics of the system simulated comply with the EU legislation. The effluent characteristics are given for the system described in Table 7 for $X_{un}(in)$ = 200 $[gCOD/m^3]$.

Table 9. Modelled system output characteristics.

Name	Value	Limit (Urban Waste Water Treatment Directive [1])	Limit (Water Framework Directive [2])	Unit
Soluble biodegradable COD in the effluent	6.45	125		$\left[\frac{gCOD}{m^3}\right]$
Soluble non-biodegradable COD in the effluent	100			$\left[\frac{gCOD}{m^3}\right]$
Total suspended solids in the effluent	negligible	30		$\left[\frac{gCOD}{m^3}\right]$
Total nitrogen in the effluent	1.07	10	2.2	$\left[\frac{gN}{m^3}\right]$
Overall methane yield	0.302			$\left[\frac{m^3(CH_4)}{kgCOD_{in}}\right]$
Fraction of methane in the gas	0.70			$[-]$

Simulation results show that the modelled system is capable of producing the effluent, that would meet the discharge standards of existing and new EU legislation.

4.5. Validity of results

As it has already been mentioned the absolute values obtained during the simulation performed in this work should be treated with caution, because the validity of ASM1 used for the modelling of bioflocculation has not been checked for the extremely low $HRTs$ and $SRTs$. And the extrapolation of the region of validity of the model should not be done unless supported by the experimental data, which is outside the scope of the present work.

Another reason to treat the results of the simulation with caution is the lack of standard procedure for the component mapping on ASM1-ADM1 model interface. While interfacing between these models is addressed in several papers [37, 38, 110], no unified opinion on component mapping exists

at the moment. In case of the system described in this work the situation is even more unclear due to the necessity to consider unflocculated biodegradable particulates X_{un}, which are not accounted for in any of the standard models. Consequently, it is very unclear to which state variables of ADM1 X_{un} should be mapped to. In this work X_{un} is assigned to the state that was meant to deal with any complex organic particulates X_c. However, such mapping is not very consistent in terms of nitrogen balance. Thus further research on this matter is strongly suggested.

Regarding the modelling of AD it should be said that the ADM1 model used for simulation is a standard model that is widely applied for the simulation of anaerobic digestion process. It is known that several important phenomena taking place in digester are neglected in ADM1 in order to simplify the model. These simplifications were already mentioned in "Anaerobic Digestion" section but need to be stressed again for further model optimization [33]:

- Production of lactate from glucose fermentation;
- Sulphate reduction and sulphide inhibition;
- Nitrate reduction;
- LCFA inhibition;
- Competitive uptake of H_2 and CO_2 between hydrogenotrophic methanogenic archaea and acetogenic bacteria;
- Solids precipitation due to high alkalinity or other chemical precipitation reactions.

Neglecting of physicochemical processes such as solids precipitation should have consequences for ADM1 applications. It is known that solids removal during AD process is partially physical [121]. Neglecting such removal in a model means that the kinetic parameters used in the model are not purely kinetic but are in fact lumped. Such lumped parameters can be expected to have different values in different systems. For this reason recalibration of the model is required for each specific case. Similar conclusion was made by Ozkan-Yucel and Gökçay [35] who studied the application of ADM1 for the simulation of full-scale anaerobic digester. The authors reported that once the model was calibrated good correlation between the measured and simulated data could be observed.

Despite the lack of experimental data to validate the results obtained from the simulation of anaerobic carbon removal block the trends revealed by these simulations look promissing and can be taken into consideration when designing a wastewater treatment plant.

4.6. Numerical issues

Numerical issues in this work were mainly associated with the simulation of anaerobic digestion process. ADM1 used for the simulation of the AD process is known to be extremely stiff, as the range of time constants utilized by the model is very large. Solving the stiff problem with the solver that uses explicit integration method (such as ODE45) may result in extensively large computational times, which is rather undesirable. Stiff solvers are also available in MATLAB that are able to deal with the stiffness problem and require relatively short computation times (such as ODE15s, ODE23s, ODE23t and ODE23tb).

However, using the stiff solver alone appeared to be insufficient to deal with the peculiarities of ADM1. To further reduce system stiffness, differential equations describing the state variables characterized by the shortest time constants might be replaced by the algebraic ones. Such

simplification reflects the fact that some state variables react much quicker on the changes in the system than the others, and can thus be considered at quasi-equilibrium at any time.

In the original paper of Batstone et al [29] pH is already given by the implicit algebraic equation (charge balance), and it is suggested that the acid-base pairs of short chain fatty acids can be assumed at equilibrium, thus can also be calculated from the algebraic equations. Rosen and Jeppsson [63] implemented such model in MATLAB/Simulink environment and reported that using algebraic equation for pH helps to reduce stiffness of the model but to a very limited extent. They further suggested using algebraic equations for both pH and S_{H_2} states. The authors reported that such simplification drastically reduced system stiffness, and as a consequence – the use of non-stiff solvers became reasonable.

Rosen and Jeppsson [63] used Newton-Raphson method to solve implicit algebraic equations for pH and S_{H_2}. In this work however different approach was used: advantage has been taken of ODE15s and ODE23t being able to solve differential-algebraic equation (DAE) problems. ODE15s was chosen because of the shorter computational time. Using the stiff solver implies that it might no longer be necessary to find S_{H_2} from algebraic equation, but it appeared that the model failed to reach steady-state when it was not done. Apart from that it was found that the model fails to converge at crude tolerances.

Generally the model analysis was dampened a lot by the model failing to converge due to the poor choice of initial conditions. It is generally acknowledged that solving DAE problems is far more difficult task compared to ODE problems [122]. Particularly, finding consistent initial conditions for DAE system is regarded as a complex problem on its own. In fact poor choice of initial conditions may cause some solvers to diverge at first step, converge slowly or converge to an undesired solution [123].

Assuming constant pH as a control handle in digester would significantly reduce the computational effort, since in that case there would be no need to consider pH as a state variable and consequently – no need to use DAE solver. For one-stage AD configuration assuming constant pH is not possible. If pH is set to 7 - an optimal value for methanogens – the first stages of the process are completely inhibited and no intermediates are produced that can be used as substrates by methanogens. Thus digestion performance is poor again. Figure 32 shows pH change in the digester for the system characterized in Table 5. It can be seen that at first stage pH in the digester is low. This is associated with the acid production by the acidogenic microorganisms. When a sufficient amount of acid is produced acetogenic and methanogenic microorganisms start to grow. These organisms consume acids so pH steadily grows and stabilizes around neutral values. This initial pH drop is very important for the process start-up and is also the main reason why it is impossible to set constant pH in one-stage AD.

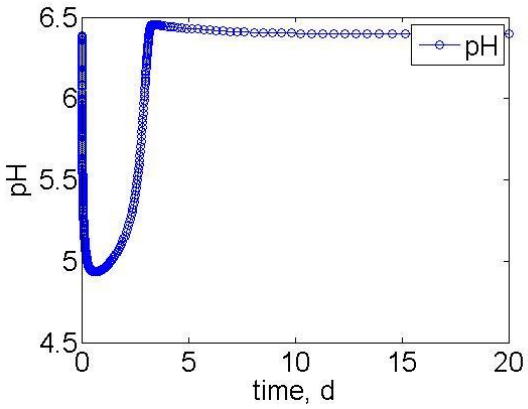

Figure 32. pH change in one-stage digester.

For two-stage configuration controlling the conditions in each of the two reactors is possible. Therefore, an optimal environment can be provided for different microorganisms. Such system appears to be both safer to operate and significantly easier to model.

5. Conclusions

Overall system

- Dynamic grey-box model for the simulation of the promising scenario for municipal wastewater treatment in the Netherlands has been developed.
- The simulation results showed that the system modelled is capable of providing the effluent that would meet the discharge standards of existing and new EU legislation.

Bioflocculation and Anaerobic Digestion

- Once the model is calibrated it can be used to adjust operational conditions in bioflocculation reactor to ensure optimal methane production in anaerobic digestion process.
- Operating the bioflocculation process at low HRT in order to concentrate COD to enhance AD performance may in fact result in an opposite effect due to the overloading of digester.
- Separating the anaerobic digestion in two stages (first stage – hydrolysis and acidogenesis, second stage – acetogenesis and methanogenesis) significantly reduces the computational effort necessary for the modelling. Furthermore, such separation makes the system more robust, since the first digester acts as a buffer for the second stage, and its overloading does not result in a whole process failure. Two-stage approach, however, might be associated with the higher investment and operational costs, as well as lower overall process sustainability. Higher costs are related to the necessity to install additional digester, while lower process sustainability – with the necessity to supply acids/bases in order to control pH in one or both digesters.

Remark. General structure of the bioflocculation model has been proposed in this work. Model calibration has not been performed. Trends predicted by the proposed model seem reasonable; however it is suggested to treat the results of the simulation with caution due to the lack of experimental proof of the proposed ideas.

Partial Nitritation and Anammox

- Models described in this work can be used to find the optimal operating conditions for partial nitritation reactor that would ensure efficient nitrogen removal in Anammox process.
- For the system described in this work, nitrogen concentration in the effluent that would meet the maximum discharge guideline value of 2.2 gN/m^3 of the new EU legislation can only be achieved when partial nitritation reactor is operated at temperatures above 25^{o}C.
- A very precise control of the operational conditions is necessary to achieve the effluent quality that would meet the requirements of new EU legislation. Controls of the system units need to be coupled with sensors to assess the influent quality. Automatic adjustment of operational conditions to changes in the influent should be provided.
- At higher temperatures less precise control is allowed. However, this comes at a cost of energy that needs to be provided to maintain the desired temperature.

6. Recommendations

Overall system

- Calculate the energy consumption and expenses associated with the process.
- Re-introduce the back-loops to the system as it was originally suggested by Khiewwijit, 2013.

Bioflocculation

- Model the process using the SMP-ASM models expanded for a bioflocculation/adsorption step.
- Calibrate the model proposed in this work using the experimental data.
- Include the effect of membrane clogging due to high biomass concentration in the reactor.
- Use air flow rate Q_G as a control handle instead of oxygen mass transfer coefficient $K_{OL}a$.

Anaerobic Digestion

- Study the effect of varying controls of AD. In this work all the values for control handles were assumed to be fixed.
- Modify the code for one-stage AD configuration to automatically adjust initial conditions vector.
- Study the interfacing between ASM and ADM1 models. Experimental data might be required.
- Consider co-digestion of different waste streams. Study the effect on combining different wastes on process performance.
- Include the inhibiting effect of sulphate.

Partial Nitritation

- Simulate the process using ASM-SMP models. These models consider SMP formation that has a major effect on membrane fouling. Such simulation results might be more accurate and more useful for practical applications since they can be used to predict cake-layer formation.
- Compare the simulation results of process taking place in MBR and CSTR without retention (SHARON process). In order to use the code to SHARON process parameter values need to be changed, because of the difference in kinetic parameters in CSTR and MBR.
- Use air flow rate Q_G as a control handle instead of oxygen mass transfer coefficient $K_{OL}a$.

Anammox

- Expand the model to account for biofilm growth.
- Consider the boundary layer around the granule.
- Model the process for PFR instead of CSTR.
- Study the effect of control handles on the process performance.
- Simulate and compare two-reactor and one-reactor (CANON or OLAND) configurations.

Phosphorus removal

- Include phosphorus removal.

Reference list

[1] E. Commission, "Council Directive 91/271/EEC of 21 May 1991 concerning urban waste-water treatment," *Official Journal No. L,* vol. 135, p. 1991, 1991.

[2] E. W. F. Directive, "EU-Water Framework Directive 2000/60/EC Council Directive 2000/60," *EC of,* vol. 23, 2000.

[3] Y. Liu and H. H. Fang, "Influences of extracellular polymeric substances (EPS) on flocculation, settling, and dewatering of activated sludge," 2003.

[4] L. Hernández Leal, H. Temmink, G. Zeeman, and C. Buisman, "Bioflocculation of grey water for improved energy recovery within decentralized sanitation concepts," *Bioresource Technology,* vol. 101, pp. 9065-9070, 2010.

[5] S. Aiyuk, I. Forrez, D. K. Lieven, A. Van Haandel, and W. Verstraete, "Anaerobic and complementary treatment of domestic sewage in regions with hot climates—A review," *Bioresource Technology,* vol. 97, pp. 2225-2241, 2006.

[6] P. McCarty, "The development of anaerobic treatment and its future," *Water science and technology: a journal of the International Association on Water Pollution Research,* vol. 44, p. 149, 2001.

[7] A. J. Ward, P. J. Hobbs, P. J. Holliman, and D. L. Jones, "Optimisation of the anaerobic digestion of agricultural resources," *Bioresource Technology,* vol. 99, pp. 7928-7940, 2008.

[8] G. Tchobanoglous, F. L. Burton, and H. D. Stensel, "Wastewater engineering: treatment and reuse. Metcalf & Eddy," *Inc., McGraw-Hill, New York,* 2003.

[9] S. Wyffels, S. W. Van Hulle, P. Boeckx, E. I. Volcke, O. V. Cleemput, P. A. Vanrolleghem, and W. Verstraete, "Modeling and simulation of oxygen-limited partial nitritation in a membrane-assisted bioreactor (MBR)," *Biotechnology and Bioengineering,* vol. 86, pp. 531-542, 2004.

[10] A. Mulder, A. Graaf, L. Robertson, and J. Kuenen, "Anaerobic ammonium oxidation discovered in a denitrifying fluidized bed reactor," *FEMS Microbiology Ecology,* vol. 16, pp. 177-184, 1995.

[11] M. S. de Graaff, H. Temmink, G. Zeeman, M. C. M. van Loosdrecht, and C. J. N. Buisman, "Autotrophic nitrogen removal from black water: Calcium addition as a requirement for settleability," *Water Research,* vol. 45, pp. 63-74, Jan 2011.

[12] M. Strous, J. Heijnen, J. Kuenen, and M. Jetten, "The sequencing batch reactor as a powerful tool for the study of slowly growing anaerobic ammonium-oxidizing microorganisms," *Applied microbiology and biotechnology,* vol. 50, pp. 589-596, 1998.

[13] L. Zhang, P. Zheng, C.-j. Tang, and J. Ren-cun, "Anaerobic ammonium oxidation for treatment of ammonium-rich wastewaters," *Journal of Zhejiang University Science B,* vol. 9, pp. 416-426, 2008.

[14] U. van Dongen, M. Jetten, and M. Van Loosdrecht, "The SHARON-Anammox process for treatment of ammonium rich wastewater," *Water science and technology: a journal of the International Association on Water Pollution Research,* vol. 44, p. 153, 2001.

[15] D. Paredes, P. Kuschk, T. Mbwette, F. Stange, R. Müller, and H. Köser, "New aspects of microbial nitrogen transformations in the context of wastewater treatment–a review," *Engineering in Life Sciences,* vol. 7, pp. 13-25, 2007.

[16] J. Vazquez-Padın, M. Figueroa, I. Fernandez, A. Mosquera-Corral, J. Campos, and R. Mendez, "Post-treatment of effluents from anaerobic digesters by the Anammox process," 2009.

[17] J. E. Bailey, "Mathematical modeling and analysis in biochemical engineering: past accomplishments and future opportunities," *Biotechnology Progress,* vol. 14, pp. 8-20, 1998.

[18] C. Picioreanu, M. v. Loosdrecht, and P. Lens, "Use of mathematical modelling to study biofilm development and morphology," 2003.

[19] J. Carstensen, P. Vanrolleghem, W. Rauch, and P. Reichert, "Terminology and methodology in modelling for water quality management—a discussion starter," *Water Science and Technology,* vol. 36, pp. 157-168, 1997.
[20] R. Romijn, L. Özkan, S. Weiland, J. Ludlage, and W. Marquardt, "A grey-box modeling approach for the reduction of nonlinear systems," *Journal of Process Control,* vol. 18, pp. 906-914, 2008.
[21] R. Aarts, "System identification and parameter estimation," 1998.
[22] G. Marais and G. Ekama, "The activated sludge process part I-steady state behaviour," *Water SA,* vol. 2, pp. 164-200, 1976.
[23] G. Ekama and G. v. R. Marais, "Dynamic behavior of the activated sludge process," *Journal (Water Pollution Control Federation),* pp. 534-556, 1979.
[24] P. Dold, G. Ekama, and G. Marais, "A general model for the activated sludge process," *Progress in Water Technology,* vol. 12, 1980.
[25] M. Henze, *Activated sludge models: ASM1, ASM2, ASM2d and ASM3* vol. 9: International Water Assn, 2000.
[26] W. Gujer, M. Henze, T. Mino, T. Matsuo, M. Wentzel, and G. Marais, "The activated sludge model No. 2: biological phosphorus removal," *Water Science and Technology,* vol. 31, pp. 1-11, 1995.
[27] M. Henze, W. Gujer, T. Mino, T. Matsuo, M. C. Wentzel, and M. Van Loosdrecht, "Activated sludge model no. 2d, ASM2d," *Water Science and Technology,* vol. 39, pp. 165-182, 1999.
[28] W. Gujer, M. Henze, T. Mino, and M. v. Loosdrecht, "Activated sludge model no. 3," *Water Science and Technology,* vol. 39, pp. 183-193, 1999.
[29] D. J. Batstone, J. Keller, I. Angelidaki, S. Kalyuzhnyi, S. Pavlostathis, A. Rozzi, W. Sanders, H. Siegrist, and V. Vavilin, "The IWA Anaerobic Digestion Model No 1(ADM 1)," *Water Science & Technology,* vol. 45, pp. 65-73, 2002.
[30] X. Hao, J. J. Heijnen, and M. Van Loosdrecht, "Model-based evaluation of temperature and inflow variations on a partial nitrification–ANAMMOX biofilm process," *Water Research,* vol. 36, pp. 4839-4849, 2002.
[31] B. J. Ni, Y. P. Chen, S. Y. Liu, F. Fang, W. M. Xie, and H. Q. Yu, "Modeling a granule-based anaerobic ammonium oxidizing (ANAMMOX) process," *Biotechnology and Bioengineering,* vol. 103, pp. 490-499, 2009.
[32] S. W. Van Hulle, E. I. Volcke, J. L. Teruel, B. Donckels, M. van Loosdrecht, and P. A. Vanrolleghem, "Influence of temperature and pH on the kinetics of the Sharon nitritation process," *Journal of Chemical Technology and Biotechnology,* vol. 82, pp. 471-480, 2007.
[33] F. Blumensaat and J. Keller, "Modelling of two-stage anaerobic digestion using the IWA Anaerobic Digestion Model No. 1 (ADM1)," *Water Research,* vol. 39, pp. 171-183, 2005.
[34] F. Boubaker and B. C. Ridha, "Modelling of the mesophilic anaerobic co-digestion of olive mill wastewater with olive mill solid waste using anaerobic digestion model No. 1 (ADM1)," *Bioresource Technology,* vol. 99, p. 6565, 2008.
[35] U. Ozkan-Yucel and C. Gökçay, "Application of ADM1 model to a full-scale anaerobic digester under dynamic organic loading conditions," *Environmental technology,* vol. 31, pp. 633-640, 2010.
[36] C. Rosen, D. Vrecko, K. Gernaey, M.-N. Pons, and U. Jeppsson, "Implementing ADM 1 for plant-wide benchmark simulations in Matlab/Simulink," *Water Science & Technology,* vol. 54, pp. 11-19, 2006.
[37] I. Nopens, D. J. Batstone, J. B. Copp, U. Jeppsson, E. Volcke, J. Alex, and P. A. Vanrolleghem, "An ASM/ADM model interface for dynamic plant-wide simulation," *Water Research,* vol. 43, pp. 1913-1923, 2009.
[38] P. A. Vanrolleghem, C. Rosen, U. Zaher, J. Copp, L. Benedetti, E. Ayesa, and U. Jeppsson, "Continuity-based interfacing of models for wastewater systems described by Petersen matrices," *Water Science & Technology,* vol. 52, pp. 493-500, 2005.

[39] O. Wanner and W. Gujer, "A multispecies biofilm model," *Biotechnology and Bioengineering,* vol. 28, pp. 314-328, 1986.
[40] J. L. Pavoni, M. W. Tenney, and W. F. Echelberger Jr, "Bacterial exocellular polymers and biological flocculation," *Journal (Water Pollution Control Federation),* pp. 414-431, 1972.
[41] S. B. Subramanian, S. Yan, R. Tyagi, R. Surampalli, and B. Lohani, "Isolation and molecular identification of extracellular polymeric substances (EPS) producing bacterial strains for sludge settling and dewatering," *Journal of Environmental Science and Health Part A,* vol. 43, pp. 1495-1503, 2008.
[42] B. Frolund, T. Griebe, and P. H. Nielsen, "Enzymatic activity in the activated-sludge floc matrix," *Applied microbiology and biotechnology,* vol. 43, pp. 755-761, 1995.
[43] E. Foresti, "Anaerobic treatment of domestic sewage: established technologies and perspectives," *Water Science & Technology,* vol. 45, pp. 181-186, 2002.
[44] T. A. Elmitwalli, J. Soellner, A. De Keizer, H. Bruning, G. Zeeman, and G. Lettinga, "Biodegradability and change of physical characteristics of particles during anaerobic digestion of domestic sewage," *Water Research,* vol. 35, pp. 1311-1317, 2001.
[45] I. Akanyeti, H. Temmink, M. Remy, and A. Zwijnenburg, "Feasibility of bioflocculation in a high-loaded membrane bioreactor for improved energy recovery from sewage," *Water Science and Technology,* vol. 61, pp. 1433-1439, 2010.
[46] H. Y. Ng and S. W. Hermanowicz, "Membrane bioreactor operation at short solids retention times: performance and biomass characteristics," *Water Research,* vol. 39, pp. 981-992, 2005.
[47] A. Fenu, G. Guglielmi, J. Jimenez, M. Spèrandio, D. Saroj, B. Lesjean, C. Brepols, C. Thoeye, and I. Nopens, "Activated sludge model (ASM) based modelling of membrane bioreactor (MBR) processes: A critical review with special regard to MBR specificities," *Water Research,* vol. 44, pp. 4272-4294, 2010.
[48] S. Rosenberger, H. Evenblij, S. Te Poele, T. Wintgens, and C. Laabs, "The importance of liquid phase analyses to understand fouling in membrane assisted activated sludge processes—six case studies of different European research groups," *Journal of Membrane Science,* vol. 263, pp. 113-126, 2005.
[49] D. J. Barker and D. C. Stuckey, "A review of soluble microbial products (SMP) in wastewater treatment systems," *Water Research,* vol. 33, pp. 3063-3082, 1999.
[50] E. Namkung and B. E. Rittmann, "Soluble microbial products (SMP) formation kinetics by biofilms," *Water Research,* vol. 20, pp. 795-806, 1986.
[51] L. G. Blackwell, "A theoretical and experimental evaluation of the transient response of the activated sludge process," Clemson University, 1971.
[52] S. H. Baek, S. K. Jeon, and K. Pagilla, "Mathematical modeling of aerobic membrane bioreactor (MBR) using activated sludge model no. 1 (ASM1)," *Journal of Industrial and Engineering Chemistry,* vol. 15, pp. 835-840, 2009.
[53] T. Janus and B. Ulanicki, "Modelling SMP and EPS formation and degradation kinetics with an extended ASM3 model," *Desalination,* vol. 261, pp. 117-125, 2010.
[54] D. F. Toerien and W. H. J. Hattingh, "Anaerobic digestion I. The microbiology of anaerobic digestion," *Water Research,* vol. 3, pp. 385-416, 1969.
[55] J. Steyer, O. Bernard, D. J. Batstone, and I. Angelidaki, "Lessons learnt from 15 years of ICA in anaerobic digesters," *Instrumentation, Control and Automation for Water and Wastewater Treatment and Transport Systems IX,* vol. 53, pp. 25-33, 2006.
[56] P. Vandevivere, "New and broader applications of anaerobic digestion," *Critical Reviews in Environmental Science and Technology,* vol. 29, pp. 151-173, 1999.
[57] G. Esposito, L. Frunzo, A. Giordano, F. Liotta, A. Panico, and F. Pirozzi, "Anaerobic co-digestion of organic wastes," *Reviews in Environmental Science and Bio/Technology,* vol. 11, pp. 325-341, 2012.

[58] L. Seghezzo, G. Zeeman, J. B. van Lier, H. Hamelers, and G. Lettinga, "A review: the anaerobic treatment of sewage in UASB and EGSB reactors," *Bioresource Technology,* vol. 65, pp. 175-190, 1998.

[59] G. Lyberatos and P. C. Pullammanappallil, "Anaerobic digestion in suspended growth bioreactors," in *Environmental Biotechnology*, ed: Springer, 2010, pp. 395-438.

[60] Y. Chen, J. J. Cheng, and K. S. Creamer, "Inhibition of anaerobic digestion process: a review," *Bioresource Technology,* vol. 99, pp. 4044-4064, 2008.

[61] J. Lauwers, L. Appels, I. P. Thompson, J. Degrève, J. F. Van Impe, and R. Dewil, "Mathematical modelling of anaerobic digestion of biomass and waste: Power and limitations," *Progress in Energy and Combustion Science,* 2013.

[62] L. De Baere, "Anaerobic digestion of solid waste: state-of-the-art," *Water Science and Technology,* pp. 283-290, 2000.

[63] C. Rosén and U. Jeppsson, "Aspects on ADM1 implementation within the BSM2 framework," *Department of Industrial Electrical Engineering and Automation, Lund University, Lund, Sweden,* 2006.

[64] A. Viturtia, J. Mata-Alvarez, F. Cecchi, and G. Fazzini, "Two-phase anaerobic digestion of a mixture of fruit and vegetable wastes," *Biological wastes,* vol. 29, pp. 189-199, 1989.

[65] M. Kayhanian, "Performance of a high-solids anaerobic digestion process under various ammonia concentrations," *Journal of Chemical Technology and Biotechnology,* vol. 59, pp. 349-352, 1994.

[66] L. De Baere, M. Devocht, P. Van Assche, and W. Verstraete, "Influence of high NaCl and NH< sub> 4</sub> Cl salt levels on methanogenic associations," *Water Research,* vol. 18, pp. 543-548, 1984.

[67] A. Hierholtzer and J. C. Akunna, "Modelling sodium inhibition on the anaerobic digestion process," *Water Science and Technology,* vol. 66, pp. 1565-1573, 2012.

[68] B. L. Vallee and D. D. Ulmer, "Biochemical effects of mercury, cadmium, and lead," *Annual review of biochemistry,* vol. 41, pp. 91-128, 1972.

[69] A. Rinzema, M. Boone, K. van Knippenberg, and G. Lettinga, "Bactericidal effect of long chain fatty acids in anaerobic digestion," *Water Environment Research,* pp. 40-49, 1994.

[70] Ž. Zonta, M. Alves, X. Flotats, and J. Palatsi, "Modelling inhibitory effects of long chain fatty acids in the anaerobic digestion process," *Water Research,* 2012.

[71] H. F. Kaspar and K. Wuhrmann, "Product inhibition in sludge digestion," *Microbial ecology,* vol. 4, pp. 241-248, 1977.

[72] Y. Miron, G. Zeeman, J. B. Van Lier, and G. Lettinga, "The role of sludge retention time in the hydrolysis and acidification of lipids, carbohydrates and proteins during digestion of primary sludge in CSTR systems," *Water Research,* vol. 34, pp. 1705-1713, 2000.

[73] P. Weiland, "Biogas production: current state and perspectives," *Applied microbiology and biotechnology,* vol. 85, pp. 849-860, 2010.

[74] M. S. Jetten, M. Wagner, J. Fuerst, M. van Loosdrecht, G. Kuenen, and M. Strous, "Microbiology and application of the anaerobic ammonium oxidation (‘anammox’) process," *Current Opinion in Biotechnology,* vol. 12, pp. 283-288, 2001.

[75] K. Third, A. O. Sliekers, J. Kuenen, and M. Jetten, "The CANON system (completely autotrophic nitrogen-removal over nitrite) under ammonium limitation: interaction and competition between three groups of bacteria," *Systematic and Applied Microbiology,* vol. 24, pp. 588-596, 2001.

[76] A. O. Sliekers, N. Derwort, J. Gomez, M. Strous, J. Kuenen, and M. Jetten, "Completely autotrophic nitrogen removal over nitrite in one single reactor," *Water Research,* vol. 36, pp. 2475-2482, 2002.

[77] L. Kuai and W. Verstraete, "Ammonium removal by the oxygen-limited autotrophic nitrification-denitrification system," *Applied and Environmental Microbiology,* vol. 64, pp. 4500-4506, 1998.

[78] Y.-H. Ahn, "Sustainable nitrogen elimination biotechnologies: A review," *Process Biochemistry,* vol. 41, pp. 1709-1721, 2006.

[79] A. Magrí, M. B. Vanotti, A. A. Szögi, and K. B. Cantrell, "Partial nitritation of swine wastewater in view of its coupling with the anammox process," *Journal of environmental quality,* vol. 41, pp. 1989-2000, 2012.

[80] S. Wyffels, P. Boeckx, K. Pynaert, W. Verstraete, and O. Van Cleemput, "Sustained nitrite accumulation in a membrane-assisted bioreactor (MBR) for the treatment of ammonium-rich wastewater," *Journal of Chemical Technology and Biotechnology,* vol. 78, pp. 412-419, 2003.

[81] Y.-J. Feng, S.-K. Tseng, T.-H. Hsia, C.-M. Ho, and W.-P. Chou, "Partial nitrification of ammonium-rich wastewater as pretreatment for anaerobic ammonium oxidation (Anammox) using membrane aeration bioreactor," *Journal of bioscience and bioengineering,* vol. 104, pp. 182-187, 2007.

[82] C. Fux, M. Boehler, P. Huber, I. Brunner, and H. Siegrist, "Biological treatment of ammonium-rich wastewater by partial nitritation and subsequent anaerobic ammonium oxidation (anammox) in a pilot plant," *Journal of Biotechnology,* vol. 99, pp. 295-306, 2002.

[83] A. Dapena-Mora, J. Campos, A. Mosquera-Corral, M. Jetten, and R. Méndez, "Stability of the ANAMMOX process in a gas-lift reactor and a SBR," *Journal of Biotechnology,* vol. 110, pp. 159-170, 2004.

[84] M. Strous, E. Van Gerven, P. Zheng, J. G. Kuenen, and M. S. Jetten, "Ammonium removal from concentrated waste streams with the anaerobic ammonium oxidation (anammox) process in different reactor configurations," *Water Research,* vol. 31, pp. 1955-1962, 1997.

[85] K. Egli, U. Fanger, P. J. Alvarez, H. Siegrist, J. R. van der Meer, and A. J. Zehnder, "Enrichment and characterization of an anammox bacterium from a rotating biological contactor treating ammonium-rich leachate," *Archives of Microbiology,* vol. 175, pp. 198-207, 2001.

[86] K. M. Udert, E. Kind, M. Teunissen, S. Jenni, and T. A. Larsen, "Effect of heterotrophic growth on nitritation/anammox in a single sequencing batch reactor," *Water science and technology: a journal of the International Association on Water Pollution Research,* vol. 58, p. 277, 2008.

[87] A. Daverey, S.-H. Su, Y.-T. Huang, S.-S. Chen, S. Sung, and J.-G. Lin, "Partial nitrification and anammox process: A method for high strength optoelectronic industrial wastewater treatment," *Water Research,* 2013.

[88] A. O. Sliekers, K. Third, W. Abma, J. Kuenen, and M. Jetten, "CANON and Anammox in a gas-lift reactor," *Fems Microbiology Letters,* vol. 218, pp. 339-344, 2003.

[89] H. De Clippeleir, S. E. Vlaeminck, F. De Wilde, K. Daeninck, M. Mosquera, P. Boeckx, W. Verstraete, and N. Boon, "One-stage partial nitritation/anammox at 15° C on pretreated sewage: feasibility demonstration at lab-scale," *Applied microbiology and biotechnology,* pp. 1-12, 2013.

[90] Y.-H. Ahn and H.-C. Choi, "Autotrophic nitrogen removal from sludge digester liquids in upflow sludge bed reactor with external aeration," *Process Biochemistry,* vol. 41, pp. 1945-1950, 2006.

[91] F.-Y. Sun, Y.-J. Yang, W.-Y. Dong, and J. Li, "Granulation of Nitrifying Bacteria in a Sequencing Batch Reactor for Biological Stabilisation of Source-Separated Urine," *Applied biochemistry and biotechnology,* vol. 166, pp. 2114-2126, 2012.

[92] S. Tsuneda, S. Park, H. Hayashi, J. Jung, and A. Hirata, "Enhancement of nitrifying biofilm formation using selected EPS produced by heterotrophic bacteria," *Water science and technology: a journal of the International Association on Water Pollution Research,* vol. 43, p. 197, 2001.

[93] J. Mulder, M. Van Loosdrecht, C. Hellinga, and R. Van Kempen, "Full-scale application of the SHARON process for treatment of rejection water of digested sludge dewatering," *Water Science and Technology,* pp. 127-134, 2001.

[94] T. Jiang, G. Sin, H. Spanjers, I. Nopens, M. D. Kennedy, W. van der Meer, H. Futselaar, G. Amy, and P. A. Vanrolleghem, "Comparison of the modeling approach between membrane

bioreactor and conventional activated sludge processes," *Water Environment Research,* vol. 81, pp. 432-440, 2009.

[95] H.-S. Shin and S.-T. Kang, "Characteristics and fates of soluble microbial products in ceramic membrane bioreactor at various sludge retention times," *Water Research,* vol. 37, pp. 121-127, 2003.

[96] W.-M. Xie, B.-J. Ni, T. Seviour, G.-P. Sheng, and H.-Q. Yu, "Characterization of autotrophic and heterotrophic soluble microbial product (SMP) fractions from activated sludge," *Water Research,* vol. 46, pp. 6210-6217, 2012.

[97] A. C. Anthonisen, R. C. Loehr, T. B. S. Prakasam, and E. G. Srinath, "Inhibition of Nitrification by Ammonia and Nitrous Acid," *Journal (Water Pollution Control Federation),* vol. 48, pp. 835-852, 1976.

[98] C. Hellinga, M. C. M. Van Loosdrecht, and J. J. Heijnen, "Model based design of a novel process for nitrogen removal from concentrated flows," *Mathematical and Computer Modelling of Dynamical Systems,* vol. 5, pp. 351-371, Dec 1999.

[99] S. Villaverde, P. Garcia-Encina, and F. Fdz-Polanco, "Influence of pH over nitrifying biofilm activity in submerged biofilters," *Water Research,* vol. 31, pp. 1180-1186, 1997.

[100] M. S. Jetten, L. v. Niftrik, M. Strous, B. Kartal, J. T. Keltjens, and H. J. Op den Camp, "Biochemistry and molecular biology of anammox bacteria," *Critical reviews in biochemistry and molecular biology,* vol. 44, pp. 65-84, 2009.

[101] E. Morgenroth, H. Eberl, M. Van Loosdrecht, D. Noguera, G. Pizarro, C. Picioreanu, B. E. Rittmann, A. Schwarz, and O. Wanner, "Comparing biofilm models for a single species biofilm system," *Water Science & Technology,* vol. 49, pp. 145-154, 2004.

[102] H. Eberl, M. van Loosdrecht, E. Morgenroth, D. Noguera, J. Perez, C. Picioreanu, B. E. Rittmann, A. Schwarz, and O. Wanner, "Modelling a spatially heterogeneous biofilm and the bulk fluid: Selected results from benchmark problem 2(BM 2)," *Water Science & Technology,* vol. 49, pp. 155-162, 2004.

[103] B. E. Rittmann, A. Schwarz, H. Eberl, E. Morgenroth, J. Perez, M. Van Loosdrecht, and O. Wanner, "Results from the multi-species benchmark problem (BM3) using one-dimensional models," *Water science and technology: a journal of the International Association on Water Pollution Research,* vol. 49, p. 163, 2004.

[104] M. Van Loosdrecht, J. Heijnen, H. Eberl, J. Kreft, and C. Picioreanu, "Mathematical modelling of biofilm structures," *Antonie van Leeuwenhoek,* vol. 81, pp. 245-256, 2002.

[105] J.-U. Kreft, C. Picioreanu, J. W. Wimpenny, and M. C. van Loosdrecht, "Individual-based modelling of biofilms," *Microbiology,* vol. 147, pp. 2897-2912, 2001.

[106] C. Picioreanu, M. C. van Loosdrecht, and J. J. Heijnen, "A new combined differential-discrete cellular automaton approach for biofilm modeling: application for growth in gel beads," *Biotechnology and Bioengineering,* vol. 57, pp. 718-731, 1998.

[107] E. Alpkvist, C. Picioreanu, M. van Loosdrecht, and A. Heyden, "Three-dimensional biofilm model with individual cells and continuum EPS matrix," *Biotechnology and Bioengineering,* vol. 94, pp. 961-979, 2006.

[108] E. Morgenroth, M. Van Loosdrecht, and O. Wanner, "Biofilm models for the practitioner," *Water Science & Technology,* vol. 41, pp. 509-512, 2000.

[109] M. N. Young, A. K. Marcus, and B. E. Rittmann, "A Combined Activated Sludge Anaerobic Digestion Model (CASADM) to Understand the Role of Anaerobic Sludge Recycling in Wastewater Treatment Plant Performance," *Bioresource Technology,* 2013.

[110] U. Zaher, P. Grau, L. Benedetti, E. Ayesa, and P. Vanrolleghem, "Transformers for interfacing anaerobic digestion models to pre-and post-treatment processes in a plant-wide modelling context," *Environmental Modelling & Software,* vol. 22, pp. 40-58, 2007.

[111] H. Siegrist, D. Vogt, J. L. Garcia-Heras, and W. Gujer, "Mathematical model for meso-and thermophilic anaerobic sewage sludge digestion," *Environmental science & technology,* vol. 36, pp. 1113-1123, 2002.

[112] M. Spérandio and M. Espinosa, "Modelling an aerobic submerged membrane bioreactor with ASM models on a large range of sludge retention time," *Desalination,* vol. 231, pp. 82-90, 2008.
[113] F. Pohland and S. Ghosh, "Developments in anaerobic stabilization of organic wastes-the two-phase concept," *Environmental Letters,* vol. 1, pp. 255-266, 1971.
[114] P. S. Jagadabhi, P. Kaparaju, and J. Rintala, "Two-stage anaerobic digestion of tomato, cucumber, common reed and grass silage in leach-bed reactors and upflow anaerobic sludge blanket reactors," *Bioresource Technology,* vol. 102, pp. 4726-4733, 2011.
[115] J. Liu, G. Olsson, and B. Mattiasson, "On-line monitoring of a two-stage anaerobic digestion process using a BOD analyzer," *Journal of Biotechnology,* vol. 109, pp. 263-275, 2004.
[116] W. Parawira, M. Murto, J. Read, and B. Mattiasson, "A study of two-stage anaerobic digestion of solid potato waste using reactors under mesophilic and thermophilic conditions," *Environmental technology,* vol. 28, pp. 1205-1216, 2007.
[117] H. Bouallagui, Y. Touhami, R. Ben Cheikh, and M. Hamdi, "Bioreactor performance in anaerobic digestion of fruit and vegetable wastes," *Process Biochemistry,* vol. 40, pp. 989-995, 2005.
[118] A. K. Vangsgaard, M. Mauricio-Iglesias, K. V. Gernaey, B. F. Smets, and G. Sin, "Sensitivity analysis of autotrophic N removal by a granule based bioreactor: Influence of mass transfer versus microbial kinetics," *Bioresource Technology,* 2012.
[119] D. Batstone, J. Keller, and J. Steyer, "A review of ADM1 extensions, applications, and analysis: 2002-2005," *Water Science & Technology,* vol. 54, pp. 1-10, 2006.
[120] J. Kauder, N. Boes, C. Pasel, and J. D. Herbell, "Combining models ADM1 and ASM2d in a sequencing batch reactor simulation," *Chemical Engineering & Technology,* vol. 30, pp. 1100-1112, 2007.
[121] G. Zeeman, H. Temmink, and C. Buisman, "Characterisation and biological treatment of greywater," *Water Science & Technology,* vol. 56, pp. 193-200, 2007.
[122] L. R. Petzold, "Recent developments in the numerical solution of differential/algebraic systems," *Computer Methods in Applied Mechanics and Engineering,* vol. 75, pp. 77-89, 1989.
[123] P. Li, Y. Li, and J. E. Seem, "Consistent initialization of system of differential-algebraic equations for dynamic simulation of centrifugal chillers," *Journal of Building Performance Simulation,* vol. 5, pp. 115-139, 2012.
[124] J. R. Welty, C. E. Wicks, G. Rorrer, and R. E. Wilson, *Fundamentals of momentum, heat, and mass transfer*: John Wiley & Sons, 2009.
[125] S. Judd, *The MBR Book: Principles and Applications of Membrane Bioreactors for Water and Wastewater Treatment*: Elsevier, 2010.
[126] D. Rosso, R. Iranpour, and M. Stenstrom, "Fifteen years of offgas transfer efficiency measurements on fine-pore aerators: Key role of sludge age and normalized air flux," *Water Environment Research,* pp. 266-273, 2005.
[127] E. Germain, F. Nelles, A. Drews, P. Pearce, M. Kraume, E. Reid, S. J. Judd, and T. Stephenson, "Biomass effects on oxygen transfer in membrane bioreactors," *Water Research,* vol. 41, pp. 1038-1044, 2007.
[128] K. Van't Riet and J. Tramper, *Basic bioreactor design*: CRC Press, 1991.
[129] D. R. Lide, "CRC handbook of physics and chemistry," *The Chemical Rubber Company, Cleveland, OH,* 2003.

Appendices

Appendix A. Mass transfer through the interface

The description of the mass transfer through the interface between phases is taken form Welty et al [124].

Any transfer process is "fuelled" by a driving force which in case of mass transfer is a concentration gradient – a difference between the bulk concentration of species to be transferred and its equilibrium concentration. When two phases come into a contact the changes occur in the system until the equilibrium is established.

If one phase is gas, the other phase is liquid and species i is transferred from one phase to the other equilibrium curve might look as it is shown on Fig. A. (concentration of i in gas phase is often given in the terms of partial pressure $S_{iG} = p_i/RT$ (S_{iG}- concentration of i in the gas phase, p_i - partial pressure of i); equilibrium curves with phase compositions given in terms of molar fractions are also very common (x_i – molar fraction of i in liquid phase, y_i – molar fraction of i in gas phase)).

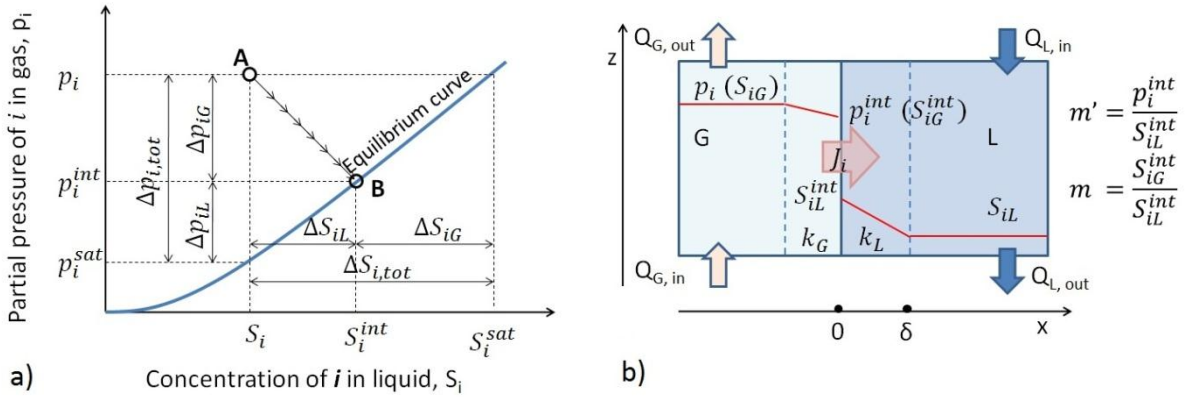

Fig. A.1. a) Equilibrium curve and concentration driving forces (taken from Welty et al [124]); b) illustration of two-film theory for a system with physical absorption.

Equilibrium curve is not a straight line but some part of it can be assumed a straight line with constant slope $m = \frac{p_i^{int}}{S_{iL}^{int}} = \frac{p_i^{sat}}{S_{iL}} = \frac{p_i}{S_i^{sat}}$ (p_i^{int}, S_{iL}^{int} - partial pressure of i in gas and concentration of i in liquid at two phase interface (there's always equilibrium at the interface), p_i^{sat} – saturation partial pressure of i which is in the equilibrium with S_{iL}, S_{iL}^{sat} – saturation concentration of i which is in the equilibrium with p_i). This is always true at low concentrations when Henry's law is obeyed; in this case **m would be equal to Henry's constant H_i**.

If specie i is transferred from the gas where its partial pressure is p_i to the liquid where its concentration is S_{iL} (point A on Fig. A.1 a)) after some time system will reach equilibrium (point B on Fig. A.1 a)). If no chemical reaction takes place flux expressions for such system would look as follows:

$$J_i = k'_G\left(p_i - p_i^{int}\right) = k'_G RT\left(S_{iG} - S_{iG}^{int}\right) = k_G\left(S_{iG} - S_{iG}^{int}\right)$$
$$J_i = k_L\left(S_{iL}^{int} - S_{iL}\right) \qquad \text{(A.1)}$$

Partial pressure and concentration at the interface are very difficult to measure. In some cases it is more convenient to express flux via overall mass transfer coefficients and overall driving force.

$$J_i = K'_G\left(p_i - p_i^{sat}\right) = K'_G RT\left(S_{iG} - S_{iG}^{sat}\right) = K_G\left(S_{iG} - S_{iG}^{sat}\right)$$
$$J_i = K_L\left(S_{iL}^{sat} - S_{iL}\right) \quad \text{(A.2)}$$

It can be shown that overall mass transfer coefficients are related to individual mass transfer coefficients:

$$\frac{1}{K_G} = \frac{1}{k_G} + \frac{m}{k_L}$$
$$\frac{1}{K_L} = \frac{1}{mk_G} + \frac{1}{k_L} \quad \text{(A.3)}$$

Another way to avoid using immeasurable interface concentrations is to express those in terms of bulk partial pressures or concentrations using ideal gas and Henry laws. Different forms of Henry's constant can be found in literature: it is often given as $H_i = p_i^{int}/S_{iL}^{int}$, but can sometimes be given as $H_i = S_{iL}^{int}/p_i^{int}$ or $H_i = S_{iG}^{int}/S_{iL}^{int}$ etc. Due to that the flux expressions given in literature can differ and care should be taken when comparing data from different sources. E.g. expression A.1 can be shown as:

$$for\ H_i = p_i^{int}/S_i^{int} \qquad J_i = k_L\left(\frac{RT}{H_i}\cdot S_{iG} - S_{iL}\right) = k_L\left(\frac{p_i}{H_i} - S_{iL}\right)$$
$$for\ H_i = S_i^{int}/p_i^{int} \qquad J_i = k_L(H_i RT\cdot S_{iG} - S_{iL}) = k_L(H_i p_i - S_{iL}) \quad \text{(A.4)}$$
$$for\ H_i = S_{iG}^{int}/S_{iL}^{int} \approx S_{iG}/S_{iL}^{int} \qquad J_i = k_L\left(\frac{S_{iG}}{H_i} - S_{iL}\right) = k_L\left(\frac{1}{H_i RT}\cdot p_i - S_{iL}\right)$$

(In the last case it is assumed that the mass transfer resistance in the gas phase is negligible and $S_{iG} \approx S_{iG}^{int}$; this is sometimes the case for some systems).

Appendix B. Mass transfer regulation

In this work mass transfer coefficient k_L or K_L $\left[\frac{m}{d}\right]$ (or alternatively $k_L a$ or $K_L a$ $\left[\frac{1}{d}\right]$) is considered a "control" – a quantity that can be regulated by a plant operator. While such assumption greatly simplifies process modelling, it should be stressed that this is not entirely true: mass transfer cannot be controlled directly, although it can be regulated via changing other control handles.

It is generally accepted that major factors that affect oxygen mass transfer are biomass characteristics and aeration system design [125].

The following expression is normally given for the oxygen mass transfer coefficient:

$$k_{OL}a = \alpha \cdot k_{OL}a_W \quad \text{(B.1)}$$

Where α is an alpha factor – a ratio between oxygen mass transfer coefficient in wastewater and in clean water, and $k_{OL}a_W$ – oxygen mass transfer coefficient in clean water.

Alpha factor decreases as the concentration of solids in the reactor increases, but the nature of the changes is system specific: alpha factor for a given wastewater depends on sludge retention time, airflow rate and tank geometry for a given wastewater [126]. Due to the complex nature of this dependency values of alpha factor measured at almost "similar" conditions might differ significantly (hence, system specific). As an example below is the alpha factor measured against mixed liquor suspended solids concentration (MLSS) , as given by Germain et al [127]:

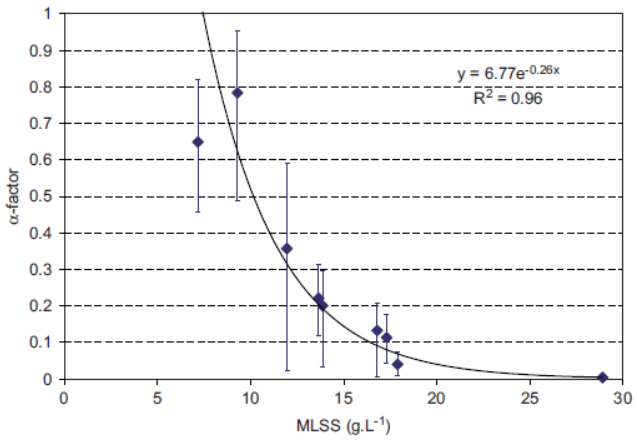

Figure B.1. Alpha factor averaged for all volumetric airflow rates (taken from Germain et al [127]).

Mass transfer coefficient for clean water $k_{OL}a_W$ can be found from the following expressions for coarse and fine bubble aeration, respectively [128]:

$$k_{OL}a_W = 0.32u_G^{0.7} \quad \text{(B.2)}$$

$$k_{OL}a_W = 0.44u_G^{0.7} \quad \text{(B.3)}$$

Where u_G – upflow velocity $\left[\frac{m}{s}\right]$.

Appendix C. Effect of temperature on oxygen solubility

Temperature dependency of oxygen saturation concentration S_O^{sat} can be described with the following expression [129]:

$$S_O^{sat}(T) = \frac{S_O^{sat}(15)}{10.5} \cdot 6791.5 \cdot K(T) \quad \text{(C.1)}$$

Where $S_O^{sat}(15) = 8\ \left[\frac{g}{m^3}\right]$ is oxygen saturation concentration at 15°C; $K(T)$ is a semi-empirical function that can be found from:

$$K(T) = 56.12e^{-66.7354+87.4755\cdot\frac{100}{T+273}+24.4526\cdot\ln\left(\frac{T+273}{100}\right)} \quad \text{(C.2)}$$

Appendix D. Matrix format and notation in ASM-family models

The example below is taken from Henze et al [25], and its purpose is to explain the format and notation used by the ASM-family models which was also further adapted in ADM1.

The example describes a simple system in which heterotrophic bacteria X_H consumes soluble substrate S_s for cell growth and energy production in aerobic environment. Energy production by bacteria is also associated with the oxygen S_O consumption. Thus these three species need to be considered in the system.

The specific symbols are assigned to species in the standard models: all insoluble (particulate) species are given the symbol X, and all soluble – S. The index of the symbol specifies individual components: index H denotes heterotrophic bacteria, S – substrate and O – oxygen.

The important part of the model development is the identification of the fundamental processes that take place in the system. In the simple system described here these fundamental processes are biomass growth and biomass decay. Substrate and oxygen utilisation are also important for the system, but these are coupled with biomass growth through stoichiometric relations, and thus should not be considered as separate processes.

The information above can be given in a very compact and clear way with the help of matrix notation (Table D.). The matrix consists of two parts: the part that contains stoichiometric coefficients and the part that contains kinetic expressions for the specific reaction rates of the individual processes.

Table D.1. Process kinetics and stoichiometry for heterotrophic bacteria growth in aerobic environment (taken from Henze et al [25]).

	→ Continuity				
↓ Mass balance	**Components i → Processes j ↓**	**1. X_H**	**2. S_s**	**3. S_O**	**Process rates, ρ_j $[ML^{-3}T^{-1}]$**
	1. Growth	1	$-\frac{1}{Y}$	$-\frac{1-Y}{Y}$	$\mu_m \frac{S_s}{K_s + S_s} X_H$
	2. Decay	-1		-1	bX_H
	Observed conversion rates $[ML^{-3}T^{-1}]$	$r_i = \sum_j r_{ij} = \sum_j \nu_{ij}\rho_j$			**Kinetic parameters:** μ_m – maximal growth rate of heterotrophic bacteria $[T^{-1}]$; K_s – half saturation constant $[ML^{-3}]$; b – decay rate of heterotrophic bacteria $[T^{-1}]$.
	Stoichiometric parameters: Y – true growth yield $[-]$.	Biomass $[M(COD)L^{-3}]$	Substrate $[M(COD)L^{-3}]$	Oxygen $[M(-COD)L^{-3}]$ (negative COD)	

Stoichiometric coefficients. Index i is assigned to each component in the system and index j – to each process. For a simple system described here i varies from 1 to 3, while j – from 1 to 2, thus forming a 2x3 matrix. The elements of the matrix represent the stoichiometric coefficients that characterize the relationships between the species in the individual processes. Positive sign in front of element ν_{ij} denotes that the species i is produced during the process j, negative – that the specie

is consumed. If ν_{ij} is zero specie i is irrelevant for process j. For example it can be seen that during the biomass growth $(+1)$ soluble substrate is utilized $\left(-\frac{1}{Y}\right)$ together with oxygen $\left(-\frac{1-Y}{Y}\right)$.

Kinetic expressions. Kinetic expressions that describe the processes are given by simple Monod-Herbert model. According to this model the biomass growth rate ρ_1 is proportional to biomass concentration in a first order manner and to substrate concentration in a mixed order manner (Monod term); but biomass decay rate ρ_2 is only proportional to biomass concentration in a first order manner.

One of the advantages of matrix notation is that it allows to easily check the fate of any specie in a system. Moving down the column that represents specie i makes it possible to see which individual processes affect the concentration of the specie and how exactly is the concentration affected. This is an important feature for setting up the mass balances which should contain net production rate for species. The net production rate for any component i (r_i) can be found as a sum of products of all the stoichiometric coefficients in column i (ν_i) with their corresponding specific reaction rates (ρ):

$$r_i = \sum_j r_{ij} = \sum_j \nu_{ij}\rho_j \qquad \text{(D.1)}$$

Another advantage of matrix notation is the possibility to check continuity. This can be done by moving horizontally along any row of the stoichiometric part of the matrix: if consistent units are used for all the coefficients in the matrix (e.g. g(COD)/m^3 or g(N)/m^3) the sum of these coefficients should be equal to zero. This feature can also be used to find unknown stoichiometric coefficients if the matrix needs to be expanded.

Appendix E. Bioflocculation model

Tabel E.1. Parameter values at 20°C (taken from [52]).

Symbol	Value	Unit	Definition
Y_H	0.69	$[gCOD_X/gCOD_S]$	Yield of heterotrophs on readily biodegradable COD
Y_A	0.28	$[gCOD_X/gN]$	Yield of autotrophs on S_{NH}
i_{NB}	0.088	$[-]$	Nitrogen content of biomass
i_{XI}	0.06	$[-]$	Nitrogen content of inert particulates X_I
f_{XI}	0.08	$[-]$	Fraction of biomass that becomes inert after decay
$\mu_H(20)$	6.9	$[1/d]$	Maximal growth rate of heterotrophs
$\mu_A(20)$	0.67	$[1/d]$	Maximal growth rate of autotrophs
$b_H(20)$	0.22	$[1/d]$	Decay coefficient of heterotrophs
$b_A(20)$	0.048	$[1/d]$	Decay coefficient of autotrophs
$K_a(20)$	0.176	$\left[\frac{m^3}{gCOD \cdot d}\right]$	Slowly biodegradable COD adsorption rate
$k_H(20)$	3	$[1/d]$	First order hydrolysis constant
$k_a(20)$	0.082		Ammonification rate
K_S	20.3	$[gCOD/m^3]$	S_s half-saturation coefficient for heterotrophs
K_{OH}	0.19	$[gCOD/m^3]$	Oxygen half-saturation coefficient for heterotrophs
K_{OA}	0.1	$[gCOD/m^3]$	Oxygen half-saturation coefficient for autotrophs
K_{NO}	0.45	$[gN/m^3]$	Nitrate half-saturation coefficient for denitrifying heterotrophs
K_{NH}	0.94	$[gN/m^3]$	Ammonia half-saturation constant for heterotrophs
$K_x(20)$	0.04	$[gCOD_S/gCOD_X]$	Half-saturation coefficient for hydrolysis of slowly biodegradable substrate
f_{ma}	1	$[gCOD_X/gCOD_X]$	Maximal amount of slowly biodegradable COD that can be adsorbed on active biomass
η_G	0.9	$[-]$	Correction factor for heterotrophic growth under anoxic conditions
η_H	0.4	$[-]$	Correction factor for hydrolysis under anoxic conditions

Tabel E.2a. Stoichiometric matrix for bioflocculation model – solubles (modified from [52]).

Coponents $\rightarrow i$ Process $\downarrow j$	1. S_O	2. S_s	3. S_{NH}	4. S_{NO}	5. S_{ND}
1. Aerobic growth of X_H	$-\frac{1-Y_H}{Y_H}$	$-\frac{1}{Y_H}$	$-i_{NB}$		
2. Anoxic growth of X_H		$-\frac{1}{Y_H}$	$-i_{NB}$	$-\frac{1-Y_H}{2.86 \cdot Y_H}$	
3. Aerobic growht of X_A	$-\frac{4.57-Y_H}{Y_H}$		$-i_{NB}-1/Y_A$		
4. Decay of X_H					
5. Decay of X_A					
6. Ammonification			1		-1
7. Flocculation					
8. Hydrolysis of X_s		1			
9. Hydrolysis of X_{ND}					1

Tabel E.2b. Stoichiometric matrix for bioflocculation model – particulates.

Coponents $\rightarrow i$ Process $\downarrow j$	6. X_{un}	7. X_s	8. X_H	9. X_A	10. X_{ND}	11. X_I
1. Aerobic growth of X_H			1			
2. Anoxic growth of X_H			1			
3. Aerobic growth of X_A				1		
4. Decay of X_H	$1-f_{XI}$		-1		$i_{NB}-i_{XI}f_{XI}$	f_{XI}
5. Decay of X_A	$1-f_{XI}$			-1	$i_{NB}-i_{XI}f_{XI}$	f_{XI}
6. Ammonification						
7. Flocculation	-1	1				
8. Hydrolysis of X_s		-1				
9. Hydrolysis of X_{ND}					-1	

Table E.2c. Reaction rates in bioflocculatio model (modified from [52]).

Process j	Specific rates
1. Aerobic growth of X_H	$\mu_H \frac{S_s}{K_s+S_s}\frac{S_O}{K_{OH}+S_O} X_H$
2. Anoxic growth of X_H	$\eta_G \mu_H \frac{S_s}{K_s+S_s}\frac{K_{OH}}{K_{OH}+S_O}\frac{S_{NO}}{K_{NO}+S_{NO}} X_H$
3. Aerobic growht of X_A	$\mu_A \frac{S_O}{K_{OA}+S_O}\frac{S_{NH}}{K_{NH}+S_{NH}} X_A$
4. Decay of X_H	$b_H X_H$
5. Decay of X_A	$b_A X_A$
6. Ammonification	$k_a S_{ND} X_H$
7. Flocculation	$K_a\left(f_{ma}-\frac{X_s}{X_H}\right) X_{un} X_H$
8. Hydrolysis of X_s	$k_H \frac{X_s/X_H}{K_x+X_s/X_H}\left(\frac{S_O}{K_O+S_O}+\eta_H\frac{K_{OH}}{K_{OH}+S_O}\frac{S_{NO}}{K_{NO}+S_{NO}}\right) X_H$
9. Hydrolysis of X_{ND}	$\frac{X_{ND}}{X_s}\cdot k_H \frac{X_s/X_H}{K_x+X_s/X_H}\left(\frac{S_O}{K_O+S_O}+\eta_H\frac{K_{OH}}{K_{OH}+S_O}\frac{S_{NO}}{K_{NO}+S_{NO}}\right) X_H$

Appendix F. Anaerobic digestion model

Table F.1. Parameter values for anaerobic digestion model, taken from [63] .

Symbol	Value	Unit	Definition
		Stoichiometric parameters	
$f_{sI,xc}$	0.1	$[-]$	Fraction of inert solubles S_I in X_c
$f_{xI,xc}$	0.2	$[-]$	Fraction of inert particulates S_I in X_c
$f_{ch,xc}$	0.2	$[-]$	Fraction of carbohydrates in X_c
$f_{p,rxc}$	0.2	$[-]$	Fraction of proteins in X_c
$f_{li,xc}$	0.3	$[-]$	Fraction of lipids in X_c
N_{xc}	0.0376/14	$\left[\frac{kmolN}{kgCOD}\right]$	Nitrogen content of X_c
N_I	0.06/14	$\left[\frac{kmolN}{kgCOD}\right]$	Nitrogen content of inerts
N_{aa}	0.007	$\left[\frac{kmolN}{kgCOD}\right]$	Nitrogen content of amino acids
C_{xc}	0.02786	$\left[\frac{kmolC}{kgCOD}\right]$	Carbon content of X_c
C_{sI}	0.03	$\left[\frac{kmolC}{kgCOD}\right]$	Carbon content of S_I
C_{ch}	0.0313	$\left[\frac{kmolC}{kgCOD}\right]$	Carbon content of carbohydrates
C_{pr}	0.03	$\left[\frac{kmolC}{kgCOD}\right]$	Carbon content of proteins
C_{li}	0.022	$\left[\frac{kmolC}{kgCOD}\right]$	Carbon content of lipids
C_{xI}	0.03	$\left[\frac{kmolC}{kgCOD}\right]$	Carbon content of X_I
C_{su}	0.0313	$\left[\frac{kmolC}{kgCOD}\right]$	Carbon content of sugars
C_{aa}	0.03	$\left[\frac{kmolC}{kgCOD}\right]$	Carbon content of amino acids
$f_{fa,li}$	0.95	$[-]$	Fraction of lipids that is hydrolysed to fatty acids
C_{fa}	0.0217	$\left[\frac{kmolC}{kgCOD}\right]$	Carbon content of fatty acids
$f_{h2,su}$	0.19	$[-]$	Unmetabolised fraction of sugars that is converted into hydrogen gas
$f_{bu,su}$	0.13	$[-]$	Unmetabolised fraction of sugars that is converted into butyrate
$f_{pro\ su}$	0.27	$[-]$	Unmetabolised fraction of sugars that is converted into propionate
$f_{ac\ su}$	0.41	$[-]$	Unmetabolised fraction of sugars that is converted into acetate
N_{bac}	0.08/14	$\left[\frac{kmolN}{kgCOD}\right]$	Nitrogen content of biomass
C_{bu}	0.025	$\left[\frac{kmolC}{kgCOD}\right]$	Carbon content of butyrate
C_{pro}	0.0268	$\left[\frac{kmolC}{kgCOD}\right]$	Carbon content of propionate
C_{ac}	0.0313	$\left[\frac{kmolC}{kgCOD}\right]$	Carbon content of acetate
C_{bac}	0.0313	$\left[\frac{kmolC}{kgCOD}\right]$	Carbon content of biomass
Y_{su}	0.1	$\left[\frac{kgCOD_X}{kgCOD_S}\right]$	Biomass X_{su} yield on sugars
$f_{h2,aa}$	0.06	$[-]$	Unmetabolised fraction of aminoacids that is converted into hydrogen gas

$f_{va,aa}$	0.23	$[-]$	Unmetabolised fraction of aminoacids that is converted into valerate
$f_{bu,aa}$	0.26	$[-]$	Unmetabolised fraction of amino acids that is converted into butyrate
$f_{pro,aa}$	0.05	$[-]$	Unmetabolised fraction of amino acids that is converted into propionate
$f_{ac,aa}$	0.40	$[-]$	Unmetabolised fraction of amino acids that is converted into acetate
C_{va}	0.024	$\left[\frac{kmolC}{kgCOD}\right]$	Carbon content of valerate
Y_{aa}	0.08	$\left[\frac{kgCOD_X}{kgCOD_S}\right]$	Biomass X_{aa} yield on amino acids
Y_{fa}	0.06	$\left[\frac{kgCOD_X}{kgCOD_S}\right]$	Biomass X_{fa} yield on fatty acids
Y_{c4}	0.06	$\left[\frac{kgCOD_X}{kgCOD_S}\right]$	Biomass X_{fa} yield on valerate and butyrate
Y_{pro}	0.04	$\left[\frac{kgCOD_X}{kgCOD_S}\right]$	Biomass X_{pro} yield on propionate
C_{ch4}	0.0156	$\left[\frac{kmolC}{kgCOD}\right]$	Carbon content of methane
Y_{ac}	0.05	$\left[\frac{kgCOD_X}{kgCOD_S}\right]$	Biomass X_{ac} yield on acetate
Y_{h2}	0.06	$\left[\frac{kgCOD_X}{kgCOD_S}\right]$	Biomass X_{h2} yield on hydrogen
		Biochemical parameters	
k_{dis}	0.5	$[1/d]$	Dissociation rate coefficient
$k_{hyd,ch}$	10	$[1/d]$	Carbohydrates hydrolysis rate coefficient
$k_{hyd,pr}$	10	$[1/d]$	Protein hydrolysis rate coefficient
$k_{hyd,li}$	10	$[1/d]$	Lipid hydrolysis rate coefficient
$K_{S,IN}$	10^{-4}	$[M]$	Nitrogen half-saturation coefficient for biomass
$k_{m,su}$	30	$[1/d]$	Maximal substrate utilisation rate of X_{su}
$K_{S,su}$	0.5	$\left[\frac{kgCOD}{m^3}\right]$	Sugars half-saturation coefficient for biomass
$pH_{UL,aa}$	6.25	$[-]$	Upper pH inhibition level for X_{aa}
$pH_{LL,aa}$	4.75	$[-]$	Lower pH inhibition level for X_{aa}
$k_{m,aa}$	50	$[-]$	Maximal substrate utilisation rate of X_{aa}
$K_{S,aa}$	0.3	$\left[\frac{kgCOD}{m^3}\right]$	Amino acids half-saturation coefficient for biomass
$k_{m,fa}$	6	$[1/d]$	Maximal substrate utilisation rate of X_{fa}
$K_{S,fa}$	0.4	$\left[\frac{kgCOD}{m^3}\right]$	Fatty acids half-saturation coefficient for biomass
$K_{Ih2,fa}$	$5{\cdot}10^{-6}$	$\left[\frac{kgCOD}{m^3}\right]$	Inhibition coefficient of X_{fa} by hydrogen
$k_{m,c4}$	20	$[1/d]$	Maximal substrate utilisation rate of X_{c4}
$K_{S,c4}$	0.2	$\left[\frac{kgCOD}{m^3}\right]$	Butyrate and valerate half-saturation coefficient for biomass
$K_{Ih2,c4}$	10^{-5}	$\left[\frac{kgCOD}{m^3}\right]$	Inhibition coefficient of X_{c4} by hydrogen
$k_{m,pro}$	13	$[1/d]$	Maximal substrate utilisation rate of X_{pro}
$K_{S,pro}$	0.1	$\left[\frac{kgCOD}{m^3}\right]$	Propionate half-saturation coefficient for biomass
$K_{Ih2,pro}$	$2.5{\cdot}10^{-6}$	$\left[\frac{kgCOD}{m^3}\right]$	Inhibition coefficient of X_{pro} by hydrogen
$k_{m,ac}$	8	$[1/d]$	Maximal substrate utilisation rate of X_{ac}
$K_{S,ac}$	0.15	$\left[\frac{kgCOD}{m^3}\right]$	Acetate half-saturation coefficient for biomass
$K_{I,nh3}$	0.0018	$[M]$	Ammonia inhibition coefficient

$pH_{UL,ac}$	7.5	$[-]$	Upper pH inhibition level for X_{ac}
pH_{LLac}	6.5	$[-]$	Lower pH inhibition level for X_{ac}
$k_{m,h2}$	35	$[1/d]$	Maximal substrate utilisation rate of X_{h2}
$K_{S,h2}$	$7{\cdot}10^{-6}$	$\left[\frac{kgCOD}{m^3}\right]$	Hydrogen half-saturation constant for biomass
$pH_{UL,h2}$	6.5	$[-]$	Upper pH inhibition level for X_{h2}
pH_{LLh2}	5.5	$[-]$	Lower pH inhibition level for X_{h2}
$k_{dec,Xsu}$	0.02	$[1/d]$	Decay rate coefficient of X_{su}
$k_{dec,Xaa}$	0.02	$[1/d]$	Decay rate coefficient of X_{aa}
$k_{dec,Xfa}$	0.02	$[1/d]$	Decay rate coefficient of X_{fa}
$k_{dec,Xc4}$	0.02	$[1/d]$	Decay rate coefficient of X_{c4}
$k_{dec,Xpro}$	0.02	$[1/d]$	Decay rate coefficient of X_{pro}
$k_{dec,Xac}$	0.02	$[1/d]$	Decay rate coefficient of X_{ac}
$k_{dec,Xh2}$	0.02	$[1/d]$	Decay rate coefficient of X_{h2}
		Physicochemical parameters	
R	0.083145	$\left[\frac{bar}{M{\cdot}K}\right]$	Universal gas constant
T_{base}	298.15	$[K]$	Reference temperature
K_w	$e^{\frac{55900}{100R}\left(\frac{1}{T_{base}}-\frac{1}{T}\right)}$	$[M]10^{-14}$	Water dissociation constant
$K_{a,va}$	10-4.86	$[M]$	Valerate dissociation constant
$K_{a,bu}$	10-4.82	$[M]$	Butyrate dissociation constant
$K_{a,pro}$	10-4.88	$[M]$	Propionate dissociation constant
$K_{a,ac}$	10-4.76	$[M]$	Acetate dissociation constant
$K_{a,co2}$	$10^{-6.35}e^{\frac{7646}{100R}\left(\frac{1}{T_{base}}-\frac{1}{T}\right)}$	$[M]$	Carbonic acid dissociation constant
$K_{a,IN}$	$10^{-9.25}e^{\frac{51965}{100R}\left(\frac{1}{T_{base}}-\frac{1}{T}\right)}$	$[M]$	Ammonium dissociation constant
P_{atm}	1.013	$[bar]$	Atmospheric pressure
$p_{gas,h2o}$	$0.0313e^{5290\left(\frac{1}{T_{base}}-\frac{1}{T}\right)}$	$[bar]$	Water vapour partial pressure
k_p	$5{\cdot}10^{4}$	$\left[\frac{m^3}{d{\cdot}bar}\right]$	
k_La	200	$[1/d]$	Mass transfer coefficient
$K_{H,co2}$	$0.035e^{\frac{-19410}{100R}\left(\frac{1}{T_{base}}-\frac{1}{T}\right)}$	$[M/bar]$	Henry's constant for CO_2
$K_{H,ch4}$	$0.0014e^{\frac{-14240}{100R}\left(\frac{1}{T_{base}}-\frac{1}{T}\right)}$	$[M/bar]$	Henry's constant for CH_4
$K_{H,h2}$	$7.8\cdot10^{-4}e^{\frac{-4180}{100R}\left(\frac{1}{T_{base}}-\frac{1}{T}\right)}$	$[M/bar]$	Henry's constant for H_2

Table F.2a. Stoichiometric matrix for anaerobic digestion model (soluble compounds), taken from [29].

Comp. $\rightarrow i$ Process $\downarrow j$	1 S_{su}	2 S_{aa}	3 S_{fa}	4 S_{va}	5 S_{bu}	6 S_{pro}	7 S_{ac}	8 S_{h2}	9 S_{ch4}	10 S_{IN}	11 S_I	12 S_{IC}
1. Disintegration											$f_{sI,xc}$	$-\sum_{i=1-9,11-24} C_i\nu_{i,1}$
2. Hydrolysis of carbohydrates	1											$-\sum_{i=1-9,11-24} C_i\nu_{i,2}$
3. Hydrolysis of proteins		1										$-\sum_{i=1-9,11-24} C_i\nu_{i,3}$
4. Hydrolysis of lipids	$1-f_{fa,li}$		$f_{fa,li}$									$-\sum_{i=1-9,11-24} C_i\nu_{i,4}$
5. Uptake of sugars	-1				$(1-Y_{su})f_{bu,su}$	$(1-Y_{su})f_{pro,su}$	$(1-Y_{su})f_{ac,su}$	$(1-Y_{su})f_{h2,su}$		$-Y_{su}N_{bac}$		$-\sum_{i=1-9,11-24} C_i\nu_{i,5}$
6. Uptake of amino acids		-1		$(1-Y_{aa})f_{va,aa}$	$(1-Y_{aa})f_{bu,aa}$	$(1-Y_{aa})f_{pro,aa}$	$(1-Y_{aa})f_{ac,aa}$	$(1-Y_{aa})f_{h2,aa}$		$N_{aa}-Y_{aa}N_{bac}$		$-\sum_{i=1-9,11-24} C_i\nu_{i,6}$
7. Uptake of LCFA			-1				$(1-Y_{fa})0.7$	$(1-Y_{fa})0.3$		$-Y_{fa}N_{bac}$		$-\sum_{i=1-9,11-24} C_i\nu_{i,7}$
8. Uptake of valerate				-1		$(1-Y_{c4})0.54$	$(1-Y_{c4})0.31$	$(1-Y_{c4})0.15$		$-Y_{c4}N_{bac}$		$-\sum_{i=1-9,11-24} C_i\nu_{i,8}$
9. Uptake of butyrate					-1		$(1-Y_{c4})0.8$	$(1-Y_{c4})0.2$		$-Y_{c4}N_{bac}$		$-\sum_{i=1-9,11-24} C_i\nu_{i,9}$
10. Uptake of propionate						-1	$(1-Y_{pro})0.57$	$(1-Y_{pro})0.43$		$-Y_{pro}N_{bac}$		$-\sum_{i=1-9,11-24} C_i\nu_{i,10}$
11. Uptake of acetate							-1		$1-Y_{ac}$	$-Y_{ac}N_{bac}$		$-\sum_{i=1-9,11-24} C_i\nu_{i,11}$
12. Uptake of hydrogen								-1	$1-Y_{h2}$	$-Y_{h2}N_{bac}$		$-\sum_{i=1-9,11-24} C_i\nu_{i,12}$
13. Decay of X_{su}												$-\sum_{i=1-9,11-24} C_i\nu_{i,13}$
14. Decay of X_{aa}												$-\sum_{i=1-9,11-24} C_i\nu_{i,14}$
15. Decay of X_{fa}												$-\sum_{i=1-9,11-24} C_i\nu_{i,15}$

16. Decay of X_{c4}												$-\sum_{i=1-9,11-24} C_i \nu_{i,16}$
17. Decay of X_{pro}												$-\sum_{i=1-9,11-24} C_i \nu_{i,17}$
18. Decay of X_{ac}												$-\sum_{i=1-9,11-24} C_i \nu_{i,18}$
19. Decay of X_{h2}												$-\sum_{i=1-9,11-24} C_i \nu_{i,19}$

Table F.2b. Stoichiometric matrix for anaerobic digestion model (particulate compounds).

Comp. → i Process ↓ j	13 X_c	14 X_{ch}	15 X_{pr}	16 X_{li}	17 X_{su}	18 X_{aa}	19 X_{fa}	20 X_{c4}	21 X_{pro}	22 X_{ac}	23 X_{h2}	24 X_I
1. Disintegration	-1	$f_{ch,xc}$	$f_{pr,xc}$	$f_{li,xc}$								$f_{xI,xc}$
2. Hydrolysis of carbohydrates		-1										
3. Hydrolysis of proteins			-1									
4. Hydrolysis of lipids				-1								
5. Uptake of sugars					Y_{su}							
6. Uptake of amino acids						Y_{aa}						
7. Uptake of LCFA							Y_{fa}					
8. Uptake of valerate								Y_{c4}				
9. Uptake of butyrate								Y_{c4}				
10. Uptake of propionate									Y_{pro}			
11. Uptake of acetate										Y_{ac}		
12. Uptake of hydrogen											Y_{h2}	
13. Decay of X_{su}	1				-1							
14. Decay of X_{aa}	1					-1						
15. Decay of X_{fa}	1						-1					
16. Decay of X_{c4}	1							-1				
17. Decay of X_{pro}	1								-1			
18. Decay of X_{ac}	1									-1		
19. Decay of X_{h2}	1										-1	

Table F.2c. Specific reaction rates for anaerobic digestion model.

Process	Specific reaction rates
1. Disintegration	$k_{dis}X_c$
2. Hydrolysis of carbohydrates	$k_{hyd,ch}X_{ch}$
3. Hydrolysis of proteins	$k_{hyd,pr}X_{pr}$
4. Hydrolysis of lipids	$k_{hyd,li}X_{li}$
5. Uptake of sugars	$k_{m,su}\frac{S_{su}}{K_{S,su}+S_{su}}X_{su}I_5$
6. Uptake of amino acids	$k_{m,aa}\frac{S_{aa}}{K_{S,aa}+S_{aa}}X_{aa}I_6$
7. Uptake of LCFA	$k_{m,fa}\frac{S_{fa}}{K_{S,fa}+S_{fa}}X_{fa}I_7$
8. Uptake of valerate	$k_{m,c4}\frac{S_{va}}{K_{S,c4}+S_{va}}X_{c4}\frac{S_{va}}{S_{va}+S_{bu}+10^{-6}}I_8$
9. Uptake of butyrate	$k_{m,c4}\frac{S_{bu}}{K_{S,c4}+S_{bu}}X_{c4}\frac{S_{bu}}{S_{va}+S_{bu}+10^{-6}}I_9$
10. Uptake of propionate	$k_{m,pro}\frac{S_{pro}}{K_{S,pro}+S_{pro}}X_{pro}I_{10}$
11. Uptake of acetate	$k_{m,ac}\frac{S_{ac}}{K_{S,ac}+S_{ac}}X_{ac}I_{11}$
12. Uptake of hydrogen	$k_{m,h2}\frac{S_{h2}}{K_{S,h2}+S_{h2}}X_{h2}I_{12}$
13. Decay of X_{su}	$k_{dec,Xsu}X_{su}$
14. Decay of X_{aa}	$k_{dec,Xaa}X_{aa}$
15. Decay of X_{fa}	$k_{dec,Xfa}X_{fa}$
16. Decay of X_{c4}	$k_{dec,Xc4}X_{c4}$
17. Decay of X_{pro}	$k_{dec,Xpro}X_{pro}$
18. Decay of X_{ac}	$k_{dec,Xac}X_{ac}$
19. Decay of X_{h2}	$k_{dec,Xh2}X_{h2}$

Appendix G. Partial nitritation model

Table G.1. Parameter values for partial nitritation model, taken from [9].

Symbol	Value	Unit	Definition
		Stoichiometric parameters	
Y_H	0.52	$[gCOD_X/gCOD_S]$	Heterotrophic yield on oxygen
Y_{AOB}	0.15	$[gCOD_X/gN]$	Autotrophic yield of AOB
Y_{NOB}	0.041	$[gCOD_X/gN]$	Autotrophic yield of NOB
Y_{HNO3}	0.44	$[gCOD_X/gN]$	Heterotrophic yield on NO_3
Y_{HNO2}	0.44	$[gCOD_X/gN]$	Heterotrophic yield on NO_2
f_i	0.15	$[-]$	Fraction of decayed biomass that forms X_I
i_{NBM}	0.0583	$[gN/gCOD_X]$	Nitrogen content of biomass
i_{NXI}	0.02	$[gN/gCOD_X]$	Nitrogen content of X_I
		Kinetic parameters (at 30°C)	
η_{NO3}	0.6	$[-]$	Correction factor for anoxic growth of X_H
η_{NO2}	0.6	$[-]$	Correction factor for anoxic growth of X_H
k_H	3	$[1/d]$	Maximal specific hydrolysis rate
K_x	0.03	$[gCOD_X/gCOD_X]$	Half saturation coefficient for slowly biodegradable substrate
μ_H	8.72	$[1/d]$	Maximal growth rate of X_H
K_{OH}	0.2	$[gO_2/m^3]$	Oxygen half-saturation coefficient for X_H
K_{SH}	50	$[gCOD/m^3]$	S_s half saturation coefficient for X_H
b_H	2.32	$[1/d]$	Decay rate coefficient for X_H
K_{NO3H}	1	$[gN/m^3]$	Nitrate half-saturation coefficient for X_H
K_{NO2H}	1	$[gN/m^3]$	Nitrite half-saturation coefficient for X_H
μ_{AOB}	2.02	$[1/d]$	Maximal growth rate of AOB
K_{OAOB}	0.235	$[gO_2/m^3]$	Oxygen half-saturation coefficient for AOB
K_{NH3AOB}	0.85	$[gN/m^3]$	Ammonia half-saturation coefficient for AOB
b_{AOB}	0.19	$[1/d]$	Decay rate coefficient for AOB
μ_{NOB}	1.36	$[1/d]$	Maxima growth rate of NOB
K_{ONOB}	1.5	$[gO_2/m^3]$	Oxygen half-saturation coefficient for NOB
$K_{HNO2NOB}$	0.00087	$[gN/m^3]$	Nitrous acid half-saturation coefficient for NOB
b_{NOB}	0.092	$[1/d]$	Decay rate coefficient for NOB

Table G.2. Stoichiometric matrix for partial nitritation model, taken from [9].

Component → i Process ↓ j	1 S_O	2 S_s	3 S_{NH}	4 S_{NO2}	5 S_{NO3}	6 X_H	7 X_{AOB}	8 X_{NOB}	9 X_s	10 X_I	Specific reaction rates
1. Hydrolysis		1							-1		$k_H \frac{X_s/X_H}{K_x + X_s/X_H} X_H$
2. Aerobic growth on X_H	$-\frac{1-Y_H}{Y_H}$	$-\frac{1}{Y_H}$	$-i_{NBM}$			1					$\mu_H \frac{S_O}{K_{OH}+S_O} \frac{S_s}{K_{SH}+S_s} X_H$
3. Anoxic growth on X_H on NO_2		$-\frac{1}{Y_{HNO2}}$	$-i_{NBM}$	$-\frac{1-Y_{HNO2}}{1.71Y_{HNO2}}$		1					$\eta_{NO2}\mu_H \frac{K_{OH}}{K_{OH}+S_O} \frac{S_s}{K_{SH}+S_s} \frac{S_{NO2}}{K_{NO2H}+S_{NO2}} X_H$
4. Anoxic growth of X_H on NO_3		$-\frac{1}{Y_{HNO3}}$	$-i_{NBM}$	$\frac{1-Y_{HNO3}}{1.14Y_{HNO3}}$	$-\frac{1-Y_{HNO3}}{1.14Y_{HNO3}}$	1					$\eta_{NO3}\mu_H \frac{K_{OH}}{K_{OH}+S_O} \frac{S_s}{K_{SH}+S_s} \frac{S_{NO3}}{K_{NO3H}+S_{NO3}} X_H$
5. Decay of X_H			$i_{NBM} - f_i i_{NXI}$			-1			$1-f_i$	f_i	$b_H X_H$
6. AOB growth	$-\frac{3.43-Y_{AOB}}{Y_{AOB}}$		$-\frac{1}{Y_{AOB}} - i_{NBM}$	$\frac{1}{Y_{AOB}}$			1				$\mu_{AOB} \frac{S_O}{K_{OAOB}+S_O} \frac{S_{NH3}}{K_{NH3AOB}+S_{NH3}} \frac{K_{IFNAAOB}}{K_{IFNAAOB}+S_{HNO2}} X_{AOB}$
7. AOB decay			$i_{NBM} - f_i i_{NXI}$				-1		$1-f_i$	f_i	$b_{AOB} X_{AOB}$
8. NOB growth	$-\frac{1.41-Y_{NOB}}{Y_{NOB}}$		$-i_{NBM}$	$-\frac{1}{Y_{NOB}}$	$\frac{1}{Y_{NOB}}$			1			$\mu_{NOB} \frac{S_O}{K_{ONOB}+S_O} \frac{S_{NO2}}{K_{NO2NOB}+S_{NO2}} \frac{K_{IFANOB}}{K_{IFANOB}+S_{NH3}} X_{NOB}$
9. NOB decay			$i_{NBM} - f_i i_{NXI}$					-1	$1-f_i$	f_i	$b_{NOB} X_{NOB}$

Appendix H. Anammox model

Table H.1. Parameter values of Anammox model, taken from [31].

Symbol	Value	Unit	Definition
		Stoichiometric parameters	
Y_H	0.67	$[gCOD_X/gCOD_S]$	Anoxic yield coefficient for X_H growth
Y_{AN}	0.164	$[gCOD_X/gN]$	Yield coefficient for X_{AN} growth
f_I	0.08	$[-]$	Fraction of decayed biomass that forms X_I
i_{NBM}	0.07	$[gN/gCOD]$	Nitrogen content of biomass
i_{NXI}	0.02	$[gN/gCOD]$	Nitrogen content of X_I
		Kinetic parameters	
η_{NOx}	0.6	$[-]$	Anoxic reduction factor
μ_H	0.5·24	$[1/d]$	Maximum growth yield of X_H on S_s
K_s	20	$[gCOD/m^3]$	S_s half-saturation coefficient X_H
b_H	0.05·24	$[1/d]$	Decay rate coefficient for X_H
K_{HNH}	0.01	$[gN/m^3]$	Ammonia half-saturation coefficient for X_H
K_{ANNH}	0.73	$[gN/m^3]$	Ammonia half-saturation coefficient for X_{AN}
K_{ANNO2}	0.55	$[gN/m^3]$	Nitrite half-saturation coefficient for X_{AN}
K_{NO2}	0.5	$[gN/m^3]$	Nitrite half-saturation coefficient for X_H
K_{NO3}	0.5	$[gN/m^3]$	Nitrate half-saturation coefficient for X_H
k_H	0.188·24	$[1/d]$	Maximal specific hydrolysis rate
K_x	1	$[gCOD/gCOD]$	Half saturation coefficient for slowly biodegradable substrate

Table H.2. Stoichiometric and kinetic matrix of Anammox model, taken from [31].

Comp. → i Process ↓ j	1 S_s	2 S_{NH}	3 S_{NO2}	4 S_{NO3}	5 S_{N2}	6 X_s	7 X_{AN}	8 X_H	9 X_I	Specific reaction rates
1. Hydrolysis	1					-1				$k_H \frac{X_s/X_H}{K_x + X_s/X_H} X_H$
2. Growth of X_{AN}		$-\frac{1}{Y_{AN}} - i_{NBM}$	$-\frac{1}{Y_{AN}} - \frac{1}{1.14}$	$\frac{1}{1.14}$	$\frac{2}{Y_{AN}}$		1			$\mu_{AN} \frac{S_{NH}}{K_{ANNH} + S_{NH}} \frac{S_{NO2}}{K_{ANNO2} + S_{NO2}} X_{AN}$
3. Decay of X_{AN}		$i_{NBM} - f_i i_{NXI}$				$1 - f_i$	-1		f_i	$b_{AN} X_{AN}$
4. Anoxic growth of X_H on NO_2	$-\frac{1}{Y_H}$	$-i_{NBM}$	$-\frac{1 - Y_H}{1.71 Y_H}$		$\frac{1 - Y_H}{1.71 Y_H}$			1		$\eta_{NOx} \mu_H \frac{S_s}{K_{SH} + S_s} \frac{S_{NO2}}{K_{HNO2} + S_{NO2}} \frac{S_{NH}}{K_{HNH} + S_{NH}} X_H$
5. Anoxic growth of X_H on NO_3	$-\frac{1}{Y_H}$	$-i_{NBM}$		$-\frac{1 - Y_H}{2.86 Y_H}$	$\frac{1 - Y_H}{2.86 Y_H}$			1		$\eta_{NOx} \mu_H \frac{S_s}{K_{SH} + S_s} \frac{S_{NO3}}{K_{HNO3} + S_{NO3}} \frac{S_{NH}}{K_{HNH} + S_{NH}} X_H$
6. Decay of X_H		$i_{NBM} - f_i i_{NXI}$				$1 - f_i$		-1	f_i	$b_H X_H$